Elucidating Temporal Variability in Organic Matter Sources and Cycling in Tropical Rivers

Erin Elizabeth Ellis

A dissertation

submitted in partial fulfillment of the

requirements for the degree of

Doctor of Philosophy

University of Washington

2012

Reading Committee:

Anitra E. Ingalls, Co-Chair

Jeffrey E. Richey, Co-Chair

Richard G. Keil

Program Authorized to Offer Degree:

School of Oceanography

University of Washington

Abstract

Elucidating Temporal Variability in Organic Matter Sources and Cycling in Tropical Rivers

Erin Elizabeth Ellis

Co-Chairs of the Supervisory Committee:
Associate Professor Anitra E. Ingalls
School of Oceanography

Professor Jeffrey E. Richey
School of Oceanography

Tropical rivers are large sources of carbon to the atmosphere and the ocean. The composition of riverine organic matter (OM) affects the size of these fluxes by governing how much carbon will be returned to the atmosphere while in transit versus exported to the ocean, where carbon can be permanently buried in marine sediments. Carbon isotopes coupled with biomarker measurements are powerful tools to elucidate the sources and cycling of OM in rivers, yet few studies have employed them in the tropics. Here I use carbon isotopes ($\delta^{13}C$ and $\Delta^{14}C$) and biomarker measurements of higher plants and soils to address the following topics: sources of organic carbon respired in rivers; terrestrial OM sources to rivers; the age of riverine OM.

In the Amazon Basin, in situ respiration rates are high enough to support the high carbon dioxide gas evasion rates occurring in many white-water rivers. C_4 grasses, C_3 plants, and phytoplankton fuel respiration, with phytoplankton being important during the low-water season. On the mainstem, C_4 grasses are an important substrate for respiration during the rising-water stage, but other sources dominate during falling water.

In the Mekong Basin, vascular plants contribute to 15-76% of the particulate organic carbon (POC) exported by the river, with phytoplankton and higher plants dominating OM composition during the dry and rainy seasons, respectively. The age of lignin exported by the Mekong is consistently young (produced within the last 15 years), and it cycles amidst POC of varying ages, ranging from contemporary during the rainy season, to over 3,000 years old during the rising-water period. The aged signal observed during the dry period is likely due to the increasing influence from carbon derived from the Upper Basin (the Chinese mountains and the Tibetan Plateau), whereas the young rainy-season values reflect carbon derived from the Lower Basin. Seasonal variability in the composition of particulate lignin corroborates these findings. Finally, the highest concentrations of branched tetraether lipids were found in floodplains and lake beds, suggesting that anaerobic environments may be a significant source of these biomarkers to the river, with production likely occurring within the river.

TABLE OF CONTENTS

LIST OF FIGURES

LIST OF TABLES

ACKNOWLEDGEMENTS

I would like to express deep gratitude to my advisors, Dr. Jeffrey Richey and Dr. Anitra Ingalls, for their continuous support and encouragement throughout the duration of my dissertation. I thank Jeff for allowing me the opportunity to conduct research in amazing places that are of global significance. I am further grateful that he consistently allowed room for scientific creativity, especially when some of my research objectives occasionally deviated slightly from his own. Also, I thank Jeff for always encouraging me keep the big picture in mind when interpreting my data. I am grateful to Anitra for her scientific guidance at many levels, from laboratory analyses to data interpretation and manuscript preparation. I thank Anitra for being my teaching mentor and my role model of a successful female scientist. Above all, I thank her for her continuous support and encouragement.

I acknowledge committee member Rick Keil with deep gratitude for his engagement in seminal discussions that aided in data interpretation. His enthusiasm for studying biomarkers was highly motivating and contributed to my pursuit of using molecular signatures to disentangle organic matter sources. I also thank committee member Robert Morris for his assistance and support. I have further benefited from discussions Paul Quay and Miles Logsdon.

I am grateful to the National Science Foundation (NSF) for providing me with a Graduate Research Fellowship, and to the University of Washington for providing me with a Huckabay Teaching fellowship. My research was supported by grants from the Office of Earth Science at the National Aeronautic and Space Administration (NASA), and from the Division of Environmental Biology at NSF.

I am indebted to many individuals for their help conducting field work in both Brazil and Cambodia, including J. Souza, E. Souza, C. Salimon, A. V. Krusche, D. Kuy, S. Kirschke, and P. Martin. Many of the chemical analyses from the Amazon were conducted at the Centro de

Estudos Nucleares na Agricultura (CENA, Piracicaba, Brazil), and I am grateful to the staff for coordinating this work, in particular R. Victoria, A. V. Krusche, A. Montebello, and G. G. Baldi. M. Sampson, A. Shantz, and the rest of the staff at Resource Development International-Cambodia (RDIC) were instrumental to collecting the Mekong samples, and this work would not have been possible without them. At the University of Washington (UW), I am grateful to the staff in Paul Quay's stable isotope lab (including J. Stutsman and M. Haught), and to the staff within the Marine Organic Geochemistry group for their assistance with the biomarker measurements (in particular L. Truxal and J. Neibauer). I also thank the Oceanography administration (in particular S. Tipple and C. Manikham) for their help in navigating many hurdles that accompany international field work. Finally, I am indebted to G. dos Santos at the Keck-CCAMS at the University of California-Irvine for handling the radiocarbon analyses.

I have benefited from discussions with past and current members of the Rivers System Research Group at the University of Washington, including E. Mayorga, A. K. Aufdenkampe. S. Remington, D. E. Lockwood, G. Holtgrieve, S. Kirschke, N. Ward, and M. Constans. I am especially grateful to S. Alin for her mentoring and for conversations that have influenced how I think about riverine processes. I also thank my fellow classmates, including K. McDuffee, E. Walsh, K. Shamberger, J. Kellogg, C.T.E. Kellogg, M. Guannel. Above all, I thank Preston Martin for being there even during the most challenging times during this dissertation. His continuous support, encouragement and sense of humor have been invaluable.

Finally, I express deep gratitude to my family for their love, support, and encouragement throughout the duration of this dissertation. It is because of the hard-working values they instilled in me that I had the confidence that I could do this in the first place.

DEDICATION

To my grandfather,

Eldren Kermit Brunsvold,

for instilling a love of learning in our family,

for being a biogeochemist without even knowing it,

for teaching me that perseverance pays off,

and for encouraging me to live a life full of adventures.

Chapter 1: Introduction

The tropics are fundamental to understanding how carbon cycles across fluvial environments. Not only do they export 65% and 72% of the global riverine dissolved and particulate organic carbon flux to the ocean, respectively [*Mayorga et al.*, 2010; E. Mayorga, personal communication], but the tropics are responsible for 60% of the global inland water carbon dioxide (CO_2) flux to the atmosphere [*Aufdenkampe et al*., 2011]. Deciphering the organic composition of the material found within these ecosystems is key to understanding these fluxes. First, the high levels of CO_2 supersaturation that drive gas evasion in the tropics are largely produced through *in situ* respiration by heterotrophs that utilize terrestrial organic matter as a substrate [*Richey et al*., 2002; *Mayorga et al.*, 2005]. Considering that the global gas evasion flux of carbon from inland waters exceeds total carbon export via rivers (1.2 Pg vs. 0.9 Pg, respectively) [*Battin et al.*, 2009; *Aufdenkampe et al*., 2011], it is imperative to decipher the source of this highly reactive material. Next, the burial of terrigenous material exported by rivers has altered the global carbon and oxygen cycles over geological time scales [*Berner*, 1989]; therefore, given the importance of the tropics in exporting organic matter to the ocean, it is imperative to elucidate the composition (and reactivity) of this material.

In the humid tropics, the biological source of riverine organic matter varies substantially between seasons, driven by strong seasonal changes in precipitation regimes [*Coynel et al.*, 2005; *Spencer et al.*, 2010]. Despite this, most studies examining riverine organic matter composition frequently miss seasonal cycles; instead, they employ snapshot sampling strategies that occur when the majority of terrigenous OM export occurs. As the chemical composition of carbon sources may vary substantially across the hydrograph, their reactivity and preservation

capabilities also change. There may specific periods when OC export most amenable to preservation occurs, and sampling only during high-water regimes could bypass such events, therefore hindering our understanding of the reactivity of this material and its potential to be preserved in ocean sediments.

The objective of my dissertation is to examine both spatial and temporal variability in the sources and cycling of organic matter carried by rivers located in the humid tropics. I do this by characterizing organic matter at the bulk and the molecular level to learn how specific biological sources of carbon cycle seasonally by using carbon isotopes ($\delta^{13}C$ and $\Delta^{14}C$) and/or biomarkers. While measurements at the bulk level are informative because they characterize the entire organic matter pool, they are often ambiguous because riverine organic matter in rivers is composed of a variety of sources with contrasting signatures. Analysis of target molecules that are representative of distinct biological sources is an alternative method to assess the origin of organic matter. Although these "biomarkers" typically only represent trace components of organic matter, they can be powerful tools to assess changes in the contribution of specific sources. Thus, combining both approaches can be highly informative in elucidating the sources of organic matter found in fluvial environments.

In chapter 2, I address the role of riverine organic matter in serving as a substrate for heterotrophic respiration in Amazonian Rivers. By taking advantage of the range of river types encountered in the Amazon Basin, I examined the relationship between organic matter size (i.e. coarse particulate, fine particulate, and dissolved organic carbon) and source (C_3 leaves, C_4 macrophytes, and algae) in fueling the high and variable respiration rates that occur throughout the central and southwestern portion of the Brazilian Amazon. By measuring the isotopic composition of respiration-derived carbon dioxide, my work demonstrates that no single

biological source consistently fuels respiration; rather, all three sources contribute to in situ respiration, with their roles varying as the availability of these sources change seasonally and spatially.

Having established the importance of source variability in fueling respiration in tropical rivers, I then focus on characterizing how organic matter sources change seasonally in chapters 3-5, using the Mekong River, of Southeast Asia, as my study site. The Mekong River is similar to the Amazon in that it is one of the largest rivers in the world, with a considerable portion of its watershed lying within the humid tropics. However, it differs in that the influence of floodplain processes is significantly diminished [*Mekong River Commission,* 2005], making it an ideal site to track seasonal changes in the mobilization of different sources of terrestrial organic matter from the watershed.

In chapter 3, I couple measurements of bulk organic matter with that of lignin-derived phenols (biomarkers for vascular plants) to deduce how the contribution of vascular plants to riverine particulate organic matter changes throughout the year. My results demonstrate that vascular plants dominate during the rainy season. Further, the sediment that is exported by the Mekong during this period reflects the predominant vascular plants growing in the Lower Basin (i.e. the basin below China), whereas the compositional signature of sediment exported by the Mekong during the dry season reflects the gymnosperm vegetation that dominates in the Upper Basin. In chapter 4, I perform compound specific radiocarbon analysis on individual lignin phenols and deduce that regardless of where the sediment originates in the basin, the age of the vascular-plant derived organic matter is consistently young, suggesting that this material is cycled on short time-scales within the basin. In contrast, the age of the bulk particulate organic matter is highly variable, ranging from contemporary to over 3,000 years old, again reflecting the

geographic influence of different regions of the basin in exporting sediment. I then apportion organic matter amongst three components (vascular plants, phytoplankton, and a slowly-cycling soil pool) and determine how the contribution of these pools to riverine organic matter changes seasonally.

In chapter 5, I again monitor seasonal changes in Mekong River sediment composition, but this time to evaluate the utility of a recently introduced proxy (the Branched and Isoprenoid Tetraether (BIT) index) that has been proposed to trace changes in the contribution of terrestrially-derived organic matter to marine sediments. By tracking changes in the branched and isoprenoid tetraether lipid composition of suspended sediments, I determine that processes occurring in the river itself significantly modify this index prior to entering marine environments, potentially complicating the use of this proxy to track changes in the delivery of terrigenous organic carbon to marine sediments.

The Mekong River Basin is currently in the midst of considerable change. China is building a series of eight dams in the Upper Basin, and up to 11 mainstem dams may be constructed between 2015 and 2030 in the Lower Basin [*Mekong River Commission*, 2009]. As dams trap organic matter that would have previously been exported, this will undoubtedly change the nature of the organic matter exported to the South China Sea. Thus, the work presented here provides a starting point in establishing a baseline by which future measurements can be assessed to evaluate how dams are affecting organic matter cycling within the catchment.

Chapter 2: Factors controlling water-column respiration in rivers of the central and southwestern Amazon Basin[1]

INTRODUCTION

Nearly all rivers and lakes across both temperate and tropical ecosystems are net sources of carbon dioxide (CO_2) to the atmosphere [*Cole et al.,* 1994; *Richey et al.,* 2002; *Duarte and Prairie,* 2005] In situ respiration of organic matter (OM) derived from upland ecosystems appears to be the primary source of CO_2 supersaturation in most of these waters [*Richey et al.,* 2002; *Mayorga et al.,* 2005*a*; *Battin et al.,* 2008]. Although aquatic ecosystems represent a small fraction of the earth's surface, over long time periods their carbon fluxes are often larger than those of the surrounding terrestrial ecosystem, giving them the ability to affect regional carbon budgets [*Cole et al.,* 2007]. In some cases, gas evasion from rivers can exceed dissolved and particulate carbon export to the ocean by an order of magnitude [*Richey et al.,* 2002]. Accordingly, it is essential to quantify respiration rates and to understand their variability given the importance of respiration in supporting gas evasion fluxes and resolving regional carbon balances.

Tropical rivers are of particular interest to biogeochemists because their areal outgassing rates typically exceed their temperate counterparts, with rivers and streams having higher rates than lakes and wetlands in both biomes [*Aufdenkampe et al.,* 2011]. The most well-studied of the tropical river basins is the Amazon, where lowland rivers and streams are highly supersaturated with CO_2, as reflected by partial pressures (P_{CO_2}) ranging from 57-3399 Pa (565-33,550 μatm) [*Mayorga et al.,* 2004, 2005*a*]. Approximately 0.5 Pg C yr^{-1} is lost to the

[1] Copyright 2012 by the Association for the Sciences of Limnology and Oceanography, Inc. Ellis, E. E., J. E. Richey, A. K. Aufdenkampe, A. V. Krusche, P. D. Quay, C. Salimon, and H. Brandao da Cunha, 2012, Factors controlling water-column respiration in rivers of the central and southwestern Amazon Basin, Limnol. Oceanograph., 57(2), 527-540.

atmosphere through ougassing throughout the basin, an amount roughly equal to the total terrestrial sequestration of carbon in the Amazon Basin [*Richey et al.*, 2002]. Respiration and gas exchange control the seasonal distribution of dissolved oxygen (O_2) and CO_2 in Amazonian rivers [*Quay et al.*, 1992; *Devol et al.*, 1995]. Specifically, CO_2 supersaturation has been hypothesized to be sustained by water-column respiration of material derived from both autochthonous and allochthonous sources, in addition to CO_2 dissolution from root respiration in forest soils, and floating and emergent macrophyte respiration [*Richey et al.*, 1990; *Richey et al.*, 2002]. Despite the potential importance of in situ respiration in fueling gas evasion, little is known about the mechanisms behind the high variability of water-column respiration rates observed across the Amazon basin (from 0.08 to 5.5 μmol O_2 L^{-1} h^{-1}) [*Richey et al*., 1990; *Benner et al*., 1995; *Devol et al*., 1995].

These observations pose the question, what combination of chemical, physical, and biological factors produces the observed variability in water-column respiration rates, and further, the distribution of CO_2 outgassing? The coupling between physical size classes of organic carbon and water-column respiration has been an area of significant research within the basin over the last twenty years; yet, our understanding of the relationships between carbon size classes and respiration remains unresolved. Measurements of the organic composition of coarse and fine particulate organic carbon (OC) (CPOC and FPOC, respectively), and dissolved OC (DOC) demonstrate that carbon becomes more degraded as its physical size decreases [*Hedges et al*., 1994; *Devol and Hedges*, 2001]. A mass balance of carbon inputs and outputs to the Amazon suggests these carbon pools are not sufficient to balance the requirements needed to support water-column respiration. Instead, it is hypothesized that a rapidly-cycling pool of labile OC likely exists within these bulk size fractions that fuels respiration [*Richey et al.*, 1990]. This

labile pool could exist within the dissolved component of DOC: elevated bacterial growth and respiration were observed during incubations with DOC size fractions > 1 kDa as compared to size fractions < 1 kDa in the Solimões (i.e., the Amazon mainstem above the confluence of the Negro River) and the Negro rivers [*Amon and Benner*, 1996]. More recently, the average age of CO_2 in equilibrium with dissolved inorganic carbon has been demonstrated to be less than 5 years old, although the age of bulk size fractions (CPOC, FPOC, and DOC) ranges from tens to thousands of years [*Mayorga et al.*, 2005*a*]. Thus, there is a growing consensus that the bulk material is of limited bioavailability, and instead, a small, labile, young pool of carbon fuels respiration [*Amon and Benner*, 1996; *Mayorga and Aufdenkampe*, 2005].

Other research has speculated on the role of different biological sources of organic matter (i.e., C_3 and C_4 plants, and phytoplankton) in supporting respiration. Isotopic work suggests C_4 vegetation (mainly grasses within river-corridors and floodplains) may be an important substrate for respiration within the central Amazon basin [*Quay et al.*, 1992; *Engle et al.*, 2008]. For example, the $\delta^{13}C$ of respiration-derived CO_2 (CO_{2resp}) indicates that C_4 grasses can support up to 40% of water-column respiration on the Solimões River during the early rising-water stage [*Quay et al.*, 1992] within the central Amazon Basin. This finding is somewhat surprising because the majority of the organic matter transported by the river has a terrestrial C_3 plant signature, and consequently this may suggest that C_4 grasses are inherently more biodegradable [*Hedges et al*., 1986; *Quay et al*., 1992; *Mayorga et al.*, 2005a].

Outside the Amazon, phytoplankton and periphyton production are important sources of labile carbon that affect respiration rates [*Kritzberg et al.*, 2004; *del Giorgio and Pace*, 2008]. Dissolved oxygen isotopes (^{18}O:^{16}O) indicate that photosynthetically-produced oxygen is found in Amazonian lakes and rivers [*Quay et al.*, 1995], yet the role of phytoplankton in supporting

respiration remains uninvestigated. This may be due to the very low photosynthesis rates observed in the sediment-rich waters of the Amazon mainstem [*Wissmar et al*., 1981], which has led to the perception that OC from phytoplankton production is of minimal importance in rivers throughout the basin.

Accordingly, to address these outstanding research questions key to understanding carbon cycling in the Amazon basin, this study examines the factors affecting the variability in water-column respiration rates across rivers and streams with contrasting organic carbon concentrations, highlighting a continuum of river sizes. Specifically, we ask is there a relationship between the situ concentrations of the physical size classes of carbon and water-column respiration rates? As different biological sources (e.g. C_3 vegetation, C_4 vegetation, or phytoplankton) may affect water-column respiration rates, we also examine the influence of these sources on respiration rates. Finally, to improve our understanding of the coupling between respiration and basin-wide gas evasion, we assess the ability of water-column respiration to support CO_2 gas evasion in rivers and streams of different water types.

Much of the previous work examining respiration in the Amazon basin represents the mainstem and lower main tributaries, often in a single "snapshot' or in controlled experiments. Although manipulations directly determine the effects of a particular variable on respiration, such studies may be biased due to bottle artifacts and the perturbation of other variables from in situ levels. In contrast, we examine relationships between respiration rates and the in situ measurement of a given variable. A caveat of this approach is that some correlations can be spurious, which must be differentiated from causal relationships. Consequently, we present our results in context with the chemical, physical, and seasonal differences between the sites that may concurrently affect respiration rates. We employ stable carbon and oxygen ($\delta^{13}C$ and $\delta^{18}O$)

isotopes to partition organic matter among sources and to identify the relative importance of photosynthesis across sites. $\delta^{13}C$ is used to differentiate between OC originating from C_3 plants (~ -28‰, typically terrestrial), C_4 plants (~-12‰, typically floodplain macrophytes), and phytoplankton (~ -33 to -37‰). Further, the $\delta^{18}O$ of dissolved O_2 provides information about the relative importance of heterotrophic respiration, autochthonous production, and gas exchange at each site [*Benson and Krause*, 1984; *Quay et al*., 1995].

METHODS

Study area

Samples were collected during 2005 and 2006 in the Brazilian states of Acre and Amaz*ô*nas (Fig. 2.1), which are located in southwestern and central *Amazônia*. Locations were chosen to represent a range of water types and conditions found in these regions. Rivers in the Amazon basin differ by both their dissolved and particulate organic and inorganic chemical contents due to the extent that they drain the Andes, Andean forelands, or highly weathered lowland shields [*Sioli*, 1984]. Due to the predominance of white-water rivers in both *Amazônas* and Acre and the logistical challenges of reaching a variety of river types in this large region, we sampled ten white-water rivers of varying sizes. We also sampled two clear-water streams (one each in *Amazônas* and Acre), and two black-water rivers in *Amazônas*. Watershed areas ranged from < 10 km^2 to 2,910,510 km^2 (Table 2.1), which were calculated as in *Mayorga et al.* [2005*b*].

Not all sites were in the same stage of the hydrograph at the time of sampling. All rivers in Acre were in the low-water stage, whereas rivers draining Amaz*ô*nas were in the falling-water stage (Table 2.1). We collected samples from 14 sites from July - September 2005, which coincided with a severe drought in the western and southern regions of the Amazon basin [*Zeng*

et al., 2008]. Eight of these sites were re-sampled during August - September 2006 of the following year (no drought).

Sample collection

Samples were collected from the thalweg of rivers using a submersible pump placed at 6/10 of the total river depth. pH, conductivity, and dissolved oxygen were measured by immersing field probes (Thermo Orion 290 A+ pH meter, a Chek Mite CD-30 conductivity meter, and a 55 YSI dissolved oxygen probe) in a continuously overflowing graduated cylinder. For small streams, samples were taken directly below the water surface to minimize disturbance. P_{CO_2} was analyzed via headspace equilibration following the methods of *Cole et al.* [1994] and modified as in *Alin et al.* [2010]. P_{CO_2} samples were either measured immediately using infra-red gas analysis via a Li-Cor LI-820 [*Alin et al*., 2010] or stored in glass bottles until analysis with a Shimadzu gas chromatograph (GC-17A equipped with flame ionization and electron capture detectors and a methanizer).

Size fractionation

Bulk size fractions (CPOC (> 63 μm), FPOC (0.7- 63 μm), and DOC (<0.7μm)) were filtered in the field, whereas size fractionation of DOC was processed in the laboratory. Coarse suspended sediment (CSS) concentrations were measured by first passing a known volume of river water through a 63 μm sieve, and then later drying and weighing the sieved material. The material collected from a plankton net was preserved with $HgCl_2$ for later analyses of weight percentages (wt%) of C, N, and $\delta^{13}C$ of CPOC. CSS concentrations were multiplied by wt% C to determine CPOC concentrations. Sieved river water was homogenized with a churn splitter [*Wilde and Radtke*, 2003] and then filtered, providing the fine suspended sediment concentration (FSS) by mass difference [*Aufdenkampe et al.*, 2001]. Sieved water was also passed through pre-

combusted glass fiber filters (GF/F), which were then analyzed for $\delta^{13}C$, wt% of C and N, and FPOC concentrations.

The filtrate of the GF/F filter (defined as DOC) was stored in precombusted glass vials and immediately preserved with $HgCl_2$ pending no further analysis. Centrifuge ultrafiltration was used to size fractionate DOC into the following categories: HMW (> 100 kDa), medium molecular weight (MMW) (5-100 kDa), and LMW (< 5 kDa) DOC, using a method modified from *Burdige and Gardner* [1998]. Water was filtered through two GF/F filters in the field, placed on ice in the dark, transported back to the laboratory, and refrigerated until analyzed (within 48 h). Centrifuge tubes (Amicon Ultra-15 Centrifugal Filter Units) were pre-cleaned by sonication with two 10% HCl rinses, followed by an Alconex rinse, and five C-free Milli-Q water rinses for an hour each. The 5 kDa filters were cleaned by centrifuging 15 mL of 0.1 mol L^{-1} NaOH through the filter unit at 4,000 x *g* for 20 min twice, followed by a third NaOH rinse for 10 min, and two Milli-Q water rinses for 10 min. 15 mL of sample was then centrifuged for 40 min. The 100 kDa filters were cleaned as follows: three 15 mL NaOH rinses for 15 min, followed by one Milli-Q water rinse, and two Milli-Q water rinses for 30 min. The sample was then centrifuged for 30 min. Controls were run using albumin to ensure that the filter was not affected by the cleaning process. The concentration factor for the retentate of the 5 kDa and 100 kDa centrifugal filter units were 104.39 and 53.39, respectively (Millipore Corporation). However, we opted to analyze the filtrate, rather than the retentate, because it was of adequate volume for DOC analyses (greater than 180 μL). Thus, the following equation was used to calculate the percentage of DOC that is less than size X ($\%DOC_{<X}$):

$$\%DOC_{<X} = \left[\frac{DOC_F V_F}{DOC_I V_I}\right] \times 100 \qquad (1)$$

where X is either 5 or 100 kDa, DOC_F and DOC_I are the DOC concentrations (mg L^{-1}) in the filtrate (F) and initial (I) (i.e., unfiltered) sample, respectively, and V_F and V_I are the volume of the filtrate and the initial sample, respectively. The average blank value associated with the filtrate was subtracted from DOC_F prior to calculating percent recoveries. To determine the concentration of DOC < 5 kDa or < 100 kDa, the unfiltered DOC concentration (i.e., DOC_I) was multiplied by $\%DOC_{<X}$. The concentration of the size fractions of DOC was obtained by subtracting the appropriate value(s) from the original DOC concentration.

DOC concentrations were measured after acidification and sparging with high temperature combustion using a Shimadzu TOC500A carbon analyzer (2005 samples) and a Shimadzu TOC-V CPH carbon and nitrogen analyzer (2006 samples). Those samples with high DIC concentrations were acidified and sparged for 20 minutes to ensure DIC removal.

Organic matter source: Carbon isotopic analyses and C:N ratios

Stable isotopes ($^{13:12}C$) of carbon were measured in both the inorganic and organic size fractions to aid in partitioning organic matter among end-member sources. Results are given in delta (δ) notation with units of per mil (‰), and were normalized relative to Vienna Peedee Belemnite. After drying coarse and fine materials in a 60°C oven, the samples were analyzed for $\delta^{13}C$ and C:N ratios using a Finnigan Delta Plus mass spectrometer coupled to a Fissions EA 1110 CHN analyzer with a precision of 0.3‰ for the mass spectrometer. For 2005 samples, the C:N ratio was obtained directly from a model 440 C:H:N analyzer made by Exeter Analytical.

The $\delta^{13}C$ of DOC was analyzed using an automated method in which DIC was sparged from the sample after adding phosphoric acid, followed by sodium persulfate oxidation of DOC to CO_2. The CO_2 gas was carried to an infra-red gas analyzer and then to a PDZ Europa-Hydra 20-20 isotope ratio mass spectrometer. Only the 2006 samples were analyzed.

DIC field collections and isotopic measurements (δ^{13}C of DIC) were conducted as in *Quay et al.* [1992] with a precision of 0.03‰ for the 2006 samples. DIC concentrations were calculated from pH and P_{CO_2} for the 2005 samples. We used temperature-dependent equilibrium constant values (K_1, K_2, and K_H) as reported in *Clark and Fritz* [1997]. To estimate the δ^{13}C of phytoplankton, we used an isotopic fractionation factor of 12‰ to 17‰ between the δ^{13}C of H_2CO_3 (calculated from the δ^{13}C of DIC (as in *Mayorga et al.*, [2004], using the equilibrium fractionation factors from *Zhang et al.*, [1995])) and phytoplankton. This fractionation factor is derived from the relationship between H_2CO_3 and POM (predominantly phytoplankton) in the surface ocean [*Goericke and Fry*, 1994].

In situ respiration rates

Respiration rates were calculated at all sites by measuring the consumption of oxygen over a 24 h period. Five initial and final replicate samples were incubated in 60-mL acid-washed Biological Oxygen Demand bottles in the dark in river water held at ambient temperatures. Bottles were agitated twice daily by gently inverting them several times to reduce aggregate formation. Oxygen concentrations were measured by Winkler Titrations [*Wetzel and Likens*, 1991] using a Hach titrator. Dissolved oxygen consumption was determined as the rate of change between the initial and final replicates over the incubation period in μmol of O_2 L^{-1} h^{-1}. To convert our measurements into CO_2 production values, we used a respiratory quotient of one to be consistent with previous work in the Amazon basin [*Devol et al.*, 1987; *Richey et al.*, 1988].

We obtained depth-integrated respiration rates by multiplying the respiration rates by the depth of the river or stream. The depth was obtained from the nearest hydrological monitoring station maintained by the Brazilian national water agency (Agência Nacional de Águas, ANA:

http://hidroweb.ana.gov.br). We used the average depth for the month of sampling as recorded in the long-term time series (> 33 years). Because there was no hydrological monitoring station nearby on the Amazon, Solimões, Madeira, and Negro rivers, we calculated depth from field measurements taken from long-term Carbon in the Amazon River Experiment (CAMREX) datasets [J. E. Richey unpubl. data]. We used Monte Carlo error analysis to obtain the error in the depth-integrated respiration rate.

Bacterial abundance measurements

Bacterial abundance measurements were made by epifluorescence microscopy using 4' 6'-diamidino-2-phenylindole (DAPI) optical filters in 2006. 40 mL samples were collected, preserved with formaldehyde to a final concentration of 2%, and analyzed within 2-4 months of collection. A surfactant (0.5% solution of Triton X-100 in distilled water) was added drop-wise to particle-rich samples, which were then sonicated for 10 minutes. Next, the sample solution was stained with Acridine Orange for three minutes. Samples were then filtered using 0.22 μm black polycarbonate-membrane filters, and then stained with DAPI for 10 minutes. Because these samples had high sediment concentrations, this dual-stain technique was necessary to illuminate the bacterial cells against the particle-rich background for counting purposes [*Schmidt et al*., 1998]. Between 250 μL to 5 mL of sample were used such that at least 200 cells were counted in 20 fields.

Measurements of $\delta^{18}O$-O_2 and $\delta^{18}O$-H_2O

Stable isotopes of oxygen dissolved in water ($\delta^{18}O$-O_2) were measured to assess the origin of O_2 [*Holtgrieve et al.*, 2010]. Samples were analyzed within three months using a Finnigan Delta XL continuous-flow mass spectrometer (Thermo Electron Corp), with an analytical error (± 1SD) of ± 0.2‰. Masses 32, 34, and 40 (^{16}O:^{16}O, ^{18}O:^{16}O, and ^{40}Ar) were simultaneously measured [*Barth et al*., 2004; *Holtgrieve et al*., 2010]. Water isotopes ($\delta^{18}O$-

H_2O), which came from a separate sample of river water, were analyzed on a Micromass Isoprime mass spectrometer. Results are given relative to Standard Mean Ocean Water (SMOW) in delta notation with units of per mil. $[O_2]$ was calculated using the ratio of O_2 to argon (Ar) and [Ar] as a function of water temperature [*Weiss*, 1970].

Gas evasion

For most sites studied in 2005, CO_2 outgassing was simultaneously determined using a floating chamber equipped with a fan. These rates are reported in *Alin et al*. [2010]. We used their published rates to determine the ability of respiration to support the outgassing flux. . However, corresponding chamber measurements were not available for several sites, so the evasion flux for these medium to large rivers (streams were excluded) were calculated as follows:

$$F = kCO_2\gamma(P_{CO_2}^{atm} - P_{CO_2}^{s}) \quad (2)$$

Where F is the outgassing of CO_2 in μmol m^{-2} s^{-1}, k_{CO2} is the temperature-dependent gas exchange coefficient for CO_2 (m day^{-1}), γ is CO_2 solubility (μmol m^{-3} μPa^{-1}) [*Weiss*, 1974], $P_{CO_2}^{atm}$ and $P_{CO_2}^{s}$ are the partial pressures of CO_2 in the atmosphere and solution, respectively. k_{CO2} was determined as a function of wind speed [*Alin et al*., 2010]. A value of k_{600}, the gas transfer velocity for freshwater at 20˚C, was selected for each wind speed based on the relationship between k_{600} and u_{10} values presented in *Alin et al.* [2010]. Monte Carlo error propagation techniques were used to determine the error of our calculated gas evasion flux.

Isotopic composition of CO_2

To analyze the $\delta^{13}C$ of CO_{2resp}, bottle incubations were conducted in which [DIC] and the $\delta^{13}C$ of DIC were measured initially and at the end of the incubation period [*Quay et al*., 1992]. 250 mL glass bottles were incubated in the dark for 3-6 days at ambient temperatures. The initial

bottle was immediately poisoned in the field with 100 μL of $HgCl_2$, whereas the final bottle was poisoned at the end of the incubation period. The $\delta^{13}C$ of CO_{2resp} was calculated using an isotope ratio mass balance.

Statistical analysis

Shapiro-Wilk's Test for normality was used to assess whether variables came from a normally distributed population prior to statistical analyses. Normality was rejected when $p < 0.01$. The following variables failed this criterion and were then log-transformed: [CSS], [DIC], [CPOC], [DOC], [SO_4], conductivity, and the $\delta^{13}C$ of CSS. Upon transformation, variables were normally distributed except for the $\delta^{13}C$ of CSS, which was then excluded from statistical analysis. Pearson correlation was performed between all variables. The site 'Campina' was also excluded because of problems with the Winkler method possibly due to the high [DOC] (31 mg L^{-1}) or nitrite or iron species interference [*Wetzel and Likens*, 1991].

Standard linear regression and step-wise backward multiple linear regression (MLR) were used to explore the relationship between environmental parameters and respiration rates. To be considered an input for the MLR, independent variables had to meet the following criteria: they must be significantly correlated with respiration rates; to avoid multicollinearity, they must not be highly correlated with each other (i.e., $r>0.7$) [*Tabachnick and Fidell*, 2001]; and there must be no more than 1 missing datum for each variable. A maximum of three independent variables at a time were considered. All statistical analyses were performed in SPSS.

RESULTS

Variation in P_{CO_2}, outgassing rates, and respiration rates

The P_{CO_2} of rivers and streams ranged from 2 to 30 times that of atmospheric equilibrium, consistent with previous work in the basin [*Mayorga et al.*, 2004, 2005*a*]. Minimum and

maximum values were found in the Acre River (87.5 Pa) and the stream, Campina (1308 Pa) (Table 2.2). Gas evasion fluxes also varied widely, with a minimum of 1.0 and a maximum of 12.7 ± 0.8 μmol C m^{-2} s^{-1} at the Purus and Negro rivers, respectively (Table 2.3).

The variability of water-column respiration rates measured in this study spanned several orders of magnitude (Fig. 2.2). The lowest rate (0.03 μmol O_2 L^{-1} h^{-1}) was observed in Barro Branco, whereas the highest rate (1.78 μmol O_2 L^{-1} h^{-1}) was measured in the Acre River. Despite the drought of 2005, there was no significant difference in respiration rates between 2005 and 2006 for rivers studied during both years (*t*-test, t = -0.129, df = 18, p = 0.898). Depth-integrated respiration rates ranged from 0.014 ± 0.007 μmol CO_2 m^{-2} s^{-1} in Barro Branco to 4.1 ± 0.8 μmol CO_2 m^{-2} s^{-1} in the Amazon River (Table 2.3). The CO_2 outgassing fluxes were consistently higher than the depth-integrated respiration rates. Accordingly, water-column respiration accounted for between 0.11 ± 0.05% to 100 ± 20% of the gas evasion flux.

Variation in $\delta^{18}O$ of O_2 and dissolved oxygen concentrations

The $\delta^{18}O$ of O_2 is affected by gas exchange, photosynthesis, and respiration. Therefore, measurements of $\delta^{18}O$ of O_2 can provide information about the relative importance of these processes between sites. If gas exchange dominates, $\delta^{18}O$-O_2 values are near 24.2‰ due to an atmospheric value of 23.5‰ and a 0.7‰ equilibrium fractionation factor during gas dissolution [*Benson and Krause*, 1984]. Respiration preferentially uptakes $^{16:16}O$ at a greater rate than $^{18:16}O$, causing an enrichment of the remaining dissolved oxygen pool by 18‰ [*Quay et al.*, 1995]. Because there is no isotopic fractionation during photosynthesis, this process produces O_2 with the $\delta^{18}O$ of the water, which ranged from -3.3 to -6.2‰ in this study. Thus, $\delta^{18}O$-O_2 values > 24.2‰ with undersaturated O_2 levels indicate that respiration exceeds photosynthesis, whereas values < 24.2‰ with supersaturation suggest that photosynthesis dominates [*Quay et al.*, 1995].

$\delta^{18}O\text{-}O_2$ values equal 24.2‰ and dissolved oxygen levels are close to saturation when gas exchange dominates.

Minimum and maximum values of $\delta^{18}O\text{-}O_2$ were in the Envira (20.8‰) and Solimões (27.6‰) rivers. O_2 concentrations ranged from a minimum of 93.8 μmol L^{-1} in the Negro River to a maximum of 247.9 μmol L^{-1} in the Envira River (Table 2.2). The fraction of dissolved O_2 saturation was negatively correlated with $\delta^{18}O\text{-}O_2$ (r = -0.916, n = 19, $p < 0.0005$) (Fig. 2.3); sites with $\delta^{18}O\text{-}O_2 > 24.2‰$ had significantly lower O_2 saturation levels (0.7 ± 0.1) than sites with $\delta^{18}O\text{-}O_2 < 24.2‰$ (where the fraction of dissolved O_2 saturation was 0.97 ± 0.04) (t-test, t = -6.052, df = 12.082, $p < 0.0005$). The latter sites consisted of medium-sized rivers in Acre that were in the low-water stage of the hydrograph (with an average depth of 1.3 m). In contrast, sites with $\delta^{18}O\text{-}O_2 > 24.2‰$ consisted of small, unshaded streams and major tributaries. The average respiration rate of sites with $\delta^{18}O\text{-}O_2$ values < 24.2‰ was over four times higher than sites with $\delta^{18}O\text{-}O_2$ values >24.2‰ (1.35 ± 0.22 vs. 0.30 ± 0.29 μmol L^{-1} h^{-1}).

Variations in the concentration and organic composition of the physical size classes of organic carbon

Concentrations of CPOC averaged 0.06 ± 0.08 mg L^{-1}, but ranged from 0 to 1.30 mg L^{-1} (Table 2.4). FPOC contained slightly more carbon (average: 1.15 ± 0.70 mg L^{-1}), and concentrations ranged from 0.07 to 2.40 mg L^{-1}. DOC ranged from 1.5 (Catuaba) to 31.3 mg L^{-1} (Campina), and averaged 3.8 ± 1.8 mg L^{-1}. Between 21% to 90% of the DOC was < 5 kDa (LMW DOC). Generally, the distribution of carbon within the size fractions varied widely (between 10-67% for the 5-100 kDa size fraction and between 0.2-55% for the > 100 kDa fraction.

The $\delta^{13}C$ and the C:N ratio of OM was measured to partition POM samples among end-member sources (i.e., C_3 plants, C_4 plants, and phytoplankton) (Fig. 2.4). The $\delta^{13}C$ of CPOC ranged from -35.8‰ to -27.9‰. There was a significant difference between the $\delta^{13}C$ of FPOC at sites with $\delta^{18}O$-O_2 values < 24.2‰ as compared to sites with $\delta^{18}O$-O_2 values > 24.2‰ ($\delta^{13}C$ =-33 ± 2‰ and -28.8 ± 0.9‰, respectively) (*t*-test, $t = 5.722$, df = 18, $p = 0.0005$). The $\delta^{13}C$ of DOC for the 2006 sites ranged from -27.2‰ to -29.9‰. The C:N of CPOC ranged from 5.8 (Purus) to 29.6 (Campina), whereas the C:N of FPOC was generally lower, and ranged from 6.0 to 23.6 (Fig. 2.4). The C:N of FPOC was significantly lower at sites with $\delta^{18}O$-O_2 values < 24.2‰ as compared to sites with $\delta^{18}O$-O_2 > 24.2‰ (7.7 ± 1.0 vs. 10.7 ± 2.2, respectively) (*t*-test: $t = 3.662$, df=17, $p = 0.002$).

The $\delta^{13}C$ of CO_{2resp} was determined in the medium to large rivers studied during 2006 to further identify the end-member sources fueling respiration. Values ranged from -30‰ to -33‰ (Fig. 2.5), with the most enriched values found on the Negro River, and the most-depleted values found on the Acre River. Values ranged between -28.3‰ to -28.7‰ in the small streams (data not shown).

Relationships between respiration rates and environmental variables

A backward selection MLR approach was used to develop a model for the dependence of respiration rates on in situ levels of environmental parameters. Out of all variables studied, the combination of [FPOC], the C:N ratio of FPOC, and O_2 concentrations explained the highest amount of the variation in respiration rates (adjusted $r^2 = 0.80$) (Table 2.5). When standard linear regression was used for variables measured during both years, [FPOC] alone explained the most variation (Fig. 2.6a), followed by the C:N of FPOC (Fig. 2.6b), and then pH ($r^2 = 0.70$, 0.61, and 0.58, respectively). [O_2] and bacterial abundance were both also positively correlated with

respiration (r^2 = 0.35 for [O_2] and r^2 = 0.78 for bacterial abundance) (Fig. 2.6c and 2.6d, respectively). Respiration rates were not correlated with the concentration of CPOC, DOC, or any of the size fractions within DOC.

pH was not included in the MLR as it was highly correlated with FPOC (r = 0.818, n = 19, $p < 0.0005$); the relationship between pH and respiration was not significant once the influence of FPOC on these variables was accounted for (r = 0.257, n = 16, p = 0.304). However, pH may be driving the positive correlation between respiration and the percentage of DOC < 5 kDa (r = 0.536, n = 16, p = 0.032): the latter was more strongly correlated with pH (r = 0.757, n = 16 p = 0.001) than respiration. Accordingly, the correlation between the percentage of DOC < 5 kDa and respiration was not significant once the variability in pH was controlled for (r = -0.101, n =13, p = 0.720).

Differences between the sites, such as seasonality or drainage basin size, affected respiration rates. Rivers in the falling-water stage of the hydrograph had significantly lower respiration rates (0.17 ± 0.11 μmol L^{-1} h^{-1}) than rivers in the low-water stage (1.09 ± 0.46 μmol L^{-1} h^{-1}) (t-test = 6.559, df = 12.818, $p < 0.0005$). Because the watershed area of the sites varied considerably, the effects of drainage basin size on respiration rates was assessed. The mean respiration rate of medium-sized rivers (1.35 ± 0.22 μmol L^{-1} h^{-1}) was significantly different than that of small (0.41 ± 0.38) or large rivers (0.20 ± 0.11) ($F_{2,17}$ = 40.7, $p < 0.005$).

DISCUSSION

This study highlights the variability of water-column respiration rates found across rivers of the central and southwestern Amazon basin: these rates vary by three orders of magnitude, from 0.03-1.78 μmol O_2 L^{-1} h^{-1}, consistent with previous studies [*Richey et al*., 1990; *Benner et*

al., 1995; *Devol et al.*, 1995]. The large variability calls into question the environmental controls that affect respiration rates.

As discussed below, our results indicate that together [FPOC], C:N ratios of FPOC, and [O_2] explain 80% of the variability of water-column respiration rates. Oxygen isotopes indicate that the highest respiration rates were found in rivers with evidence for photosynthetic production. Considering that these rivers also have the highest FPOC concentrations, we argue below that the strong correlation between respiration and the aforementioned parameters is because each of these parameters is reflective of photosynthetic activity. Thus, rather than identifying a particular size fraction that is predictive of respiration rates, we conclude that respiration rates are controlled by the interplay of biogeochemical processes occurring within the water column. This study demonstrates that FPOC derived from autochthonous origins is associated with high respiration rates, indicating that phytoplankton and/or periphyton production can significantly influence river metabolism even in rivers carrying high sediment loads. This is in contrast with previous work, which has assumed that high sediment loads inhibit in situ production [*Wissmar et al*., 1981]. This research further demonstrates that multiple sources (C_3 plants, C_4 grasses, and phytoplankton) serve as the substrate for respiration basin-wide, suggesting that the type of carbon preferentially consumed during respiration is affected by hydrograph stage and/or floodplain connectivity.

Relationships between organic carbon size fractions and respiration rates

A long-standing hypothesis for the Amazon mainstem is that a small, rapidly-cycling pool of labile OC fuels respiration [*Richey et al*., 1990]. This labile pool likely coexists within the larger pool of refractory materials that comprise the bulk size fractions of CPOC, FPOC and DOC [*Richey et al.*, 1990; *Amon and Benner*, 1996, *Mayorga et al*., 2005*a*]. Recently,

measurements of the $\Delta^{14}C$ and $\delta^{13}C$ of the bulk size fractions and CO_2 gas in equilibrium with DIC suggests that the CO_2 produced through respiration is younger and disproportionately composed of C_4 grasses relative to the bulk size fractions [*Mayorga et al*., 2005*a*], providing evidence that an isotopically-distinct pool of OC (relative to the bulk size fractions) may support river metabolism. Accordingly, a major objective of this study was to assess the relationship between bulk OC size fractions, and size fractions within the DOC pool, with respiration rates.

FPOC was the only bulk size fraction that was significantly correlated with respiration. Further, out of all parameters studied during both years, it explained the highest amount of the variability in respiration rates (Fig. 2.6a, Table 2.5), suggesting that it may contain a labile pool of OM. Previous work has shown that although the majority of the FSS carried by Amazonian lowland rivers originates in the Andes, the $\delta^{13}C$ of FPOC of these rivers reflects organic matter derived from the lowlands. This indicates near-complete remineralization of Andean-derived FPOC [*Mayorga et al.*, 2005a], suggesting it is a labile size fraction. Furthermore, the $\delta^{13}C$ of FPOC carried by the Solimões and Amazon rivers mirrors the high-altitude enrichment of terrestrial plants expected of 1‰ for every 1,000 m change in elevation [*Hedges et al.*, 2000; *Mayorga et al*., 2005*a*].

Although FPOC may be an inherently labile size fraction, the positive correlation between respiration rates and FPOC observed in this study is primarily due to the influence of phytoplankton production at sites with high FPOC concentrations. The average respiration rate at sites with $\delta^{18}O\text{-}O_2$ values < 24.2‰ was over four-fold greater than that observed at sites with $\delta^{18}O\text{-}O_2$ values >24.2‰. At the former sites, FPOC concentrations were over twice that at sites with $\delta^{18}O\text{-}O_2 > 24.2‰$, demonstrating that photosynthetic production of dissolved oxygen was occurring at sites with high suspended loads. This is not unexpected as these rivers with high

sediment concentrations were sampled during the low-water stage, and consequently they were shallow, unshaded, and visually tinted green. They inherently had high suspended loads due to the high-relief nature of their drainage basins, but the particulate carbon concentrations were likely enhanced by autochthonous production. In contrast, sites with $\delta^{18}O\text{-}O_2 > 24.2‰$ consisted of small, shaded streams throughout the study area, and major tributaries (the average depth was 34 m) with deep and highly turbid water-columns.

Primary production can directly stimulate water-column respiration rates through multiple pathways. First, previous work within the basin suggests that the lack of a bioavailable substrate limits bacterial growth and respiration in large whitewater rivers of the Amazon [*Benner et al*., 1995]. Autochthonous production produces labile carbon [*Sun et al*., 1997; *del Giorgio and Pace*, 2008], and in Amazonian-floodplain lakes, respiration is positively correlated with chlorophyll *a* concentrations and phytoplankton cell carbon [*Wissmar et al*., 1981]. Therefore, one direct pathway by which increased photosynthetic activity can lead to elevated respiration rates is via providing a labile substrate for heterotrophs, thereby increasing heterotrophic respiration rates. Our bacterial abundance measurements support this notion, as the highest abundances were found at sites with $\delta^{18}O\text{-}O_2 < 24.2‰$, and abundances ware positively correlated with respiration rates (Fig. 2.6d). However, primary production may elevate water-column respiration due to autotrophic respiration. This is unlikely to be significant at sites with $\delta^{18}O\text{-}O_2 > 24.2‰$, which have the lowest respiration rates observed in our study, but it may be a significant factor at sites with $\delta^{18}O\text{-}O_2 < 24.2‰$. Regardless of the direct mechanism by which respiration is stimulated, these results indicate that the low-water stage of the hydrograph is an important time of carbon processing.

The composition of POM provides further support that autochthonous production is occurring at sites with $\delta^{18}O\text{-}O_2 < 24.2‰$. Plotting $\delta^{13}C$ values against C:N ratios demonstrates that the FPOC of these sites lie within the range expected for carbon influenced by phytoplankton end-members (Fig. 2.4), whereas FPOC from sites with $\delta^{18}O\text{-}O_2 > 24.2‰$ (i.e., shaded streams and large tributaries) is likely derived from forest soils. In contrast, CPOC appears to be primarily sourced from forest soils and C_3 vegetation in both areas, indicating that autochthonous production is predominantly found in the fine fraction. This is consistent with previous work in the Amazon Basin, where phytoplankton has previously been shown to significantly contribute to POM composition in the Andean headwaters of the Amazon during the dry season [*Townsend-Small et al*., 2007].

Accordingly, the results from the MLR demonstrate that respiration is well predicted by a model that includes FPOC, $C:N_{FPOC}$, and O_2 (r^2=0.80) (Table 2.5, Fig. 2.6) because each of these parameters reflect photosynthetic production. The significant inverse relationship between the $C:N_{FPOC}$ and respiration demonstrates that as FPOC becomes more similar to phytoplankton end-members, respiration rates increase (Fig. 2.6b). Similarly, the inclusion of O_2 in the MLR is likely because it reflects the importance of oxygen produced from photosynthesis. Thus, we conclude that FPOC is associated with high respiration rates when it can be demonstrated to have characteristics of autochthonous production.

Conversely, any relationship between in situ concentrations of DOC size classes and respiration rates is less clear. It has been speculated that a labile pool of carbon may exist within the dissolved pool that partially fuels respiration [*Mayorga and Aufdenkampe*, 2002]. For example, previous work on the Solimões and Negro rivers have demonstrated higher rates of bacterial growth and respiration during incubations amended with high molecular weight DOC

(i.e., DOC > 1 kDa) as compared to incubations with DOC < 1 kDa [*Amon and Benner*, 1996]. Thus, DOC > 1 kDa is hypothesized to be of more recent origin (and more bioavailable) than DOC < 1 kDa [*Amon and Benner*, 1996]. As a test of this conceptual model, we examined the relationship between respiration rates and the in situ concentrations of size fractions of DOC.

We found no relationship between respiration and [DOC] or the concentration of any of the size fractions of DOC. There are several mechanisms that could account for the lack of a significant correlation. First, the influence of pH, which ranged from 4.0 to 8.6 at our sites, may obscure any relationship between DOC size classes and respiration rates. pH has been shown to affect the molecular weight distribution, size, and shape of fulvic acids leached from soils due to influences caused by changes in hydrogen bonding and van der Waal's forces [*Schnitzer*, 1978; *De Haan et al.*, 1983]. Therefore, the positive correlation between the percentage of the total DOC pool that was less than 5 kDa in size and pH could potentially be explained by those factors. Although respiration rates were positively correlated with the percentage of DOC < 5 kDa, the positive correlation between the percentage of DOC < 5 kDa and pH was stronger. Accordingly, after controlling for pH via partial correlation analyses, the relationship between respiration and the percentage of DOC < 5 kDa was no longer significant (*Results*).

The lack of correlation between respiration and DOC concentrations (both bulk and size fractions) suggest that other variables, such as in situ primary production, play a larger role in influencing respiration rates than the in situ concentrations of the DOC size classes examined in this study. The occurrence of autochthonous respiration at sites with $\delta^{18}O\text{-}O_2 < 24.2‰$ could obfuscate any correlations. Such respiration would obscure relationships between dissolved size fractions and respiration as autochthonous respiration is not dependent upon these size fractions. Accordingly, the discrepancy between our results and that of *Amon and Benner* [1996] likely

reflects differences in methodology (i.e., comparisons of relationships between respiration rates and in situ concentrations verses manipulated bottle incubations) and/or the effects of other variables in controlling the molecular weight distribution of DOC.

Potential biological sources of CO_2 produced from respiration

In contrast to previous work that has suggested that C_4 grasses are preferentially consumed during respiration [*Mayorga et al*., 2005a], our results demonstrate that a variety of sources are consumed across the basin. We measured the $\delta^{13}C$ of CO_2 produced during dark-bottle incubations at select sites to further our understanding of the origin of CO_2 produced from respiration. The $\delta^{13}C$ of CO_{2resp} was -33.2 ± 0.6‰ and -31 ± 2‰ (Fig. 2.5) at sites where $\delta^{18}O\text{-}O_2$ < 24.2‰. If this CO_2 was produced entirely from the consumption of phytoplankton, the (calculated) $\delta^{13}C$ of CO_{2resp} would be expected to range between -32‰ to -37‰ at these sites. Conversely, if the CO_2 was produced entirely from C_3 or C_4 substrates, the $\delta^{13}C$ of CO_{2resp} would be expected to range between -26‰ to -31.3‰, and between -12‰ to -16‰, respectively [*Hedges et al*., 1986; *Bernardes et al*., 2004; *Mayorga et al*., 2005*a*]. Therefore, the similarity of the $\delta^{13}C$ of CO_{2resp} to that of these potential end-members suggests that the $\delta^{13}C$ of CO_{2resp} produced during bottle incubations is derived from the consumption of both phytoplankton and/or periphyton and C_3 plants at sites with $\delta^{18}O\text{-}O_2$ < 24.2‰.

In contrast, at most sites where $\delta^{18}O\text{-}O_2$ > 24.2‰, the $\delta^{13}C$ of CO_{2resp} appears to be coming from C_3 sources (Fig. 2.5). For example, in the streams (Catuaba and Humaita), the $\delta^{13}C$ of CO_{2resp} ranged from -28.3‰ to -28.7‰ (data not shown), whereas it was -30‰ on a major tributary (the Negro). These values are substantially more enriched than our estimates of phytoplankton in these rivers (-37‰ to -45‰).

Perhaps the most surprising result is that that the $\delta^{13}C$ of CO_{2resp} from the Solimões River was -33 ± 3‰. The $\delta^{13}C$ of phytoplankton should range from -35‰ to -40‰, suggesting that the $\delta^{13}C$ of CO_{2resp} is derived from C_3-plants and phytoplankton in August. The Solimões shows little evidence of autochthonous production based on $\delta^{18}O$-O_2 and the composition of organic matter (Figs. 3 and 4). However, algal material could be produced in nearby floodplain lakes [*Wissmar et al*., 1981]. During this time period (the early stages of falling water), these lakes drain into the river channel, possibly transporting labile carbon that could stimulate riverine metabolism. As previous work has suggested that a rapidly cycling pool of labile carbon is needed to support water-column respiration along the mainstem [*Richey et al*., 1990; *Mayorga et al.*, 2005*a*], we suggest that phytoplankton-derived OM may provide this substrate during certain times of the year.

The $\delta^{13}C$ of CO_{2resp} reported here for the Solimões River differs significantly from the one measurement that has been reported previously (-22‰). It was taken during the early-rising water stage, and implied that 40% of the water-column respiration on the Solimões River was supported by floodplain grasses [*Quay et al*., 1992]. Given the discrepancy between these results, we measured the $\delta^{13}C$ of CO_{2resp} on the Solimões at the same location during the rising-water stage (April 2007). It was -23 ± 3‰ (data not shown), consistent with the results of *Quay et al.* [1992]. Accordingly, the CO_2 produced through respiration appears to be highly dynamic given that its isotopic signature may vary by as much as 10‰ depending upon the time of the year that sampling occurs. The variability may be explained by differences in the production of C_4 grasses on the floodplain. For example, the biomass of grasses in an Amazonian floodplain lake in April was demonstrated to be over twice that in August, with a higher monthly biomass loss to the mainstem occurring in April relative to August [*Engle et al*., 2008].

In conclusion, our bottle incubation results suggest that phytoplankton and C_3 plants are important substrates for respiration at sites where $\delta^{18}O\text{-}O_2 < 24.2‰$. In contrast, at sites with $\delta^{18}O\text{-}O_2 > 24.2‰$, C_3 plants typically play a larger role fueling respiration rates than phytoplankton, and respiration rates are reduced. However, all of these end-members (C_3 and C_4 plants, and phytoplankton and/or periphyton) are important substrates for respiration throughout the basin, and their role in supporting respiration likely reflects temporal variability caused by changes in hydrograph stage.

Comparisons between the $\delta^{13}C$ of respiration-derived CO_2 and organic carbon size fractions

Several studies have suggested that $\delta^{13}C$ of CO_2 produced through respiration is isotopically enriched relative to the bulk size fractions carried by rivers in the Amazon Basin [*Quay et al*., 1992; *Mayorga et al*., 2005*a*], suggesting that the C_4 grasses lining river corridors are inherently more biodegradable than the bulk organic matter transported by the Amazon River, which resembles C_3 plants. To assess whether this finding holds under the continuum of rivers examined in this study, we compared the $\delta^{13}C$ of CO_{2resp} to that of the bulk size fractions. We found that the error associated with the $\delta^{13}C$ of CO_{2resp} often overlaps with the isotopic signature of bulk organic matter (Fig. 2.5), suggesting that this material (which is isotopically consistent with C_3-plant origins) supports respiration in rivers ranging from major black-water and white-water tributaries (i.e., the Negro River and the Purus River, respectively) to small forested streams (Catuaba and Humaita: data not shown). However, isotopically depleted C is respired relative to the bulk size fractions found in the Acre and Solimões rivers, suggesting that phytoplankton may be preferentially consumed in certain rivers. Thus, the coupling between the bulk size fractions and respired carbon is also substantially more variable than suggested previously.

Role of water-column respiration in fueling CO2 outgassing

Finally, to what extent does water-column respiration support CO_2 gas evasion fluxes in Amazonian waters? The role of respiration is highly variable, with depth-integrated respiration rates accounting for between 0.1% to 100% of the outgassing flux during the low- and high-falling water seasons (Table 2.3). As water-column metabolism is typically less than 3.5% of the total ecosystem metabolism in streams draining the Hudson River watershed [*Bott et al.*, 2006], it may be expected that water-column respiration would compose a small percentage of the outgassing flux in small streams. Indeed, respiration fuels less than 6% of the outgassing flux for all streams in this study. In such streams, inputs of CO_2 from ground-water via soil and root respiration are likely significant contributors to the gas evasion flux, and work within the Amazon basin has demonstrated that 90% of CO_2 transported by groundwater is evaded in the headwater reaches of 1st and 2nd order Amazonian streams [*Johnson et al*., 2008]. Accordingly, as streams scale in size, the influence of respiration increases: it accounted for an average of 26 ± 27% of the outgassing flux in the medium-sized rivers.

The contribution of water-column respiration to gas evasion is also highly variable in large tributaries, and the extent that respiration fuels gas evasion appears to be influenced by water-chemistry type. For example, the aerial respiration flux accounts for between 8-18% of the outgassing flux during the falling-water stage on the Negro, suggesting that additional CO_2 production mechanisms may be important in black-water rivers, such as photo-oxidation [*Remington et al*., 2011]. In contrast, 62 ± 34% of outgassing CO_2 is accounted for by water-column respiration in large white-water rivers (Amazon, Madeira, and Solimões) (Table 2.3). We hypothesize this variability is due to changes in wind speed affecting gas evasion rates or due

to fluctuation of respiration rates. Our results suggest that *in situ* water-column respiration rates are capable of supporting the high outgassing rates in large white-water rivers.

Implications towards our understanding of carbon cycling in Amazonian rivers

A significant implication of this work is that the coupling between organic matter sources and respiration is highly variable. At any point in time, rivers within the Amazon basin vary dramatically in terms of their drainage basin size, chemical composition, and stage of the hydrograph. Therefore, it may be expected that respiration rates will vary significantly throughout the basin as light availability, floodplain connectivity, and land-water coupling dynamics differ across river types.

One of the primary objectives of this work was to assess the relationship between respiration rates and size fractions of organic carbon. Our results indicate that respiration is controlled by a variety of biogeochemical processes, rather than a single size fraction. We found that when FPOC is derived from algal sources, it is associated with high water-column respiration rates as both autotrophic respiration and heterotrophic respiration are stimulated (the latter being due to the production of a labile substrate).

Relative to regional carbon budgets, how consistent are the results here with the partitioning of basin outgassing into the potential sources terms estimated by *Richey et al.* [2002]? They viewed outgassing as direct carbon losses from upland forests and floating and emergent macrophytes. Based on calculations of floodplain production of macrophytes and the area of the floodplain in the central Amazon, they estimated that about 25% of the flux could be due to C_4 decomposition and respiration. The results here are consistent, in that a significant C_4 signal is detected. However, given that we have demonstrated that this signal is highly variable, this estimate likely needs revision. Furthermore, the presence of autochthonous production at

certain times of the year does not change our perspective of Amazonian rivers as processors of terrestrial carbon [*Quay et al*., 1992; *Richey et al*., 2002; *Mayorga et al*., 2005*a*]. As phytoplankton fix inorganic carbon generated via weathering and respiration, CO_2 produced from the consumption of phytoplankton (or from autotrophic respiration) should still be considered to be a carbon loss from upland ecosystems.

Future studies should strive to incorporate temporal and spatial variability in their sampling designs to further our understanding of the diverse array of processes that control carbon cycling in tropical rivers. Specifically, studies are needed to quantify the temporal and spatial variability of autochthonous production, including scaling work to evaluate its significance to the regional carbon budget. Previously, autochthonous production has been discounted as a significant source of OC in sediment-rich rivers of the Amazon Basin [*Wissmar et al.*, 1981]. Here we provide evidence that OC derived from autochthonous production occurs even in rivers with high sediment loads, suggesting that it could potentially be a source of rapidly-cycling labile carbon that stimulates respiration in other rivers throughout the basin.

Table 2.1. Site characteristics.

Name	Abbreviation	Date	Lat. (˚S)	Long. (˚W)	Watershed area (km^2)	Stage of hydrograph	Water type	Depth (m)
Campina	Cm	17 Aug 2006	2.589	60.033	< 10	falling	black	0.3
Barro Branco	BB	16 Jul 2005 29 Aug 2006	2.930	59.974	< 10	falling	clear	0.4
Negro	Ng	02 Aug 2005 11 Aug 2006	3.062	60.285	716,770	falling	black	34
Catuaba	Ct	30 Aug 2005 25 Sept 2006	10.073	67.614	< 10	Low	clear	0.5
Humaita	Hm	26 Aug 2005 15 Sep 2006	9.751	67.672	< 10	Low	white	0.3
Amazon	Am	19 Jul 2005	3.358	58.746	2,910,510	Falling	white	51
Solimões	So	02 Aug 2005 21 Aug 2006	3.285	60.041	2,241,320	falling	white	24
Madeira	Ma	19 Jul 2005	3.405	58.771	1,381,590	falling	white	25
Acre	Ac	02 Sep 2005 14 Sep 2006	10.011	67.843	20,750	Low	white	1.3
Moa	Mo	18 Aug 2005	7.652	72.700	8710	Low	white	0.6
Jurua	Jr	18 Aug 2005	7.682	72.660	34,450	Low	white	2.0
Tarauaca	Tr	20 Aug 2005	8.175	70.773	7607	Low	white	1.0
Envira	En	20 Aug 2005	8.170	70.391	12,570	Low	white	1.3
Purus	Pr	02 Sep 2005 22 Sep 2006	8.999	68.596	46,220	Low	white	1.5

Table 2.2. Measurements of aquatic chemical parameters.

Site	Year	Temperature (°C)	pH	P_{CO_2} (Pa)	DO (μmol L^{-1})	DIC (μmol L^{-1})	$\delta^{13}C$ DIC (‰)
Campina	2006	25.1	4.0	1308	102.6	344.7	-26.6
Barro Branco	2005	25.6	4.6	970	186.9	327.4	-22.4
Barro Branco	2006	25.8	4.7	731	196.1	279.9	-24.3
Negro	2005	29.2	5.1	659	101.3	208.5	-25.2
Negro	2006	29.1	4.8	491	93.8	222.8	-25.6
Catuaba	2005	23.5	6.2	201	207.7	121.0	-16.9
Catuaba	2006	24.0	5.1	163	217.9	108.5	-20.2
Humaita	2005	27.9	5.6	281	156.5	104.9	-17.1
Humaita	2006	25.4	6.3	251	168.9	310.1	-18.6
Amazon	2005	28.4	6.6	365	104.8	333.1	-17.0
Solimões	2005	28.5	6.7	627	105.9	676.5	-15.4
Solimões	2006	29.8	6.8	426	126.3	592.5	-16.5
Madeira	2005	29.7	6.9	293	200.8	450.4	-13.6
Acre	2005	30.5	7.3	119	201.5	415.1	-12.0
Acre	2006	28.8	7.3	88	213.3	910.0	-11.6
Moa	2005	28.4	7.5	148	221.7	747.4	-11.4
Jurua	2005	28.5	7.9	400	200.2	4895.7	-14.7
Tarauaca	2005	28.5	8.2	174	228.6	4852.3	-12.9
Envira	2005	28.4	8.4	195	247.9	8796.6	-12.8
Purus	2005	29.9	8.6	139	232.0	8263.8	-12.4
Purus	2006	32.0	8.3	103	225.9	4503.5	-11.6
Average		28.1	6.6	341	181.9	1856.0	-16.6
Standard deviation		2.2	1.3	244	49.6	2787.8	4.7

Table 2.3. Comparison between the depth-integrated respiration flux and the gas evasion flux.

Site	Year	Depth-integrated respiration flux (μmol CO_2 m^{-2} s^{-1})[a]	Gas evasion flux (μmol CO_2 m^{-2} s^{-1})[b]	Percentage of gas evasion accounted for by respiration (%)
Barro Branco	2005	0.014 ± 0.007	12.41	0.11 ± 0.05
Negro	2005	1.0 ± 0.4	12.7 ± 0.8[c]	8 ± 3
Negro	2006	0.8 ± 0.4	4.3 ± 0.5[c]	20 ± 10
Catuaba	2005	0.024 ± 0.008	2.87	0.8 ± 0.3
Humaita	2005	0.06 ± 0.03	1.13	6 ± 2
Amazon	2005	4.1 ± 0.8	4.2 ± 0.5[c]	100 ± 20
Solimões	2005	2.2 ± 0.4	7.7 ± 0.8[c]	29 ± 6
Solimões	2006	1.9 ± 0.2	2.2 ± 0.7[c]	90 ± 30
Madeira	2005	0.8 ± 0.3	2.09	36 ± 16
Acre	2005	0.5 ± 0.2	4.07	11 ± 4
Acre	2006	0.7 ± 0.3	1.2 ± 0.3[c]	56 ± 26
Moa	2005	0.21 ± 0.08	6.41	3 ± 1
Jurua	2005	0.8 ± 0.3	9.1	9 ± 3
Tarauaca	2005	0.3 ± 0.1	6.8	5 ± 2
Envira	2005	0.5 ± 0.2	6.75	7 ± 2
Purus	2005	0.5 ± 0.1	1.0	48 ± 12
Purus	2006	0.6 ± 0.1	0.8 ± 0.1[c]	70 ± 20
Average		0.9	5	29
Standard deviation		1	4	32

[a] The respiratory flux was calculated by converting measurements of oxygen consumption to CO_2 production by using a respiratory quotient of 1, as in previous work within the basin [*Devol et al.*, 1987; *Richey et al.*, 1988].
[b] The gas evasion flux is that which is reported by *Alin et al.* [2010] unless otherwise indicated.
[c] The gas evasion rate was calculated as described in this study.

Table 2.4. The concentration of organic carbon size fractions and total suspended solids. All units are in mg L^{-1}. TSS is total suspended solids and TOC represents total organic carbon. - indicates the size fraction could not be calculated due to methodological problems.

Site	Year	TSS	TOC	CPOC	FPOC	DOC	DOC > 100 kDa	DOC 5-100 kDa	DOC < 5 kDa
Campina	2006	4.0	32.8	1.30	0.18	31.3	3.6	21.1	6.6
Barro Branco	2005	0.5	3.4	0.17	0.08	3.2	-	-	2.2
Barro Branco	2006	0.3	2.4	0.03	0.07	2.2	0.1	1.3	0.9
Rio Negro	2005	0.4	9.6	0	0.56	9.0	2.9	3.0	3.1
Rio Negro	2006	6.6	7.6	0.06	0.35	7.2	1.3	4.1	1.9
Catuaba	2005	4.2	2.1	0.01	0.50	1.6	0.8	0.2	0.5
Catuaba	2006	9.3	2.6	0.03	1.05	1.5	0.8	0	0.7
Humaita	2005	4.6	4.2	0.05	0.48	3.7	1.1	-	-
Humaita	2006	13.7	4.0	0.24	1.03	2.8	1.0	0.3	1.4
Amazon	2005	133.7	6.7	0.22	1.63	4.8	0	1.7	3.3
Solimões	2005	74.8	5.6	0.06	1.07	4.4	1.3	0	3.3
Solimões	2006	102.1		0.17		3.6	0.3	1.3	2.1
Madeira	2005	45.4	4.3	0	0.80	3.5	-	-	3.0
Acre	2005	29.1	5.3	0	1.25	4.0	1.2	-	-
Acre	2006	87.2	5.5	0.01	2.40	3.1	0.4	0.4	2.3
Moa	2005	29.7	4.6	0.01	1.78	2.8	-	-	1.6
Jurua	2005	25.8	6.9	0.02	2.26	4.6	-	-	3.8
Tarauaca	2005	77.8	4.9	0.11	1.79	3.0	0	0.4	2.6
Envira	2005	22.8	5.2	0.01	1.61	3.6	0	0.3	3.2
Purus	2005	30.6	5.6	0.01	1.67	3.9	0.7	-	-
Purus	2006	47.9	4.2	0.01	1.49	2.7	-	-	-
Average		37.2	5.0	0.06	1.15	3.8	0.8	1.1	2.2
Standard deviation		38.7	1.9	0.08	0.70	1.8	0.8	1.3	1.0

Table 2.5. Statistical relationships between respiration rates and environmental variables.

Independent Variable	Model[a]	R^2	F	df	p
[FPOC], [O_2], C:N_{FPOC}	**Rsp = 0.43FPOC – 0.084C:N_{FPOC} + 0.003O_2 + 0.485**	**0.80**[b]	**25.1**	**(3,15)**	**<0.0005**
Bacterial Abundance[c]	Rsp = 2.94 x 10^{-7} BA – 0.22	0.78	17.7	(1,5)	0.008
FPOC	Rsp = 0.70FPOC – 0.084	0.70	39.1	(1,17)	<0.0005
C:N_{FPOC}	Rsp = -0.20C:N_{FPOC} – 2.6	0.61	26.6	(1,17)	<0.0005
pH	Rsp = 0.34pH – 1.52	0.58	25.3	(1,18)	<0.0005
$\delta^{13}C_{FPOC}$	Rsp = -0.15$\delta^{13}C_{FPOC}$ – 3.9	0.37	10.6	(1,18)	0.004
O_2	Rsp = 0.007O_2 – 0.55	0.35	9.7	(1,18)	0.006
$\%DOC_{< 5\ kDa}$	Rsp = 0.015$\%DOC_{<5k\ Da}$ – 0.32	0.29	5.7	(1,14)	0.032

[a]The model in bold is the best parameterized for this study. Stepwise backwards MLR was used to examine the influence of multiple variables on respiration rates (Rsp), whereas standard linear regression was used to assess the dependence of respiration on only one variable. BA is bacterial abundance, and $\%DOC_{<5\ kDa}$ is the percentage of the total DOC concentration < 5 kDa. All other variables are defined in the text.
[b]Refers to the adjusted R^2 as it was generated from a MLR. All others are standard coefficients of determination.
[c]Only contained data from 2006.

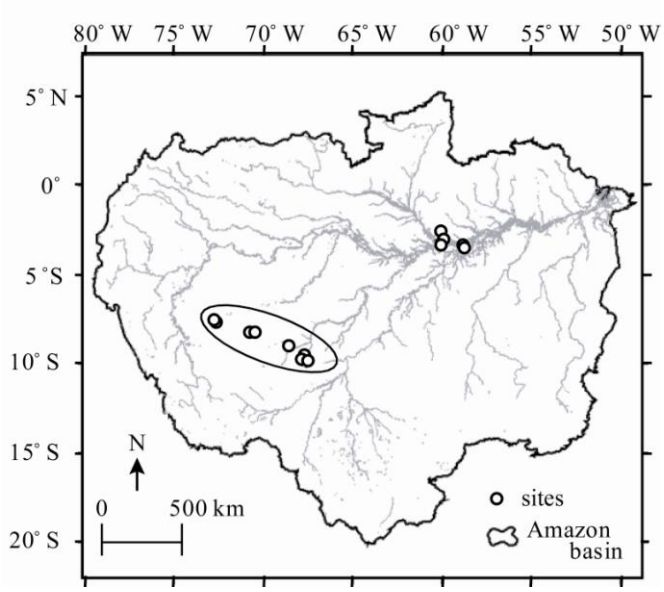

Figure 2.1. Map of study sites within the Amazon River basin. Major tributaries are in grey. The circled sites are located in the state of Acre, whereas the others are in the state of Amazônas.

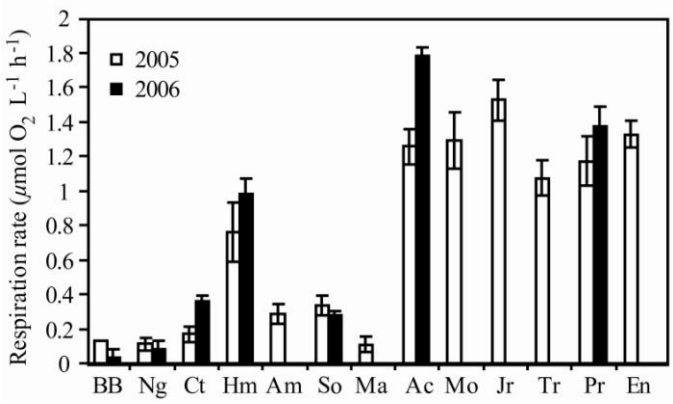

Figure 2.2. Respiration rates measured at various sites during 2005 and 2006. See Table 2.1 for the abbreviation of each site.

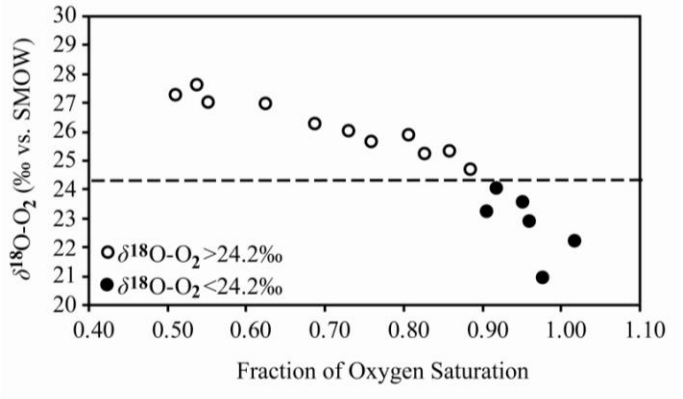

Figure 2.3. The relationship between δ^{18}O-O_2 and the fraction of dissolved O_2 saturation. The horizontal line at 24.2‰ represents the δ^{18}O value of dissolved oxygen in the water at atmospheric equilibrium. SMOW refers to the standard (standard mean ocean water).

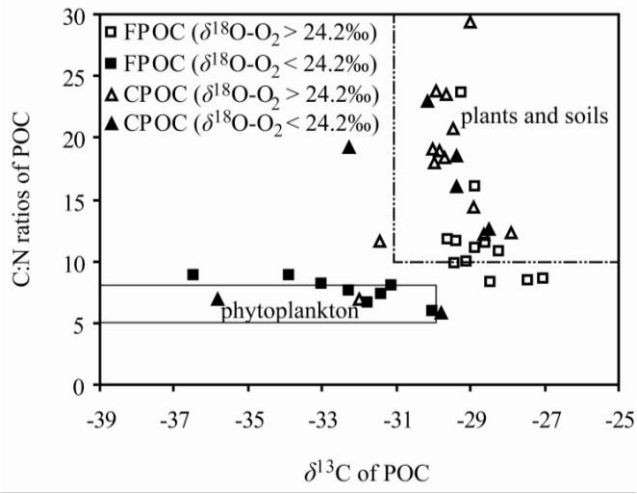

Figure 2.4. The relationship between the $\delta^{13}C$ and C:N ratios of POC in the Amazon Basin. C:N ratios of phytoplankton, soil, and leaves range between 5-8, 10-27, and 21-106, respectively [*Hedges et al.*,1986; *Trumbore*, 1993; *Devol and Hedges*, 2001]. The $\delta^{13}C$ of C_3 plants range from -26‰ to -31‰, whereas C_4 grasses found on floodplains and in pastures are more enriched (-12‰ to -16‰) [*Hedges et al*., 1986; *Bernardes et al.*, 2004; *Mayorga et al.*, 2005*a*]. The $\delta^{13}C$ of phytoplankton range from -30‰ to -45‰ in rivers and lakes *[Araujo-Lima et al., 1986; Hedges et al*., 1986; *Mayorga et al*., 2005*a*]. The $\delta^{13}C$ of soil generally spans the range of the vegetation types [*Bernardes et al*., 2004].

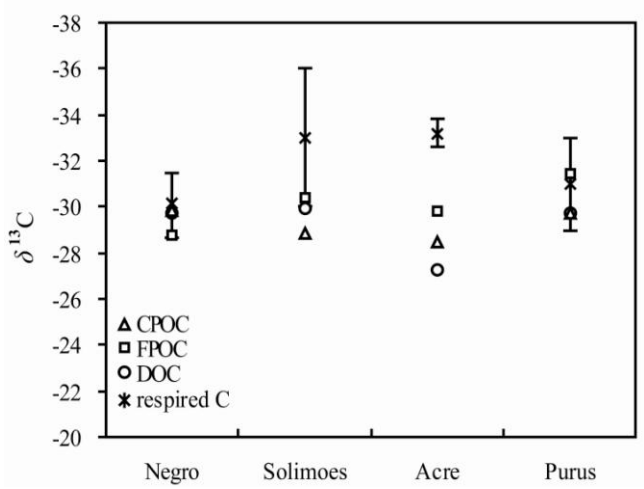

Figure 2.5. The $\delta^{13}C$ (‰) of bulk size fractions and respiration-derived CO_2 from sites studied in 2006.

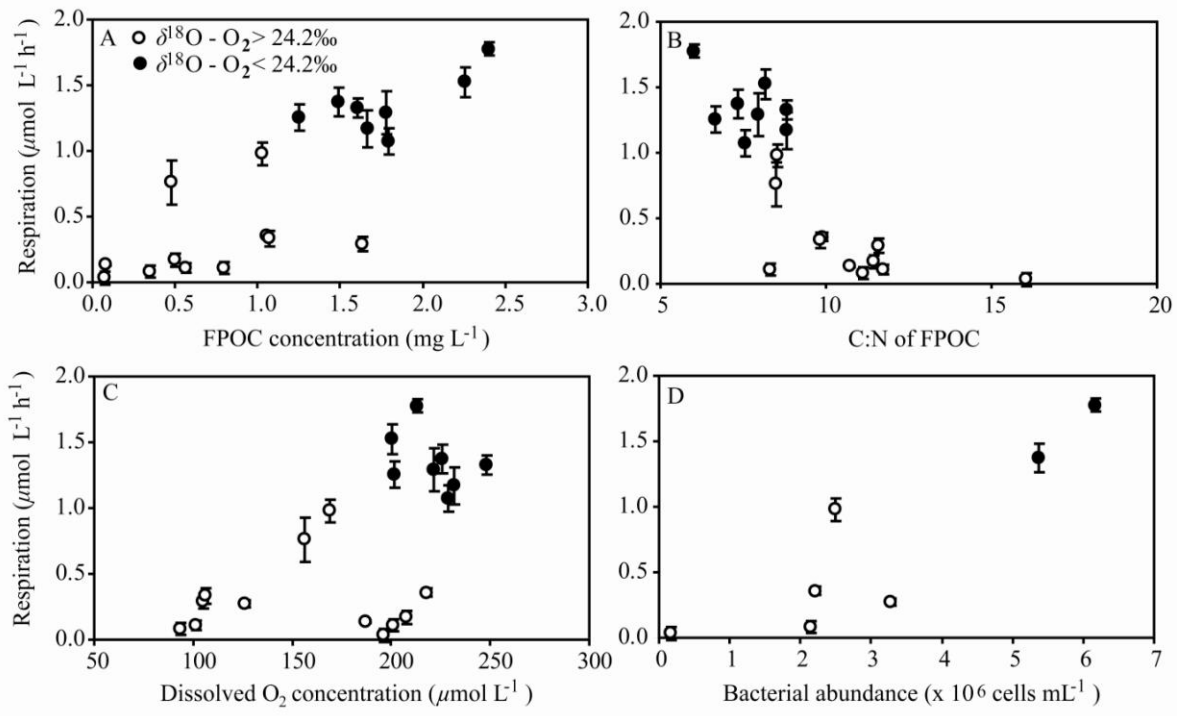

Figure 2.6. Correlations between respiration rates and some of the environmental variables analyzed in this study. Respiration rates (μmol O_2 L^{-1} h^{-1}) were significantly correlated with (A) FPOC concentration, (B) C:N ratios of FPOC, (C) dissolved O_2 concentration, and (D) bacterial abundance.

Chapter 3: Seasonal variability in the sources of particulate organic matter of the Mekong River as discerned by elemental and lignin analyses[2]

INTRODUCTION:

The role of rivers as transporters and processors of carbon (C) has recently been recognized to be a fundamental component of the global C cycle [*Cole et al.* 2007; *Tranvik et al.,* 2009; *Aufdenkampe et al.,* 2011]. Inland waters receive 2.7 Pg C/year [*Battin et al.,* 2009; *Tranvik et al.,* 2009], which is a flux nearly equal to the size of the terrestrial sink for anthropogenic C (2.8 Pg C/yr) [*Canadell et al.,* 2007; *Battin et al., 2009*]. Understanding the fate of C received by inland waters is of considerable interest, whether it is exported to the ocean, buried within the watershed, or lost to the atmosphere via gas evasion. The particulate organic carbon (POC) carried by rivers is an integral component of each of these fluxes. For example, POC comprises half of the organic carbon (OC) flux discharged by rivers to the ocean [*Degens et al.,* 1991; *Stallard et al.,* 1998]. Deciphering the composition of this material is critical to assessing how much of this material will be permanently buried in marine depositional settings upon reaching saline waters [*Hedges and Keil*, 1995], versus oxidized via respiration while in transit. Understanding particulate organic matter (POM) composition also aids in understanding carbon reallocation on land in response to anthropogenic change. For example, it has recently been suggested that in-land reservoirs exceed OC burial in the ocean by at least 1.5-fold [*Cole et al.,* 2007]. As impoundments trap sediment from the watershed, deciphering the composition of the POM associated with these sediments is key to understanding the reactivity, and ultimate fate of this material. Further, knowledge of compositional attributes may aid in

[2] Reproduced by permission of American Geophysical Union. Ellis, E. E., R. G. Keil, A. E. Ingalls, J. E. Richey, and S. R. Alin, Seasonal variability in the sources of particulate organic matter of the Mekong River as discerned by elemental and lignin analyses, J. Geophys. Res. Biogeosci., 117, G01038, doi:10.1029/2011JG001816, 2012. Copyright 2012 American Geophysical Union.

predicting the magnitude of C sequestration in terrestrial settings beyond the lifetime of impoundments (as dams themselves are short lived) [*Cole et al*., 2007; *Tranvik et al*., 2009].

Riverine POM may be derived from a variety of sources, including vascular plants, sedimentary rocks, and phytoplankton [*Hedges et al.*, 1986; *Devol and Hedges*, 2001; *Blair et al.*, 2004; *Coynel et al*. 2005]. The organic composition of each of these sources differ, and as does their lability. While in transit, the composition of these starting materials can be modified by numerous processes, including respiration, leaching, sorption, photoxidation, and lateral exchange with the floodplain [*Amon and Benner*, 1996; *Aufdenkampe et al.*, 2001; *Hernes et al.*, 2007; *Eckard et al.*, 2007; *Spencer et al., 2010; Galy et al.*, 2011]. The interplay of these processes can be seasonally and spatially dynamic, leading to substantial variation in the quantity and quality of the organic C exported, particularly in tropical rivers experiencing intense seasonality in precipitation [*Richey et al.*, 1990; *Paolini et al.*, 1995; *Coynel et al.*, 2005]. Such variability may then affect whether carbon is oxidized in transit or preserved in depositional environments. Despite the inherent importance of understanding seasonal variability in POM composition, time-series studies documenting changes in the organic matter source of POM are generally lacking. This issue is especially important in the tropics as 64% of the global riverine organic C flux, and 60% of the inland-water gas evasion flux occurs in this region [*Meybeck*, 1982; *Aufdenkampe et al.*, 2011]; yet, the tropics remain poorly studied.

Biomarkers, or compounds indicative of a unique biological source, can be powerful tools to trace the origin, transformation, and preservation of POM [*Goni and Hedges*, 1995; *Tareq et al*., 2004; *Rezende et al.*, 2010], especially in systems, such as rivers, with a vast heterogeneity of sources. In this study we use time series measurements of biomarker composition to enhance our understanding of these simple, yet, fundamental questions regarding

C cycling in fluvial systems: 1) what are the biological sources of POM carried by a large tropical river? and 2) how does the source and degradation-state of POM vary with the hydrological cycle? To answer these questions, we monitored monthly changes in the organic composition of suspended sediment carried by the Mekong River, a globally significant tropical river basin. Specifically, we measured nitrogen:carbon (N:C) ratios and stable isotopes ($\delta^{13}C$) of the fine suspended POM pool. At the molecular-level, we targeted the terrestrial component of fine POM (FPOM) by using lignin-derived phenols, which are biomarkers unique to vascular plants. In large tropical rivers, the carbon contained in fine suspended POM (or fine POC (FPOC)) represents 95% of total riverine particulate carbon [*Richey et al.*, 1990].

Higher-plant derived biomass is an important reservoir of fixed carbon, and lignin represents 40% of the biomass of vascular plants. Consequently, lignin-phenols have been used extensively to understand the fate of terrestrially-derived OM in fresh-water and marine settings [*Hedges et al.*, 1982; *Hedges et al.*, 1986; *Walsh et al.*, 2008; *Rezende et al.* 2010]. As a basis for determining the vascular-plant contribution to riverine FPOC, we analyzed the composition of the fresh-plant sources from which lignin originates: bark, leaf, and wood tissues from angiosperms found within the Mekong Basin. Considering that higher plants can be degraded to form soil-derived OM, and ultimately converted to carbon dioxide through respiration, comparing the lignin-phenol composition of riverine OM to the original vascular-plant signature provides information about the continental-level processing that occurs as this material travels from source to sink.

The Mekong ranks in the top ten rivers of the world in terms of average sediment load and mean water discharge [*Milliman and Svytski*, 1992; *Mekong River Commission*, 2005]. Although three dams currently exist on the mainstem, the flow regime continues to be dominated

by an annual monsoonal flood pulse [*Mekong River Commission*, 2005]. However, this may change in the near future. China is building a series of eight reservoirs along the mainstem in the Upper Basin, and in September 2010, the Lao People's Democratic Republic petitioned the Mekong River Commission to install eleven dams along the mainstem in the Lower Basin [*Grumbine and Xu*, 2011]. In addition to altering the OM flux and composition, these changes will likely impact the Tonle Sap Lake, which is one of the world's most productive freshwater fisheries, as the seasonal inputs of sediment and nutrients from the Mekong River have been suggested to be important to the fishery [*Mekong River Commission*, 2005; *Kummu et al.*, 2008]. Despite the potentially large downstream effects of changing the Mekong's sediment load, no study has examined the organic composition of material carried by the Mekong. Our dataset is the first attempt to characterize the flow of C through the Mekong prior to major alteration from the building of these dams. Further, an estimate of the flux of particulate organic carbon exported by the Mekong is currently absent from the literature. We consequently present a conservative estimate of the annual flux of suspended sediment, particulate organic carbon, and particulate lignin exported by the Mekong River for the 2006 hydrologic year.

METHODS:

Study area

The Mekong River originates in the mountains of the Tibetan Plateau at an elevation of 4,968 m, and flows through China, Myanmar, the Lao People's Democratic Republic, Thailand, Cambodia, and Viet Nam during a 4,800 km journey to the South China Sea (Fig. 3.1) [*Hori*, 2000]. The drainage basin (795,000 km^2) has been divided into two regions: the Upper and Lower Basin. In the Upper Basin, the river flows 2,200 km from the headwaters in Tibet to the Lower Basin boundary at the Chinese border. During this journey, it descends 4,000 m in an

incised channel, where it is primarily confined to narrow, deep gorges, with few opportunities for sediment deposition [*Mekong River Commission*, 2005; *Gupta et al.*, 2005]. Although its area is only 24% of the watershed, 50% of the sediment exported by the Mekong River comes from the Upper Basin [*Kummu and Varis*, 2007; *Walling*, 2005]. The Lower Basin consists of the portion of the watershed draining the countries downstream of China (the Lao People's Democratic Republic, Myanmar, Cambodia, Thailand, and Viet Nam). This 2,600 km stretch of the mainstem begins almost entirely mountainous, but then gradually enters a low-relief region, with the flow of the river slowing and the channel widening. Although there are few opportunities for sediment deposition, the main sediment sink on the mainstem of the Lower Basin is from Luang Prabang to Nong Khai [*Wang et al.*, 2011], possibly due to local geomorphology in which sediment is stored in the channel against cut banks [*Gupta et al.*, 2002]. It is not until Kratie, Cambodia, that an extensive floodplain develops. The first distributaries form at Phnom Penh, marking the beginning of the Mekong River delta [*Mekong River Commission*, 2005].

The basin is home to over 70 million people and has experienced extensive anthropogenic change. In both the Upper and Lower basins, forests have been replaced with agricultural lands and rice production is widespread [*Mekong River Commission*, 2005; *Costa-Cabral et al*., 2008]. Sixty-four dams are currently in operation within the basin. Most of these are small to medium-sized reservoirs found on tributaries of the Mekong River, although three are located on the mainstem in the Upper Basin [*Xue et al.*, 2011]. The impact of the latter impoundments on the sediment load of the river remains unclear due to the sporadic measurements of long-term suspended sediment concentrations prior to dam installation [*Wang et al*,. 2011; *Xue et al.*, 2011]. Regardless, the Mekong River is currently considered to be one of

the few large river basins that has not been irreversibly modified by dams [*Kummu and Sarkkula*, 2008].

The climate of the Lower Mekong basin has two monsoon seasons, with the southwest and northeast monsoons dominating during the rainy and dry seasons, respectively. Due to the arrival of the southwest monsoon in May, the Mekong rises from discharges less than 2,500 m^3/s during the low-water period (December through May) to peak flows exceeding 40,000 m^3/s during the rainy season [*Mekong River Commission*, 2005]. During this period, the highest precipitation occurs in the Lower Basin, specifically in south-western Cambodia and in the Eastern Highlands of Laos (where annual precipitation exeeds 2,500 mm), where rainfall peaks in August. Lowest-year round precipitation occurs in the Himalayan Highlands of the Upper Basin (500 mm), where precipitation falls largely as snow [*Costa-Cabral et al.*, 2008]. Runoff is dominated by snowmelt from China during the dry season. Much of the annual temporal variability in runoff results from these monsoonal precipitation patterns in addition to basin-wide topography. However, soil moisture levels can explain a significant proportion of the variability, which lags the precipitation peak [*Costa-Cabral et al.*, 2008]. As a result, the Upper Basin contributes to over 35% of the Mekong's total flow during the dry season, but only 18% over the entire year, indicating that runoff derived from the Upper Basin is disproportionately important during the dry season relative to the rainier periods [*Mekong River Commission,* 2005; *Kummu and Varris*, 2007]. During the latter time, inputs from tributaries from the Lower Basin dominate the hydrograph, with tributaries from Laos being particularly important [*Mekong River Commission,* 2005]. Part of the dry season flow, and the initial rise during the rainy season, is due to the delivery of snowmelt from the mountains [*Kummu and Varris*, 2007; *Wang et al.*, 2011].

In 2006 (the year of this study), the hydrograph was defined by an unusual second peak in discharge that occurred during the first week of October in response to the tropical storm Xangsane. This storm was widespread over the central and southern portion of the Mekong Basin, with some areas receiving as much as 400-500 mm of rain. Without this storm, the volume of water discharged during the flood season in the Lower Basin would have been among the lowest ever recorded over the past 80 years [*Mekong River Commission*, 2007].

Field measurements

Water samples were collected on the Mekong River just north of the confluence with the Tonle Sap River (11.595617 N 104.94299 E). This site was selected because it is not affected by seasonal changes in flow from the Tonle Sap Lake, and it is the most downstream point on the Mekong River that remains uninfluenced by tides and/or salinity [*Mekong River Commission*, 2005]. Samples were collected once to twice a month between 6 January 2006 to 1 November 2006. Water samples were collected at half of the total depth of the river using an in-line submersible pump. This depth was chosen as it has been previously demonstrated to yield a representative sample of the silt and clay-sized particles as compared to sediments obtained from a depth-integrated sampling scheme [*Moody and Meade*, 1994].

Coarse particulate organic carbon (CPOC) was first removed with a 63 μm sieve due to the observation that it comprises a small proportion of the total organic carbon pool of similar large tropical rivers [*Richey et al.*, 1990]. Sieved river water was homogenized with a churn splitter [*Wilde and Radtke*, 2003], then filtered onto a pre-weighed 0.45 μm cellulose acetate filter. The fine suspended sediment (FSS) concentration was determined by the mass difference of the dry filter weighed before and after FSS collection. A known quantity of sieved water was

also passed through a precombusted GF/F filter, which was later analyzed for N:C ratios, $\delta^{13}C$, and lignin-derived phenols. All filters were dried for 24 hours at 60°C.

A variety of plant end-member types from various aquatic and upland areas around Cambodia were collected, including the Tonle Sap Lake, the Mekong River, the Kulen Mountains (upland primary forest), and agricultural settings outside of the cities of Siem Reap and Phnom Penh, taking care to select vegetation that is representative of that which is growing in the basin. Vegetation was air-dried and coarsely ground prior to analysis. When necessary, bark was first removed from wood samples. Wood, bark, and leaves were analyzed for lignin-derived phenols from 17 angiosperm species.

Hydrograph measurements

We used the definitions applied by the Mekong River Commission to determine the onset of the different stages of the hydrograph [*Mekong River Commission*, 2007]. The rising water stage began when discharge rose to over twice that of the annual minimum. The flood season occurred when the daily discharge was greater than the mean annual discharge, and the falling water stage began when a consistent decrease in daily flow of 1% was observed daily for a two-week period. Discharge at Kratie, Cambodia was obtained from records provided by the Mekong River Commission.

Laboratory analyses

Carbonates were removed from FSS on GF/F filters by vapor-phase acidification prior to organic C analyses [*Komada et al.*, 2008]. Wetted filters were placed in a glass desiccator with 125 mL of 12 N HCl overnight. Acidified filters were then air-dried for 24 hours, and then dried at 60°C overnight. N:C ratios and $\delta^{13}C$ were measured using a PDZ Europa ANCA-GSL elemental analyzer interfaced to a PDZ Europa 20-20 isotope ratio mass spectrometer (IRMS) at

the Stable Isotope Facility at the University of California-Davis with a precision of 0.2‰. Samples were run with laboratory standards calibrated against NIST standard reference materials. $\delta^{13}C$ is expressed relative to PeeDee Belemnite. FPOC concentrations were obtained by multiplying weight % OC by the FSS concentration. The weight % OC and $\delta^{13}C$ of the vegetation end-members were analyzed at the University of Washington's IsoLab using a Thermo-Finigan MAT 253 IRMS coupled with a Costech ECS4010 elemental analyzer with a precision that ranged from 0.1 to 0.3‰.

To liberate lignin phenols from sample matrices, samples were subjected to microwave CuO oxidation [*Goni and Montgomery*, 2000]. Prior to microwaving, the sample (either the finely-ground plant or the GF/F filter containing the sediment) was placed in an acid-washed Teflon vessel with copper (II) oxide powder, ferrous ammonium sulfide, and 20 mL of 2 M NaOH. For each sample, the size was adjusted so that between 3-5 mg of OC was present in each vessel. Nitrogen-purged vessels were microwaved in a MARS 5 Accelerated Reaction System that was held at 144°C for ninety minutes at a pressure that ranged from 45-70 PSI. Once the reaction was complete, 50 µL of 1 mM recovery standards (ethyl vanillin and trans-cinnamic acid) were added. The sample was acidified to pH 1, and phenols were extracted using ethyl acetate. Water was removed using sodium sulfate, and the extract was dried under a gentle stream of N_2 gas at 45°C. The sample was then resuspended in pyridine, and lignin-derived phenols were derivitized with trimethylsilyl ethers and esters using BSTFA (N,O-bis(trimethylsilyl) trifluoroacetamide) and TCMS (trimethylchlorosilane). Phenols were quantified by gas chromatography using flame ionization detection (GC-FID). Blank GF/F filters were used to calculate blank-corrected lignin phenol concentrations. Filters were subject to a solvent extraction step prior to being microwaved so that the extracts could be used for

subsequent lipid analyses. Comparisons between extracted and non-extracted samples indicated that solvent extraction did not affect lignin recovery.

The effects of over-drying the ethyl acetate extracts on the recovery of phenols were assessed because this can lead to significant loss of adehyldes and ketones [*Keil and Neibauer*, 2009]. The recovery standard, ethyl vanillin, was subject to more loss than trans-cinnamic acid. The following phenols were corrected for loss during drying from post-microwave processing using ethyl vanillin: 4-hydroxybenzaldehyde, vanillin, and acetovanillin. All others were corrected with trans-cinnamic acid.

λ_8 is reported as the sum of the eight phenolic products within the individual vanillyl (V), syringyl (S), and cinnamyl (C) families, normalized by 100 mg of OC (i.e. mg V+S+C /100 mg OC) [*Hedges and Mann*, 1979]. Further, Σ_8 is the sum of these same 8 phenols normalized to 10 g of bulk sediment (i.e. mg V+S+ C/ 10 g sediment). We report C:V and S:V ratios (the ratio of the lignin-phenol derivatives in the cinnamyl and syringyl families to that of the vanillyl family) to differentiate samples among tissue types. We also express the ratio of the acidic functional group (ad) to the aldehyde (al) group within the vanillyl and syringyl families (denoted as (ad:al)v and (ad:al)s) as an indicator of degradation [*Hedges et al.*, 1982; *Ertel and Hedges*, 1984]. Finally, we calculated the Lignin Phenol Vegetation Index (LPVI) for both plant end-members and sediments to further identify the vegetation source of riverine POM [*Tareq et al.*, 2004]:

$$LPVI = [S(S+1)/(V+1) + 1]*[C(C+1)/(V+1) + 1] \quad (1)$$

where V, S, and C are expressed in % of the λ_8.

The total flux of FSS, FPOC, and particulate lignin exported by the Mekong River at Phnom Penh was calculated for the 2006 hydrologic year. The FSS flux was calculated by

linearly interpolating between the field measurements of FSS to produce daily values, which were then multiplied by daily discharge values, and then summed over one year. To obtain a FPOC flux, percent OC values were taken from field measurements, linearly interpolated between samples to a daily record, and then multiplied by the daily FSS flux, and summed accordingly. Finally, the particulate lignin flux was calculated from daily interpolations of the percent lignin from the FSS flux.

Statistical analyses

All statistical analyses were performed in version 15.0 of SPSS. Only comparisons between mean values of environmental parameters were made between the dry and rainy season, as only two samples were collected during the rising-water period. We used the Mann-Whitney U-test to determine significant differences in a variable between two groups, the Kruskal-Wallis test to determine differences among more than two groups. Further, Spearman's rank correlation procedure was used to determine associations between variables.

RESULTS:

Plant end-members in the Mekong Watershed

The % OC of plant end-members ranged from 34.7 to 50.7 across all vegetation types, but was similar within vegetation types (Table 3.1). On average, angiosperm barks had the highest % OC values (45.7 ± 4.1%) and grasses had the lowest values (38.2 ± 4.6%). $\delta^{13}C$ values ranged from -11.9‰ to -34.5‰; grasses were the most enriched (averaging -23.0 ± 9.7‰) and angiosperm barks were the most depleted (averaging -31.8 ±1.6‰).

Angiosperm woods could be statistically differentiated from other angiosperm tissues by the high amount of lignin-derived phenols normalized to both C (λ_8) and gram dry weight (gdw) (for λ_8, χ^2=34.201, df=2, p<0.0005 and for Σ_8, χ^2=34.238, df=2, p<0.0005). Woody tissue λ_8

values averaged 18.9 ± 4.3 mg (100 mg of OC)$^{-1}$, whereas Σ_8 averaged 806.4 ± 189.4 mg (10 gdw)$^{-1}$). Leaves had considerably lower yields, with λ_8 averaging 5.7 ± 3.0 mg (100 mg of OC)$^{-1}$ and Σ_8 averaging 236.4 ± 125.6 mg (10 gdw)$^{-1}$. Bark fell between these values (Table 3.1).

The average C:V ratio, which differentiates wood from non-woody vegetation [*Hedges and Mann*, 1979], increased among angiosperm tissues taken from trees and shrubs as follows: wood had the lowest C:V ratio (C:V = 0.02 ± 0.01), whereas barks were intermediate (0.20 ± 0.21), and leaves had the highest values (0.34 ± 0.27). Out of all vegetation types studied, macrophytes (grasses and aquatic plants) had the highest C:V values observed (1.20 ± 0.15 and 1.08 for grasses and aquatic plants, respectively) (Table 3.1). The S:V ratio differentiates angiosperms from gymnosperms, as expected, since gymnosperms do not make syringyl-phenol derivatives [*Hedges and Mann*, 1979]. Angiosperm wood had the highest S:V ratio (1.92 ± 0.82), and bark, leaves, and grasses had S:V ratios near 1 (see Table 3.1). Aquatic plants can be physically separated from other vegetation types based on the low S:V ratio (0.14) and high C:V ratio (1.08).

The LPVI has recently been proposed to be an additional tool to partition OM among end-member sources [*Tareq et al*., 2004]. Although the average LPVI value of angiosperm leaves was higher than that of wood and bark (Table 3.1), the high variability of the leaves (411.9 ± 553.7) and similar values of wood and bark tissues (124.5 ± 68.6 and 172.3 ± 230.1, respectively) indicates that it is not statistically possible to differentiate between these three tissue types using the LPVI (χ^2=3.464, df=2, p=0.177). Grasses had the highest LPVI value of 1589.6 ± 900.5, but the range of LPVI values for angiosperm leaves overlaps with the grasses.

Mekong River sediment fluxes, concentrations and organic matter compositions

In 2006, the rising-, flood-, falling-, and low-water stages for the Lower Basin were from 13 May – 5 July, 6 July – 1 November, 2 November – 28 November, and 29 November – 30 May, respectively [*Mekong River Commission,* 2007]. FSS concentrations varied by two orders of magnitude throughout 2006, with a minimum of 6.1 mg/L and a maximum of 259.8 mg/L (Table 3.2, Fig. 3.2a). They were positively correlated with discharge ($r=0.850$, $p=<0.0005$, $n=18$), with higher concentrations observed during the flood season compared to the dry season (185.0 ± 52.6 vs. 10.4 ± 6.3) ($u=0.000$, $p=0.001$, $n=16$). The total annual flux of FSS for 2006 was 76.3 MT/yr.

FPOC concentrations ranged from 0.5 to 6.3 mg/L (Table 3.2) and were also positively correlated with discharge ($r=0.904$, $p=<0.0005$, $n=18$) and FSS ($r=0.941$, $p<0.0005$, $n=18$). FPOC was five-fold higher during the flood-period than the low-water period (3.9 ± 1.2 mg/L vs. 0.7 ± 0.1) ($u=0.000$, $p=0.001$, $n=16$). The flux of FPOC exported by the Mekong at Phnom Penh was 1.67 MT/yr.

The % OC of FSS also exhibited significant seasonal variability, with values ranging from 1.5 to 10.7% (Table 3.2, Fig. 3.2b). It was inversely correlated with discharge ($r=-0.847$, $p=<0.0005$, $n=18$) and FSS concentrations ($r=-0.943$, $p<0.0005$, $n=18$). Values sharply declined from 10.7 to 4.0 % as FSS concentrations increased from 7 to 29 mg/L, and then plateaued between 2-3% as FSS values increased to 260 mg/L thereafter. Dry-period values were higher than those from the rainy period (7.9 ± 2.4 vs. 2.2 ± 0.4%, respectively) ($u=0.000$, $p=0.001$, $n=18$). Maximum values peaked during the first-half of the low-water season (Feb. 17), and declined to high-water values during the remainder of the low-water period.

The N:C ratio of FPOM ranged from 0.06 to 0.11 and averaged 0.09 ± 0.02 (Table 3.2, Fig. 3.2c). It increased from 0.06 to 0.11 throughout the low-water season and was negatively correlated with discharge (r=-0.479, p=0.044, n=18). However, there was no significant difference between the low-water and high-water N:C ratios (u=17.500, p=0.137, n=16). The $\delta^{13}C$ of FPOC ranged between -27.7 to -31.3‰ with no seasonal trends (Table 3.2).

Measurements of lignin-derived phenols associated with FPOM

Lignin concentrations in the FPOM fraction ranged from 2.00 to 62.7 µg/L (Table 3.3) and were positively correlated with the hydrograph (r= 0.909, p<0.0005, n=18). Average high-water values (41.7 ± 15.9 µg/L) were over fourteen-fold greater than low-water values (2.84 ± 0.58 µg/L). Vanillyl phenol concentrations were always the highest, followed by concentrations from the syringyl family, and then the cinnamyl family. The total lignin flux exported by the Mekong at Phnom Penh was 0.019 MT/yr.

Σ_8 ranged from 1.04 to 3.81 mg (10 gdw)$^{-1}$ (Table 3.3), and there was no significant correlation between Σ_8 and discharge (r=-0.416, p=0.086, n=18). Total lignin yields (λ_8) ranged from 0.34 to 1.47 mg (100 mg OC)$^{-1}$ (Table 3.3 and Fig. 3.2d). Values were positively correlated with discharge (r=0.857, p<0.0005, n=18), with the dry season having lower λ_8 values (0.40 ± 0.05 mg (100 mg OC)$^{-1}$ than the flood period 1.1 ± 0.3 (100 mg OC)$^{-1}$ (u=0.000, p=0.001, n=16). When λ_8 was divided into individual phenol families ($\lambda_{vanillyl,}$ $\lambda_{syringyl,}$ and $\lambda_{cinnamyl}$), the vanillyl family contributed the highest proportion of OC, followed by the syringyl, and then the cinnamyl families (mean $\lambda_{v,}$= 0.4 ± 0.2, λ_s = 0.2 ± 0.2 $_{and}$ λ_c = 0.05 ± 0.03 mg C/100 mg OC) (data not shown). The S:V ratio ranged from 0.37 to 0.80 and the C:V ratio ranged from 0.07 to 0.18 (Table 3.3). Both parameters were significantly correlated with discharge (r=0.866 and 0.724 for S:V and C:V, respectively) and each other (r=0.830, p<0.0005, n=18). Values of

(Ad:Al)v and (Ad:Al)s ranged from 0.29 to 0.77 and 0.22 to 0.72, respectively (Table 3.3). Neither was correlated with discharge, and no difference between these ratios was observed between seasons. However, the (Ad:Al)s ratio clearly peaked during the middle of the low-water season (Fig. 3.2e). LPVI ranged from 15.9 to 93.0 and was also positively correlated with discharge ($r=0.857$, $p<0.0005$, $n=18$) (Table 3.3, Fig. 3.2f), with dry season FPOM samples having lower LPVI values (29.4 ± 15.0) than rainy season samples (74.6 ± 17.3) ($u=2.000$, $p=0.002$, $n=16$).

DISCUSSION

The discharge and concentration of fine suspended sediment of the Mekong River varied by almost two orders of magnitude during the 2006 study period, with both parameters being dominated by the annual monsoonal flood pulse. Given this extreme variability, one might expect vast differences in POM composition between seasons. However, intensity in rainfall is not unique to the Mekong Basin, nor is seasonal variability in sediment concentrations. The Amazon River, which is perhaps the most thoroughly studied of the large tropical rivers, experiences little variability in POM composition relative to the large changes observed between dissolved and particulate organic matter [*Hedges et al.*, 1986; *Quay et al.*, 1992]. Such homogeneity is likely due to the role of the extensive lowland floodplain in both storing and resuspending previously deposited sediment during various stages of the hydrograph [*Hedges et al.*, 1986; *Hedges et al.*, 1994; *Dunne et al.*, 1998]. Although a floodplain does develop when the Mekong River reaches Cambodia, the Mekong is largely constrained to its channel during the vast majority of its journey [*Mekong River Commission*, 2005]. Accordingly, distinct compositional differences are observed in Mekong POM composition at both the bulk and the molecular level. We argue below that the variability in riverine POM source signatures over the

course of one year is due to seasonal differences in autochthonous production, degradation, and the mobilization of sediment from different regions of the Mekong Basin.

Variability in lignin-derived phenols in regional vascular plants

As organic matter composition is inherently linked to remineralization and carbon preservation in both marine and terrestrial reservoirs, understanding the biological source of riverine organic matter, and its associated reactivity, will improve our understanding of the global carbon cycle. Riverine organic matter is important to understanding the inland-water gas evasion flux because it is a substrate for heterotrophic respiration, which drives gas evasion [*Richey et al.*, 2002; *Cole et al.*, 2007; *Tranvik et al.*, 2009]. Several studies suggest that suspended particles contain labile OM that support bacterial metabolism and respiratory carbon dioxide fluxes in rivers [*Grossart and Ploug*, 2000; *Mayorga et al*., 2005; *Ellis et al.*, 2012a]. As a starting point to assess riverine OM source, it is first necessary to compare the same compositional signatures found in riverine POM to that found in the potential end-members from which this material is derived.

Accordingly, we used lignin-phenols to deduce whether riverine FPOM is derived from vascular plants, and to assess how the vascular-plant contribution to riverine POM changes seasonally. The range of lignin-phenol compositions for fresh angiosperms found within the Mekong Basin suggests that riverine POM can potentially be partitioned among three angiosperm end-members as they have distinct signatures: 1) woods, 2) leaves and barks, and 3) macrophytes (Table 3.1, Fig. 3.3). To the best of our knowledge, ratios for barks have not previously been reported in the tropics, but the values reported here are similar to previous results from a watershed in the South of France [*Cotrim da Cunha et al.*, 2001]. Although there are gymnosperms growing within the basin [*Rundel*, 2009; *Costa-Cabral* et al., 2008], none were

found in the pristine forests visited in this study. Accordingly, the non-overlapping S:V ratios between fresh angiosperms from this study and gymnosperms reported from the literature [*Hedges and Mann*, 1979; *Opsahl and Benner*, 1995] enables riverine POM to be partitioned between these respective sources.

The composition of Mekong angiosperms suggests that the LPVI may be of diminished utility as a tool to partition POM among end-member sources in this watershed. This index linearizes the S:V and C:V ratios to a single value [*Tareq et al.*, 2004]. Its presumed advantage is that each vegetation type and tissue type has non-overlapping boundary lines along this index. However, in this study, the LPVI of angiosperm woods, barks, leaves, and aquatic plants significantly overlap with each other (Fig. 3.4, Table 3.1) making differentiation between these sources using only the LPVI tenuous. The low amount of cinnamyl and/or syringyl phenols in some of the angiosperm leaf samples analyzed in this study (relative to those presented in *Tareq et al.* [2004]) could account for the overlap between the LPVI of angiosperm leaves and woods.

Seasonal variability in vascular-plant derived particulate organic matter transported by the Mekong River

As the Mekong River descends from its headwaters to the sea, it drains a landscape with a rich diversity of vascular plant types, and transitions from cool temperate to tropical climates. Along the way, the Mekong passes through numerous vegetation zones with distinct communities. In the Upper Basin, subalpine shrublands and alpine meadows are found at elevations greater than 5,000 m, whereas coniferous forests dominate between 1,000 to 4,000 m in elevation, and evergreen and deciduous broad-leaved forests are found at elevations below 1,000 m [*Costa-Cabral et al.*, 2008; *Rundel*, 2009]. Although conifers are found in some montane forests of the Lower Basin, agriculture production and broadleaf forests cover much of

the lowlands [*Costa-Cabral et al.,* 2008], with deciduous dipterocarp (angiosperms) forests being the most common forest type of the Lower Basin [*Rundel,* 2009]. Therefore, considering that approximately twice as much flow (40%) comes from the Upper Basin during the dry season relative to the rainy season (20%) [*Mekong River Commission*, 2005], it is possible that the vascular plant composition of riverine FPOM could reflect seasonal variation in the origin of flow and the associated regional vascular-plant-derived OM that is concurrently mobilized.

Our results indicate that vascular plants comprise a significant component of riverine FPOM (λ_8 values range between 0.34 and 1.47 mg (100 mg OC)$^{-1}$), with significant compositional changes observed between seasons. The most striking compositional trend observed using lignin phenols is that Mekong FPOM lies on a mixing line between angiosperm bark/leaf tissues and gymnosperm wood tissues, with clear compositional changes between seasons (Fig. 3.3). Dry season samples had lower S:V and C:V ratios than rainy season samples, suggesting that gymnosperms exert a larger influence on FPOM composition during this period, whereas the higher ratios during the rainy season suggest that angiosperms are proportionally more important. However, this trend could potentially be explained without invoking a change in sources between seasons, as degradation can cause the same compositional patterns. Degradation by white-rot fungi preferentially removes precursors of syringyl and cinnamyl phenols relative to vanillyl phenols, so degradation tends to force S:V and C:V ratios towards the origin [*Hedges et al.*, 1988; *Benner et al.*, 1991]. Thus, an alternative possibility is that all of the FPOM originates from angiosperm bark/leafy tissues, and seasonal differences in degradation state, not variability in tissue type, drives this compositional trend.

To assess this possibility, we monitored the acid/aldehyde ratios of lignin phenols. Previous work has demonstrated they can be used to assess degradation given that ratios in

diagenetically-altered samples are elevated relative to those found in fresh plants [*Ertel et al.*, 1984; *Hedges et al.*, 1988; *Opsahl and Benner*, 1995]. Although the (Ad:Al)s and (Ad:Al)v ratios for FPOM were higher than our plant end-members (Table 3.1 and Table 3.3), there was no observable difference between (Ad:Al)v and (Ad:Al)s between the dry and rainy season.

As a second test to ensure that degradation is not driving the variability in C:V and S:V ratios between seasons, relationships between the LPVI and Ad:Al ratios were examined. As proposed by Rezende et al. [2010], the LPVI should decrease with diagenesis given that cinnamyl and syringyl phenols are preferentially removed relative to vanillyl phenols during degradation [*Hedges et al.*, 1988; *Benner et al.*, 1991]. Accordingly, a negative correlation between Ad:Al ratios and LPVI should be observed if degradation is affecting FPOM signatures. No correlation was found for the whole data set (Fig. 3.4), likely because both (Ad:Al)v and (Ad:Al)s were equally scattered within the dry and rainy season. In contrast, LPVI values were significantly lower during the dry season, with FPOM values lying within the range reported for gymnosperm leaves (12-27) [*Tareq et al.*, 2004], while rainy season FPOM values overlapped with the LPVI of angiosperms from the Mekong basin. Thus, the separation of dry and wet season samples by LPVI (which may be influenced by both diagenesis and OM source), but not (Ad:Al) (primarily affected by degradation), provides further support for changes in vegetation type being an important driver of variability in FPOM composition between seasons.

While great differences in composition were observed between the wet and dry seasons, significant compositional changes were also observed within seasons. During the low-water period, the FPOM derived from angiosperms became more degraded as the dry season initially progressed, with (Ad:Al)s ratios abruptly peaking in the middle of the dry season (Fig. 3.2e and Fig. 3.4). Degradation by white-rot fungi occurs in subaerial environments [*Hedges et al.*, 1988],

so it may be expected that degradation would increase as soils dry out. Therefore, the initial decline in the LPVI to gymnosperm values (from sample 1 to samples 4-8) that is accompanied by elevated (Ad:Al)s ratios could be explained by the progressive degradation of FPOM derived from an angiosperm source as the low water season progresses. However, after reaching its peak (sample 5), (Ad:Al)s fell from 0.72 to 0.41, consistent with less degraded material being transported at the end of the dry season. Interestingly, the LPVI experienced little change during this period, continuing to reflect a gymnosperm source. The large change in degradation state without a concurrent change in the LPVI suggests: 1) the LPVI is relatively insensitive to changes in degradation relative to (Ad:Al)s and/or 2) the importance of angiosperms relative to gymnosperms has become significantly reduced as the dry season progresses. Either way, both of these possibilities suggest that the decline in LPVI during the dry season is primarily controlled by the increasing importance of gymnosperms as the dry season progresses, with degradation being of secondary importance.

Compositional variability occurs within the rainy period as well. The freshest angiosperm tissues may be transported during the beginning of the rainy season, likely being derived from undegraded angiosperm bark/leaf sources (Fig. 3.4). As the rainy season progresses, the (Ad:Al)s ratio of these angiosperms indicate that they generally become more degraded. Therefore, although the LPVI is consistent with the mean for angiosperm-bark end-members, the elevated (Ad:Al)s of these samples suggests that angiosperm leaves and wood may have been the ultimate starting material (Fig. 3.4). The high variability observed in compositional signatures may be expected as many different mechanisms transport FPOM to the river during this period (i.e. overland flow, through flow, mass wasting, sediment resuspension, etc.).

Mechanisms for a seasonal shift in vascular plant composition

It is likely that vascular-plant compositional changes in riverine FPOM are ultimately caused by seasonal differences in the contribution of various regions of the basin to the flow of the Mekong River. In addition to having proportionally more flow coming from the Upper Basin during the dry season relative to the wet season [*Mekong River Commission*; 2005; *Costa-Cabral et al.,* 2008], research conducted in the Lower Basin (in Laos) suggests that eroded material is simply redistributed among the hill slope initially during the rainy season; it is not until after the catchment is sufficiently saturated that precipitation-induced runoff is able to transport sediment [*Chaplot et al.*, 2005]. Therefore, it is possible that soils from the Lower Basin may become an increasingly important source of sediment as the rainy season progresses. Similarly, with more of the flow originating from the Upper Basin during the dry season, a greater proportion of dry season FPOM could be expected to be derived from Upper Basin sources relative to the rainy season. Therefore, the predominance of gymnosperms observed in dry season samples may reflect the abundance of coniferous forests of the Upper Basin. Similarly, the predominance of angiosperms during the wet-season may reflect the relative importance of these plant types in the Lower Basin [*Rundel,* 2009].

To assess the likelihood that dry-season FPOM is derived from the Upper Basin, we analyzed POM samples taken from two locations from the mainstem in the Chinese portion of the Upper Basin during the low-water period (i.e. April 2006). These samples cluster within the variability of the S:V and C:V ratios of our lowland dry-period samples (Fig. 3.3b), and their origin is consistent with gymnosperms. Therefore, they provide further support that the FPOM exported from the Mekong Basin during the dry season has a gymnosperm compositional signature that emanates from the Upper Basin.

Compositional parameters that are linked to sediment coming from different regions of the basin could be a useful tool to assess the impacts of reservoir construction in different regions. For example, China is building eight reservoirs along the mainstem in the Upper Basin [*Grumbine and Xu*, 2011], with a likely consequence being that carbon that would otherwise have different downstream fates will likely remain trapped in the Upper Basin. Accordingly, a diminished gymnosperm signal could be expected in POM exported by the Mekong during the dry season. However, 200 other reservoirs are projected to be completed basin-wide over the next several decades [*Xue et al.*, 2011], making predictions as to how that could affect organic matter composition complex.

Variability in the vascular plant contribution to particulate organic matter

Lignin-phenol concentrations (μg/L) of POM from the Mekong River followed the hydrograph, indicating that more plant-derived material is transported from the watershed during the wet season (Table 3.3). This is consistent with studies of POM on the Tech River in the South of France [*Cotrim da Cunha et al.*, 2001], and studies of dissolved OM in the Congo River basin [*Spencer et al.*, 2010]. In the Congo basin, higher Σ_8 and λ_8 values of dissolved OM occurred during the flush relative to the post-flush/dry season, which was attributed to the intense leaching of the organic-rich surface horizons and increased runoff rates during the rainy season. Low values during the dry season, in turn, were likely due to increased RT (enabling more degradation), and the extensive leaching of the source material during the preceding flush period [*Spencer et al.*, 2010]. In this study, Σ_8 values of FPOM were not significantly different between seasons, suggesting that there was no variability in the dilution of the lignin pool by mass with sediment between seasons. However, it is possible that sampling at a higher resolution (i.e. more frequently than twice a month) may have been necessary to see significant

differences in Σ_8, especially during the rising-water period when discharge increases rapidly. Regardless, the higher concentration of lignin (μg/L) observed during the rainy season is likely a result of more sediment mobilization caused by increased precipitation.

Normalizing lignin yields by OC content (λ_8) indicates that a greater fraction of Mekong FPOC is derived from vascular plants during the wet season relative to the dry period: λ_8 is twice as high during the rainy season (Fig. 3.2d, Table 3.3). Dilution of λ_8 by phytoplankton occurs in other river systems, such as the Mississippi [*Bianchi et al.*, 2007]. To assess this possibility, we examined the % OC of FSS. The global riverine average of 1% typically reflects the high mineral content of FSS, whereas higher values may be indicative of algae, which can be up to 50% OC [*Meybeck, 1982*]. Indeed, a strong inverse relationship was observed between suspended sediment concentrations and the % OC on the Mekong (Fig. 3.2b). A likely explanation for this relationship is light inhibition of *in situ* production during the rainy season [*Ittekot and Laane*, 1991]. Alternatively, although there are generally few opportunities for sediment deposition along the Mekong, this same trend could be caused by an increase in sediment resuspension during the rainy season in the Lower Mekong. However, simultaneous work at this exact location demonstrated that the ratio of gross photosynthesis to community respiration was twice as high during the dry season relative to the rainy season during the period examined in this study [*D. E. Lockwood*, unpublished data, 2006]. Accordingly, increased phytoplankton production during the dry season is likely the primary mechanism that elevates OC contents and dilutes λ_8 values during the dry season.

To further assess the influence of phytoplankton, N:C ratios and the isotopic signature ($\delta^{13}C$) of FPOM were also measured. Unfortunately, $\delta^{13}C$ was of limited utility due to the overlap between phytoplankton $\delta^{13}C$ values with that of leaves and needles (Fig. 3.5). An

increase in N:C ratios was observed throughout the low-water season (Fig. 3.2c, Fig. 3.5), suggesting that FPOM transitions from a vascular-plant source with low N:C ratios towards a phytoplankton source with high values as the dry season progresses. However, there was no observable difference between seasons, due to the variability in N:C ratios during both the dry and rainy seasons. High N:C ratios may also be a result of the sorption of nitrogen-rich dissolved OM onto minerals [*Aufdenkampe et al.*, 2001]. Soils from Laos have N:C ratios range from 0.07 to 0.13 [*de Rouw et al.*, 2010], which is considerably lower than the vascular plant N:C ratios reported here. Accordingly, the rising/high-water FPOM likely reflects mixing between leaf and soil-derived FPOM. Despite no significant difference between the N:C ratios and the $\delta^{13}C$ of POM between seasons, the increase in N:C ratios throughout the low-water period combined with the strong seasonal signals in % OC further suggests that phytoplankton are significantly contributing to the FPOM composition of the dry period.

CONCLUSIONS

Riverine POM is intricately tied to understanding long-term C burial in marine sediments and elucidating CO_2 production mechanisms, such as respiration, in rivers. Therefore, understanding the provenance of POM signatures and their variability will improve our understanding of these important aspects of the C cycle. In contrast to the Amazon Basin, where little seasonal variability is observed in POM composition relative to the large compositional differences between the coarse and fine fraction [*Hedges et al.*, 1986], distinct seasonal patterns are observed at both the bulk and molecular-level in this large tropical river draining a high-relief catchment. We speculate that such temporal variability occurs because the Mekong is generally constrained to its channel during much of its journey to the South China Sea, with a short transit

time from source to sink. Temporal changes in the composition of this material have implications for POM reactivity and preservation.

First, measurements made at the bulk level suggest that FPOM has more of an autochthonous influence during the low-water season relative to the flood season. In the Amazon basin, high rates of water-column respiration support high CO_2 gas evasion fluxes [*Richey et al.*, 2002], and recent work examining the variability in basin-wide respiration rates demonstrates that the highest rates are observed in rivers in which the FPOM was derived from autochthonous origins [*Ellis et al.*, 2012a]. Thus, given the lability of phytoplankton [*Sun et al.*, 1997], a high proportion of FPOM carried by the Mekong during the dry season would be expected to be consumed while in transit rather than preserved in coastal sediments.

In contrast, during the rainy season, the autochthonous signal carried by Mekong FSS is quickly diminished and the proportion of vascular-plant-derived FPOM increases. However, this does not indicate that this material is of limited bioavailability. Consistent increases in organic C concentrations and dissolved CO_2 with discharge, and simultaneous declines in dissolved oxygen have been observed across a continuum of river sizes in the Amazon Basin [*Richey et al.*, 2009]. These data are consistent with terrestrially-derived material supporting water-column respiration during the rainy season. Further support for the reactivity of plant-derived FPOM comes from the observation that downstream changes in the $\delta^{13}C$ of FPOC carried by the Solimões and Amazon rivers mirrors the expected high-altitude enrichment of 1‰ for every 1,000 m change in elevation for terrestrial plant biomass [*Hedges et al.*, 2000]. This occurs even though the majority of the sediment originates in the Andes. Finally, lignin in soils is highly reactive [*Kiem et al.*, 2003]. Taken together, a strong case can be made in support of the idea that material derived from higher-plants is bioavailable. Accordingly, it appears likely that although the

composition of the material exported by the Mekong differs between seasons, there are labile pools of carbon available to support riverine metabolism throughout the hydrograph.

Gymnosperms contribute to a higher proportion of vascular-plant material during the dry-season, whereas the FPOM transported during the rainy season predominantly reflects angiosperm leaf and bark material. We hypothesize that this variability reflects changes in the proportion of flow coming from the Upper and Lower regions of the Mekong, and speculate that differences in the vascular plant composition of these regions explains the compositional changes observed in riverine FPOM downstream. Thus, we have identified compositional parameters that may be linked to sediment coming from different regions of the basin, which could potentially be used to evaluate the impact of reservoirs on sediment mobilization within the basin.

We estimate that the total annual flux of FSS, FPOC, and lignin exported by the Mekong River was 76.3 MT/yr, 1.67 MT/yr, and 0.019 MT/yr during the 2006 hydrologic year. This material was then delivered to the Mekong Delta and then on to the South China Sea. An important question is, what are the implications of current and future dams on the composition and magnitude of these fluxes? Three dams are currently in operation on the Mekong mainstem in the Upper Basin, and 200 more are projected to be completed within the basin over the next several decades [*Xue et al.*, 2011]. As reservoirs trap material that would have otherwise had another fate, the impacts of these dams will likely have a profound impact on both the quantity and quality of C leaving the catchment via fluvial export. More terrestrially-derived C will likely be preserved within the basin rather than being carried downstream and respired, and more autochthonous C will likely be produced due to sediment settling in reservoirs, increasing light penetration [*Downing et al.*, 2008]. These impacts will likely affect Asia's largest freshwater

fishery, the Tonle Sap Lake, considering that Mekong sediments are hypothesized to be important in sustaining it [*Mekong River Commission, 2005; Kummu et al.,* 2008]. This study provides the beginning of the composition and flux data necessary to assess the impacts of future anthropogenic change within the basin.

Table 3.1. The organic composition of angiosperm end-members[a] found in the Mekong River Basin

Name	Type[b]	Tissue[c]	N:C	$\delta^{13}C$	% OC	S:V	C:V	(Ad:Al)v	(Ad:Al)s	λ_8	Σ_8	LPVI
Aglaia pisifera	A	W		-27.3	38.4	1.48	0.01	0.11	0.15	20.1	773.1	90.0
Alstonia scholaris	A	W		-29.5	43.0	1.89	0.03	0.15	0.18	21.9	943.8	130.2
Antidesma ghaesembilla	A	W		-29.6	40.1	1.82	0.02	0.13	0.16	21.2	852.6	120.0
Artocarpus heterophylus	A	W		-32.4	41.8	3.48	0.02	0.09	0.12	26.5	1107.9	285.8
Baccaurea ramiflora	A	W		-29.1	37.4	0.67	0.04	0.17	0.18	13.3	497.4	31.7
Cassia siamensis	A	W		-31.0	46.2	2.15	0.01	0.14	0.13	21.5	994.9	147.2
Dipterocarpus alatus	A	W		-33.2	42.3	2.02	0.03	0.11	0.34	9.1	385.3	140.0
Feroniella lucida	A	W		-30.8	42.1	1.29	0.01	0.18	0.17	19.2	808.3	73.4
Garcinia lanessani	A	W		-30.2	41.9	0.72	0.02	0.15	0.01	17.9	747.5	32.1
Irvingina malayana	A	W		-30.5	42.0	1.58	0.01	0.13	0.18	17.1	715.8	98.0
Lagerstroemia calyculata	A	W		-29.3	45.4	1.86	0.01	0.13	0.16	18.2	825.6	122.2
Nephelium hypoleucum	A	W		-27.2	43.6	3.02	0.01	0.14	0.18	24.8	1081.1	223.3
Peltophorum dasyrachis	A	W		-30.4	41.1	2.15	0.01	0.12	0.13	19.0	782.4	147.6
Schleicheria oleosa	A	W		-29.6	46.9	1.43	0.01	0.12	0.10	12.7	594.5	86.0
Streblus asper	A	W		-33.1	45.0	1.38	0.03	0.14	0.15	20.6	926.6	84.2
Tamarindus indica	A	W		-30.1	42.5	1.31	0.01	0.18	0.21	18.7	793.9	75.5
Srol wood	A	W		-29.6	43.3	3.04	0.02	0.13	0.12	20.3	877.9	229.2
	Wood average (n=17):			*-30.2*	*42.5*	*1.92*	*0.02*	*0.14*	*0.16*	*18.9*	*806.4*	*124.5*
	Standard deviation:			*1.7*	*2.5*	*0.82*	*0.01*	*0.02*	*0.07*	*4.3*	*189.4*	*68.6*
Aglaia pisifera	A	B	0.052	-29.5	46.4	0.98	0.86	0.18	0.29	2.2	103.7	939.0
Alstonia scholaris	A	B	0.039	-32.1	41.8	0.72	0.10	0.18	0.25	8.0	332.9	48.8
Antidesma ghaesembilla	A	B		-29.7	48.5	2.13	0.16	0.20	0.22	8.3	402.4	264.0
Artocarpus heterophylus	A	B	0.062	-34.0	46.7	0.85	0.11	0.23	0.33	8.6	409.0	67.0
Baccaurea ramiflora	A	B	0.048	-30.6	40.2	0.46	0.08	0.25	0.33	8.0	323.1	22.8
Cassia siamensis	A	B	0.054	-33.0	46.5	0.96	0.09	0.26	0.29	10.9	506.3	68.7
Dipterocarpus alatus	A	B		-33.4	46.2	1.78	0.10	0.11	0.61	6.7	310.0	159.1
Feroniella lucida	A	B	0.042	-31.7	48.1	0.74	0.58	0.20	0.22	5.7	275.6	386.6
Garcinia lanessani	A	B		-31.4	44.4	0.74	0.14	0.17	0.21	10.0	445.3	63.6
Irvingia malayana	A	B		-30.6	49.1	0.98	0.06	0.24	0.34	9.6	471.4	58.7
Lagerstroemia calyculata	A	B	0.047	-31.0	45.3	0.48	0.13	0.27	0.37	9.7	437.5	34.6
Nephelium hypoleucum	A	B	0.037	-32.1	49.7	0.91	0.09	0.20	0.23	8.7	434.3	63.1
Peltophorum dasyrachis	A	B		-34.5	46.7	0.66	0.11	0.20	0.23	5.6	261.3	147.3
Schleicheria oleosa	A	B	0.034	-30.4	50.7	0.47	0.19	0.17	0.17	4.2	212.3	48.9
Srol bark	A	B	0.043	-30.6	50.2	1.33	0.36	0.21	0.18	4.3	216.6	400.7
Streblus asper	A	B	0.065	-34.5	35.0	1.16	0.15	0.25	0.33	8.5	298.6	122.5

Table 3.1 continued.

Name	Type[b]	Tissue[c]	N:C	$\delta^{13}C$	% OC	S:V	C:V	(Ad:Al)v	(Ad:Al)s	λ_8	Σ_8	LPVI
Tamarindus indica	A	B	0.035	-32.2	41.6	0.63	0.07	0.18	0.19	9.2	383.4	33.3
Bark Average (n=17):			*0.046*	*-31.8*	*45.7*	*0.94*	*0.20*	*0.21*	*0.28*	*7.6*	*342.6*	*172.3*
Standard deviation			*0.010*	*1.6*	*4.1*	*0.45*	*0.21*	*0.04*	*0.10*	*2.4*	*107.7*	*230.1*
Aglaia pisifera	A	L	0.048	-29.6	47.0	0.15	0.35	0.03	0.15	2.4	110.8	26.6
Alstonia scholaris	A	L	0.046	-29.2	36.5	1.25	0.24	0.09	0.14	2.2	81.5	224.0
Antidesma ghaesembilla	A	L	0.038	-31.8	34.1	0.87	0.16	0.11	0.13	3.2	110.5	92.4
Artocarpus heterophylus	A	L	0.050	-34.0	40.2	1.33	1.14	0.10	0.17	2.7	109.3	1981.3
Baccaurea ramiflora	A	L	0.042	-29.5	36.3	0.73	0.17	0.13	0.17	3.6	130.8	76.9
Borassus flabellifer	A	L	0.035	-32.2	38.0	2.20	0.14	0.13	0.18	14.0	530.4	247.5
Cassia siamensis	A	L	0.045	-31.7	45.9	1.03	0.32	0.17	0.20	6.3	288.4	258.3
Dipterocarpus alatus	A	L	0.039	-33.8	46.2	0.48	0.04	0.13	0.17	5.3	245.5	18.8
Feroniella lucida	A	L	0.054	-31.8	40.6	0.72	0.43	0.15	0.24	6.4	258.1	246.9
Garcinia lanessani	A	L	0.038	-30.8	43.3	1.41	0.16	0.11	0.13	7.0	300.9	166.5
Irvingina malayana	A	L	0.031	-30.0	43.0	0.77	0.13	0.16	0.20	8.0	344.3	65.0
Lagerstroemia calyculata	A	L	0.033	-30.2	46.0	0.99	0.09	0.12	0.16	6.4	294.4	71.3
Nephelium hypoleucum	A	L	0.039	-31.0	41.8	1.14	0.51	0.10	0.12	9.9	415.3	556.8
Peltophorum dasyrachis	A	L	0.031	-32.7	45.7	1.42	0.46	0.12	0.15	5.5	249.8	594.6
Schleicheria oleosa	A	L		-32.4	44.3	0.47	0.14	0.17	0.29	7.7	342.6	34.3
Srol leaves	A	L	0.049	-29.7	38.7	2.07	0.71	0.19	0.21	4.8	184.4	1641.7
Streblus asper	A	L	0.051	-32.9	33.4	1.66	0.48	0.11	0.12	2.1	68.9	744.6
Tamarindus indica	A	L	0.052	-32.6	38.2	0.89	0.47	0.14	0.19	5.0	189.9	366.5
Leaf Average (n=18):			*0.043*	*-31.4*	*41.1*	*1.09*	*0.34*	*0.13*	*0.17*	*5.7*	*236.4*	*411.9*
Standard Deviation:			*0.008*	*1.5*	*4.4*	*0.54*	*0.27*	*0.04*	*0.04*	*3.0*	*125.6*	*553.7*
Tonle Sap	M_g	L	0.064	-29.9	36.3	0.84	1.03	0.18	0.45	10.7	388.4	978.2
Treng	M_g	L	0.049	-11.9	43.4	0.79	1.28	0.16	0.46	10.2	441.8	1166.9
Bamboo	M_g	L	0.065	-27.3	34.7	1.70	1.29	0.16	0.28	15.7	531.8	2623.6
Eichornia crassipes	M_a	L	0.058	-29.7	40.6	0.08	0.98	0.45	0.36	1.0	40.3	65.8
Ipomoea aquatic	M_a	L	0.088	-28.0	36.4	0.19	1.19	0.27	0.31	2.3	82.6	165.1
Macrophyte Average (n=5)			*0.065*	*-25.3*	*38.3*	*0.72*	*1.15*	*0.24*	*0.37*	*8.0*	*297.0*	*999.9*
Standard Deviation:			*0.015*	*7.6*	*3.6*	*0.65*	*0.14*	*0.12*	*0.08*	*6.2*	*221.5*	*1028.8*
Grass Average (n=3)			*0.059*	*-23.0*	*38.2*	*1.11*	*1.20*	*0.17*	*0.39*	*12.2*	*454.0*	*1589.6*
Standard Deviation:			*0.009*	*9.7*	*4.6*	*0.51*	*0.15*	*0.01*	*0.10*	*3.1*	*72.5*	*900.5*
Aquatic plants (n=2)			*0.065*	*-28.8*	*38.5*	*0.14*	*1.08*	*0.36*	*0.33*	*1.6*	*61.5*	*115.5*

Table 3.1 continued.

[a]Attributes of the organic composition of angiosperms are defined as follows: N:C = nitrogen to carbon ratio, $\delta^{13}C$= ^{13}C of the bulk organic matter, % OC = percent organic carbon, S:V = syringyl to vanillyl ratio, C:V = cinnamyl to vanillyl ratio, (Ad:Al)v = acid to aldehyde ratio of vanillyl phenols, (Ad:Al)s = acid to aldehyde ratio of syringyl phenols, $\lambda 8$ = mg of 8 lignin phenols (100 mg OC)$^{-1}$, $\Sigma 8$ = mg of 8 lignin phenols (10 gdw)$^{-1}$, and LPVI = Lignin Phenol Vegetation Index.
[b]Type denotes the type of angiosperm: A is a tree or shrub, M_g is grass, and M_a is an aquatic plant.
[c]Tissue types W, B, and L refer to wood (W), bark (B), and leaves (L).

Table 3.2. Bulk characteristics of fine suspended sediment.

Date	FSS[a] *mg/L*	FPOC[b] *mg/L*	% OC	N:C	$\delta^{13}C$ *‰*
		Low-water Stage			
06 Jan. 2006	26.2	0.94	3.6	0.06	-30.3
20 Jan. 2006	10.8	0.86	8.0	0.07	-29.9
03 Feb. 2006	6.1	0.50	8.2	0.10	-31.3
17 Feb. 2006	6.7	0.72	10.7	0.09	-29.2
02 Mar. 2006	7.0	0.73	10.5	0.09	-28.8
17 Mar. 2006	7.9	0.68	8.6	0.10	-30.4
31 Mar 2006	6.1	0.58	9.5	0.09	-29.4
21 Apr. 2006	12.4	0.61	5.0	0.10	-29.3
19 May 2006	10.5	0.72	6.9	0.12	-27.7
Average	*10.4*	*0.71*	*7.9*	*0.09*	*-29.6*
Standard deviation	*6.3*	*0.14*	*2.4*	*0.02*	*1.0*
		Rising-water Stage			
09 Jun. 2006	29.3	1.17	4.0	0.07	-30.4
23 Jun. 2006	36.7	1.04	2.8	0.07	-30.5
Average	*33.0*	*1.10*	*3.4*	*0.07*	*-30.5*
Standard deviation	*5.2*	*0.09*	*0.8*	*0.00*	*0.1*
		High-water Stage			
07 Jul. 2006	196.7	3.99	2.0	0.09	-29.5
21 Jul. 2006	136.3	3.28	2.4	0.09	-29.3
04 Aug. 2006	259.8	6.34	2.4	0.08	-30.1
18 Aug. 2006	173.6	3.78	2.2	0.09	-29.0
06 Oct. 2006	219.6	4.41	2.0	0.08	-29.7
20 Oct. 2006	103.1	2.71	2.6	0.06	-31.1
01 Nov. 2006	206.1	3.04	1.5	0.09	-29.8
Average	*185.0*	*3.94*	*2.2*	*0.08*	*-29.8*
Standard deviation	*52.6*	*1.21*	*0.4*	*0.01*	*0.7*
Overall Average	*80.8*	*2.01*	*5.2*	*0.09*	*-29.8*
Standard deviation	*91.4*	*1.75*	*3.3*	*0.01*	*0.9*

[a]FSS denotes the FSS concentration (measured in units of mg/L)

[b]FPOC is the FPOC concentration (in mg/L). All other variables are defined in Table 3.1.

Table 3.3. Riverine vascular-plant biomarker concentration[a] and composition of FPOM.

Date	Total Lignin *μg/L*	Vanillyl *μg/L*	Syringyl *μg/L*	Cinnamyl *μg/L*	S:V	C:V	(Ad:Al)v	(Ad:Al)s	λ_8	Σ_8	LPVI
				Low-water Stage							
06 Jan. 2006	3.82	2.14	1.36	0.32	0.64	0.15	0.34	0.30	0.41	1.46	57.9
20 Jan. 2006	3.12	1.96	0.96	0.20	0.51	0.11	0.71	0.49	0.36	2.53	34.0
03 Feb. 2006	2.00	1.19	0.60	0.21	0.50	0.17	0.31	0.38	0.40	3.30	47.4
17 Feb. 2006	2.47	1.69	0.63	0.14	0.37	0.09	0.43	0.64	0.34	3.66	17.0
02 Mar. 2006	2.63	1.81	0.68	0.13	0.38	0.07	0.62	0.72	0.36	3.74	15.9
17 Mar. 2006	3.02	2.04	0.77	0.21	0.40	0.10	0.43	0.54	0.44	3.81	19.7
31 Mar. 2006	2.28	1.49	0.66	0.13	0.44	0.09	0.52	0.46	0.39	3.74	22.1
21 Apr. 2006	2.44	1.66	0.64	0.14	0.39	0.08	0.39	0.41	0.40	1.97	17.6
19 May 2006	3.76	2.28	1.27	0.22	0.56	0.10	0.29	0.42	0.52	3.59	32.8
Average	*2.84*	*1.81*	*0.84*	*0.19*	*0.46*	*0.11*	*0.45*	*0.48*	*0.40*	*3.09*	*29.4*
Standard deviation	*0.58*	*0.31*	*0.26*	*0.06*	*0.09*	*0.04*	*0.14*	*0.14*	*0.05*	*0.92*	*15.0*
				Rising-water Stage							
09 Jun. 2006	6.35	4.13	1.83	0.39	0.44	0.09	0.50	0.36	0.54	2.17	23.4
23 Jun. 2006	4.88	2.94	1.57	0.37	0.53	0.13	0.52	0.41	0.47	1.33	38.3
Average	*5.62*	*3.53*	*1.70*	*0.38*	*0.49*	*0.11*	*0.51*	*0.38*	*0.51*	*1.75*	*30.9*
Standard deviation	*1.03*	*0.84*	*0.18*	*0.02*	*0.06*	*0.02*	*0.01*	*0.04*	*0.05*	*0.59*	*10.5*
				High-water Stage							
07 Jul. 2006	31.97	18.35	11.22	2.40	0.62	0.13	0.47	0.22	0.80	1.63	52.2
21 Jul. 2006	32.73	16.60	13.19	2.94	0.79	0.18	0.62	0.52	1.00	2.40	93.0
04 Aug. 2006	62.66	32.00	25.75	4.90	0.80	0.15	0.48	0.43	0.99	2.41	79.6
18 Aug. 2006	55.67	28.37	22.24	5.06	0.78	0.18	0.49	0.49	1.47	3.21	89.9
06 Oct. 2006	55.71	28.78	22.32	4.60	0.78	0.16	0.43	0.35	1.26	2.54	79.1
20 Oct. 2006	31.65	17.87	11.55	2.23	0.65	0.12	0.77	0.59	1.17	3.07	49.2
01 Nov. 2006	21.44	11.21	8.32	1.90	0.74	0.17	0.47	0.58	0.70	1.04	79.4
Average	*41.69*	*21.88*	*16.37*	*3.43*	*0.74*	*0.16*	*0.53*	*0.46*	*1.06*	*2.33*	*74.6*
Standard deviation	*15.90*	*7.77*	*6.86*	*1.37*	*0.08*	*0.02*	*0.12*	*0.13*	*0.27*	*0.77*	*17.3*
Overall Average	*18.26*	*9.81*	*6.98*	*1.47*	*0.57*	*0.13*	*0.49*	*0.46*	*0.67*	*2.64*	*47.1*
Standard deviation	*21.45*	*10.95*	*8.73*	*1.81*	*0.16*	*0.04*	*0.13*	*0.13*	*0.36*	*0.91*	*26.9*

[a]Total lignin concentration is the sum of the vanillyl, syringyl, and cinnamyl phenol concentrations in (μg/L). All other variables are defined in Table 3.1.

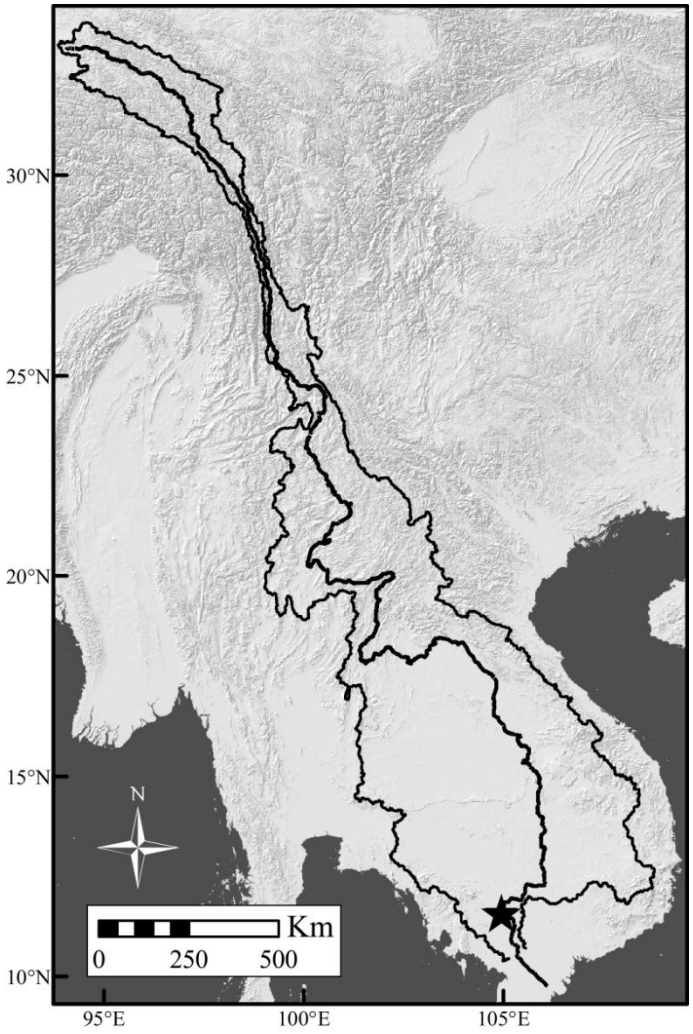

Figure 3.1. The Mekong River Basin in southeast Asia. The location at which sampling was conducted for this study is denoted with a star.

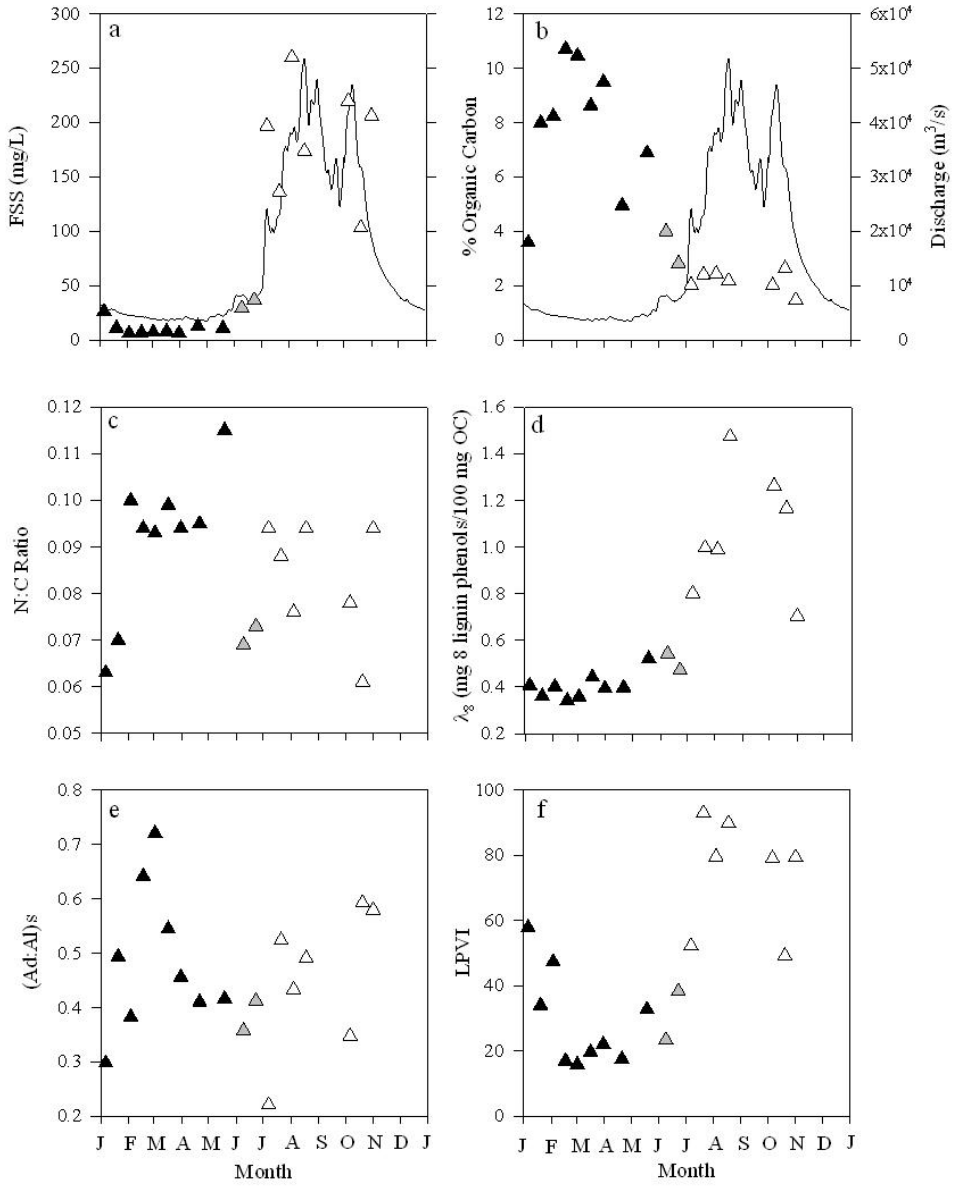

Figure 3.2. Seasonal variability in suspended sediment attributes found in the Mekong River at Phnom Penh. The hydrograph is plotted concurrently with (a) FSS concentration, (b) % organic carbon of FSS, (c) N:C ratio of FPOM, (d) λ_8 (mg lignin (100 mg OC)$^{-1}$), (e) (Ad:Al)s ratio, and (f) the LVPI of suspended sediment. The low-water, rising-water, and high-water periods are denoted by black triangles, gray triangles, and white triangles, respectively.

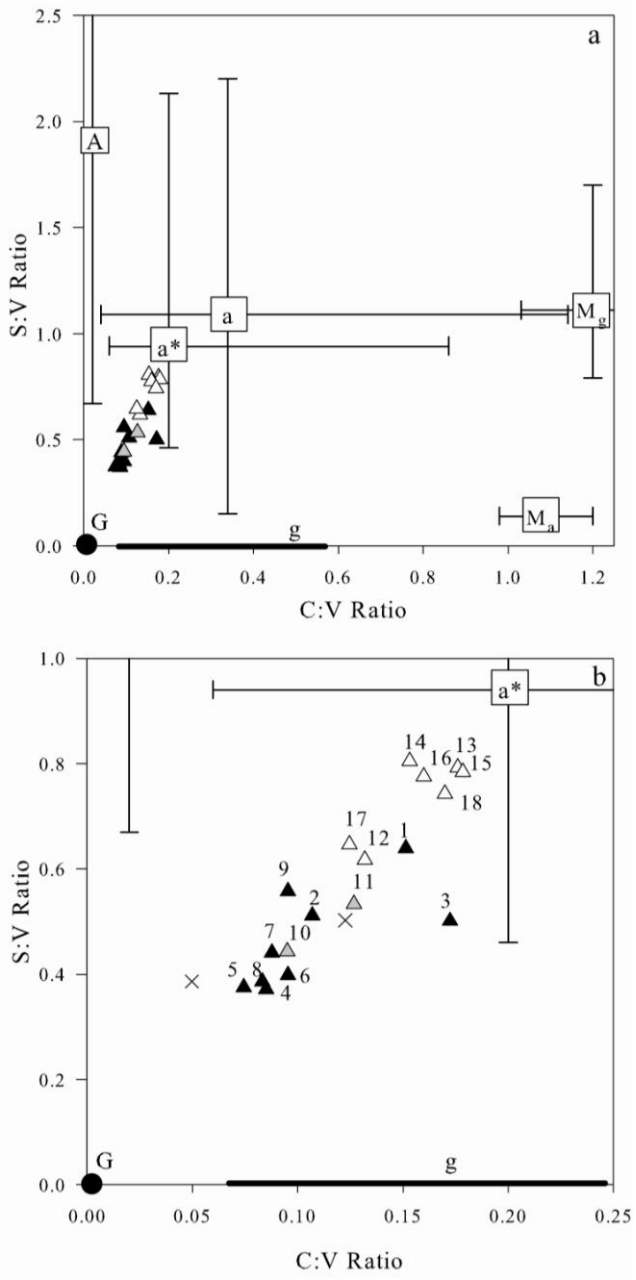

Figure 3.3. The S:V and C:V ratios of Mekong River FPOM and vegetation end-member tissues specific to the Mekong River Basin. FPOM samples from different seasons are differentiated using the same symbols described in Fig. 3.2. End-member types are indentified as follows: angiosperm woods (A), angiosperm leaves (a), angiosperm barks (a*), gymnosperm woods (G), gymnosperm leaves (g), grasses (M_g), and floating aquatic plants (M_a). Error bars indicate the range of values observed for each tissue type. Gymnosperm values were taken from [*Hedges and Mann*; 1979] and [*Opsahl and Benner*, 1995] as none were analyzed in this study. FPOM is plotted amongst all the end-members in Fig. 3.3a, whereas Fig. 3.3b is scaled with a higher resolution so that seasonal patterns can be observed. Samples are numbered in the order that they were collected, with the first collection occurring close to the beginning of the low-water period. Two additional samples from the Upper Basin are plotted in Fig. 3.3b, which are represented with an "x".

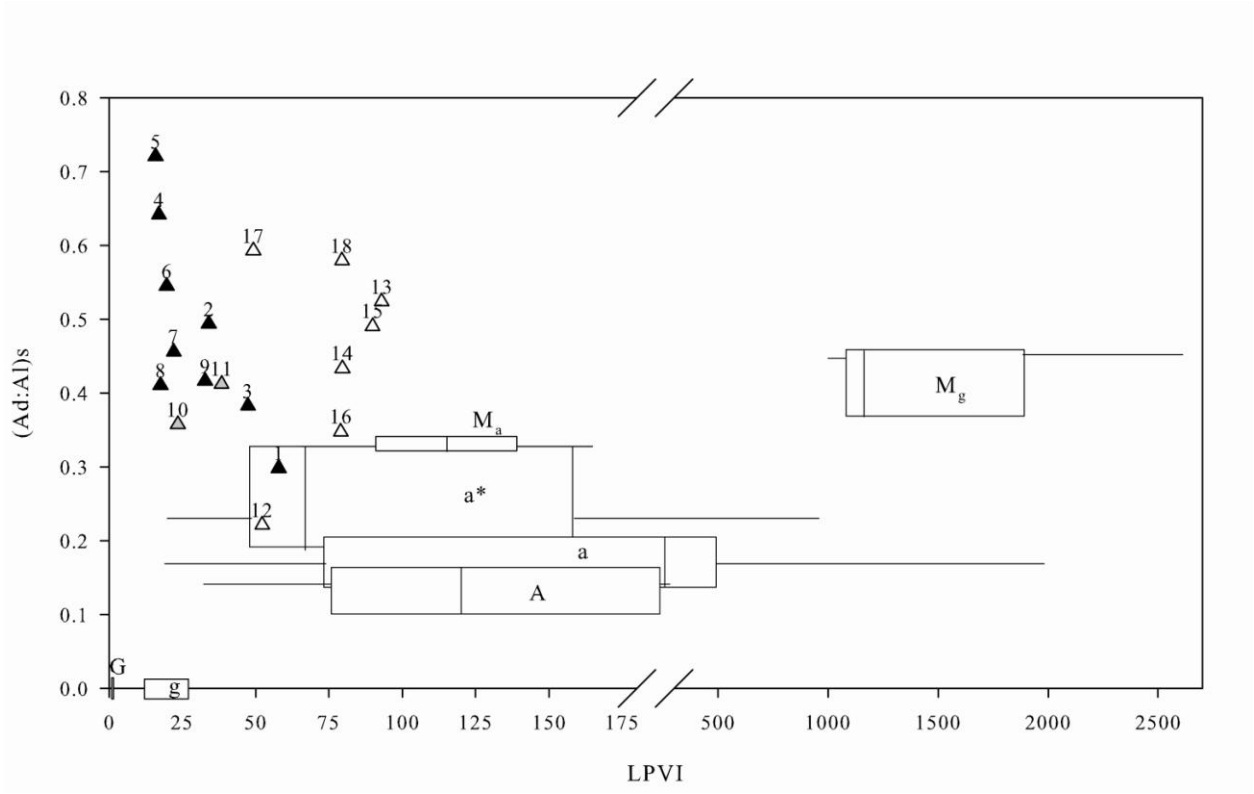

Figure 3.4. Lignin Phenol Vegetation Index as a function of the acid-to-aldehyde ratio of syringyl phenols of Mekong River FPOM samples. Symbols are as in Fig. 3.2, and vegetation tissue is identified as in Fig. 3.3. The LPVI and (ad:al)s of angiosperm end-members from this study are displayed using box-and-whisker plots. The range of LPVI values for gymnosperm samples are taken from [*Tareq et al.*, 2004]. Samples are numbered in the order that they were collected (see the Fig. 3.3 caption).

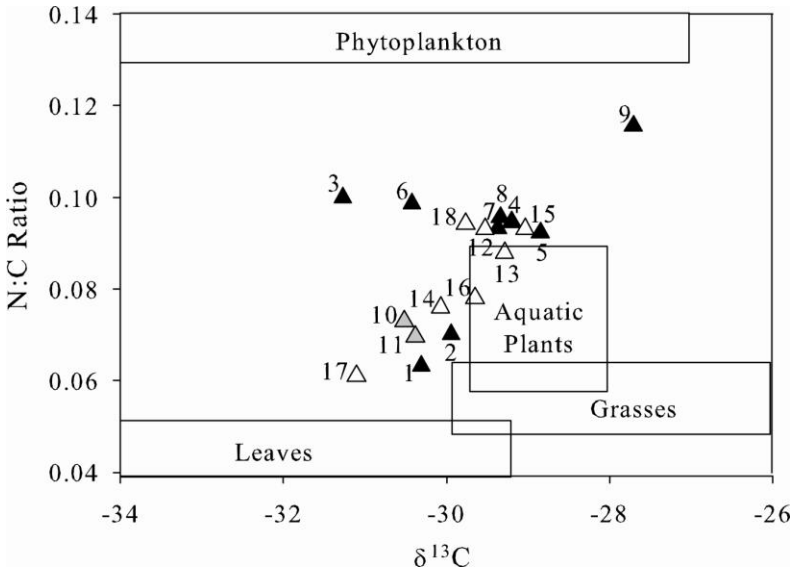

Figure 3.5. Partitioning of Mekong FPOM among end-members sources using $\delta^{13}C$ and N:C ratios. Symbols are described in the caption of Fig. 3.2, and each point is labeled as in Fig. 3.3. Boxes indicate the range of values reported for each end-member. The $\delta^{13}C$ and N:C ratios of vascular plants are from Table 3.1 in this study. The N:C of phytoplankton was calculated from the C:N ratios reported for phytoplankton from the Amazon Basin (5 to 8) [*Devol and Hedges*, 2000]. The $\delta^{13}C$ of phytoplankton was estimated from the $\delta^{13}C$ of DIC and the fractionation that occurs between DIC and phytoplankton (-21 to -24‰) [*Tan and Strain*, 1983]. Because DIC ranged from -6‰ to -14‰ from the dry to the rainy season [J. E. Richey, *unpublished data*], autochthonous OM should be between -27‰ to -38‰. However, during the dry season, it should be on the enriched side of this range. The δ^{13} of grasses extends to -11.9‰, which is beyond the scale of this figure.

Chapter 4: Young plant-derived organic matter is consistently exported from sediments of the Mekong River Basin despite high variability in the age of the bulk sediments

Vascular plants are the largest pool of living biomass on earth, and therefore represent a significant component of the actively-cycled pool of organic carbon [*Bianchi et al.,* 2011]. Changes in the residence time of plant-derived carbon in tropical ecosystems will have major implications for the concentration of carbon dioxide in the atmosphere. Rivers integrate biogeochemical processes occurring across the catchment, making the organic matter exported by rivers a useful tool to determine the residence time of different pools of carbon in terrestrial ecosystems [*Galy et al.,* 2011]. However, few studies have been able to constrain the sources and cycling time of the organic matter carried by rivers due to the complex nature of this material. Here we use radiocarbon dating of individual lignin phenols (a major component of vascular plants) to show that lignin carried by fine suspended sediment of the Mekong River of Southeast Asia is consistently young (i.e. produced within the last 15 years) and represents between 15-76% of the fine particulate organic carbon carried by the Mekong. This modern lignin is present even when the ages of the particulate pool vary seasonally across the hydrograph, from contemporary during the rainy season, to over 3,000 years old during the rising-water period. Therefore, our results demonstrate that plant-derived organic matter is cycled on short time-scales across the basin, consistent with recent work in soils [*Rasse et al.,* 2006; *Marschner et al.,* 2008]. The tropics are anticipated to experience unprecedented heat more within the next two decades [*Diffenbaugh and Scherer*, 2011]. Considering the recent debate on how the tropics will respond to rising temperatures, our results are a starting point from which future measurements of plant residence times can be assessed to further our understanding of the response of terrestrial ecosystems to climate change.

INTRODUCTION

Tropical terrestrial ecosystems are currently a source of carbon (C) to the atmosphere, although there is high uncertainty in the magnitude of this flux (1.5 ± 1.2 Pg) [*Aumont et al.*, 2001; *Houghton et al.*, 2007]. Climate change anticipated over the next century will have consequences for the balance of C in these ecosystems. However, little consensus has arisen regarding the potential impacts of such change on C cycling due to the complexity of assessing how increased temperatures will affect vascular plants and the subsequent cycling of plant-derived organic matter (OM) in soils. Some studies suggest that drought increases forest productivity [*Saleska et al*., 2003; *Hutyra et al.*, 2007], whereas others indicate increasing temperatures will result in a decline in tree growth rates [*Clark et al.*, 2003; *Feely et al*., 2007]. It is clear that any change in net primary productivity will affect the ability of soil OM to store C. C stocks in soils result from the balance between inputs from leaf and root detritus and outputs dominated by the efflux of carbon dioxide (CO_2) produced through microbial decomposition of soil OM [*Davidson and Janssens*, 2006]. Although the rate at which microbial enzymes decompose OM increases with temperature, the mechanisms controlling temperature sensitivity for the decomposition of different pools of OM remains poorly understood [*Schmidt et al*., 2011]. Therefore, if increased inputs of plant-derived C exceed microbial decomposition, soils could exert a negative feedback on climate change by increasing the rate at which they store C. Alternatively, if decomposition exceeds plant inputs, a positive feedback would be expected [*Davidson and Janssens*, 2006]. Considering that the tropics account for at least 30% of the global terrestrial primary production [*Malhi et al*., 2006; *Field et al.*, 1998], even a small change in net C fluxes can have major implications for atmospheric CO_2 concentrations.

The residence time (RT) of C in terrestrial ecosystems is determined by the size of the reservoir and the rate at which C is exchanged between reservoirs. Accordingly, many of the

factors that influence the RT of vascular-plant derived OM in soils are projected to be impacted by climate change. Molecular structure has classically been thought to govern the stability of OM in soils, but recent work suggests that stability is strongly affected by physiochemical and biological processes occurring at the ecosystem level [*Schmidt et al.,* 2011]. The heterogeneity of soils makes it difficult to extrapolate the RT of a single pool of C found in soils to the watershed, given that soils vary considerably with changes in bedrock, microclimate, disturbance, relief, and biological activity. Alternatively, soil-derived OM is mobilized into streams and rivers by erosion and fluvial transport, making the material exported at the mouth of certain rivers an integrative account of the biogeochemical processes controlling OM composition across the catchment [*Galy et al.,* 2011]. As such, analysis of the radiocarbon content ($\Delta^{14}C$) of select biomarkers exported by rivers offers the ability to estimate residence times of a particular pool of C in a catchment.

The complexity of riverine OM makes it difficult to determine the RT of terrestrial C as it is derived from a mixture of sources with contrasting radiocarbon ($\Delta^{14}C$) contents [*Raymond and Bauer,* 2001; *Mayorga et al.,* 2005]. Petrogenic C contains ^{14}C-depleted C ($\Delta^{14}C$ of -1000‰) [*Dickens et al.,* 2004; *Drenzek et al.,* 2009; *Galy et al.,* 2011], whereas the $\Delta^{14}C$ of phytoplankton and vascular plants is determined by variability in the C source utilized during photosynthesis [*Raymond et al.,* 2004; *Mayorga et al.,* 2005; *Galy et al.,* 2011]. Here we take advantage of recently developed methodology [*Ingalls et al.,* 2010] to determine the $\Delta^{14}C$ of lignin-derived phenols isolated from suspended sediments carried by the Mekong River (Fig. 4.1). Lignin is ideal for this study as it is diagnostic for vascular plants, abundant, and transported fluvially [*Hedges et al.,* 1997; *Huang et al.,* 1999]. As the $\Delta^{14}C$ value obtained for an individual lignin phenol is derived from a composite with varying ages, it can be used as a proxy for the average RT of vascular plant C exported by rivers within the basin. Because the

coarse fraction of C was excluded from suspended sediment (i.e. > 63 μm), the $\Delta^{14}C$ of lignin analyzed here is representative of the remnants of vascular plants found in soils. Comparisons between the $\Delta^{14}C$ of lignin with that of the bulk fine particulate organic carbon (FPOC) further enables FPOC to be partitioned amongst end-members.

The Mekong River (Fig. 4.1) lies within the top 10 rivers in the world with respect to sediment load and discharge [*Milliman and Syvitski*, 1992; *Mekong River Commission*, 2005]. The importance of various sources of OM to Mekong sediments varies substantially between the dry and rainy seasons [*Ellis et al.*, 2012b]. Hence, we measured the concentration, the $\Delta^{14}C$, and the stable isotopic ($\delta^{13}C$) composition of dissolved organic carbon (DOC) and FPOC between September 2008 – February 2010. We also measured C:N ratios, the weight percent organic carbon (wt% OC) of fine particulate OM (FPOM), as well as the $\Delta^{14}C$ of particulate lignin phenols exported just above the mouth of the Mekong in Cambodia during the rainy season (September 2008) and the rising-water season (June 2009 and July 2009).

RESULTS AND DISCUSSION

The close coupling between the $\Delta^{14}C$ of the FPOC and suspended sediment concentrations is striking (Fig. 4.2a and b). $\Delta^{14}C$ values range from -327.7 ± 1.6‰ to 25.9 ± 2.2‰, with the most contemporary C exported by the Mekong during the flood season (in associated with the highest sediment concentrations), whereas the oldest C was transported at the end of the dry season/beginning of the rising-water period (with low sediment concentrations) (Table 4.1, Table S4.1). Values of $\Delta^{14}C$ higher than zero indicate that $^{14}CO_2$ was fixed from the atmosphere recently ($\Delta^{14}C$ reached a maximum close to 900‰ in 1964 due to the testing of nuclear weapons, and has subsequently decreased as $^{14}CO_2$ exchanged with the surface ocean and biosphere [*Levin and Hesshaimer*, 2000; *Randerson et al*. 2002]). Our post-bomb $\Delta^{14}C$ results suggest that the youngest FPOC is dominated by organic matter fixed within the last 50

years (with an average $\Delta^{14}C$ value of 25.9± 2.2‰), while the oldest predominantly contains organic C that exceeds 3,000 years in age (with an average Δ14C value of -327.7 ± 1.6‰). The $\Delta^{14}C$ of DOC ranged between -55.7 ± -11.2‰ to 51.6 ± 32.5‰, with no detectable seasonal trends (Fig. 4.2b, Table S4.2). The enrichment of DOC relative to POC has been observed across many rivers and estuaries [*Raymond and Bauer*, 2001; *Mayorga et al.*, 2005], with the younger ages likely due to the leaching of young soil OM (including leaf litter) and the short transit times required for DOC export [*Raymond and Bauer*, 2001].

The $\Delta^{14}C$ of the lignin phenols collected during the rising- and high-water periods demonstrate that young plant-derived OC is consistently exported from the basin, despite the high ^{14}C variability in the bulk C. The concentration-weighted average values ranged between 91 ± 27‰ to 92 ± 4‰, whereas the $\Delta^{14}C$ of FPOC varied between 25.9 to -308.4‰ during these intervals (Fig. 4.2b). The $\Delta^{14}C$ of individual lignin monomers also varied minimally, with all samples having post-bomb $\Delta^{14}C$ values (Fig. 4.3, Table S4.3). Further, there were no trends in ^{14}C ages across lignin phenol families or functional groups. Atmospheric ^{14}C levels were last at 91-92‰ between 1996-1997, suggesting that vascular plants exported by rivers have a RT of ~ 15 years. Although similar atmospheric $\Delta^{14}C$ values were observed during the rising of the bomb curve (post-bomb ages were calibrated using CaliBomb [*Reimer et al.*, 2004; Hua and Barbetti, 2004], the consistency in the ^{14}C values of the individual phenols suggests that lignin is more recent and association with the $\Delta^{14}C$ values of the declining portion of the bomb curve [*Randerson et al.*, 2002].

Lignin has classically been viewed as recalcitrant [*Dagley*, 1975]. Recent work suggests otherwise, with lignin dynamics in soils being characterized by two pools. In the rapidly-cycling pool, over 90% of the lignin (in the form of undegraded plant residues) is degraded on timescales less than a year [*Rasse et al.*, 2006; *Marschner et al.*, 2008]. The remaining pool has a RT near

two decades, and appears to be associated with fine minerals [*Rasse et al*., 2006; *Marschner et al*., 2008 and references cited therein]. In this study, lignin appears to lie in the slowly-cycling pool, whose persistence in soils is likely controlled by a myriad of environmental factors, including primary production, compound chemistry, substrates to "prime" decomposition, availability of decomposers, reactive mineral surfaces, water, and oxygen [*Bianchi et al*., 2011; *Schmidt et al*., 2011]. However, this does not mean that it is unreactive. The similarity between the $\Delta^{14}C$ of DOC with that of particulate lignin suggests that there may be a close coupling between these pools via sorption and desorption of lignin from minerals [*Hernes et al.*, 2007] amongst other factors. However, the ^{14}C value of DOC suggests there are additional sources of old C that are important to the dissolved pool.

The seasonal variability in the $\Delta^{14}C$ of Mekong FPOM appears to be due to the several contributions of different ^{14}C sources within it. Previous work suggests the contribution of plants to lowland FPOC diminishes during the low-water period due to the increasing influence of phytoplankton [*Ellis et al.*, 2012b]. Although C:N ratios and $\delta^{13}C$ values of FPOM vary little between seasons [Table S4.1; *Ellis et al.*, 2012b], the elevated dry-season wt % OC values are suggestive of phytoplankton (Fig. 4.2c) [*Meybeck et al.*, 1982]. The $\Delta^{14}C$ of phytoplankton can be estimated from the $\Delta^{14}C$ of DIC, which was previously measured to be -82‰ and -106‰ during the low and rising-water periods during 2004, respectively. Considering that the $\Delta^{14}C$ of FPOC is more depleted (i.e. older) than this during the dry season, an additional aged C source is needed. We propose that this source is derived from the Upper Basin (Fig. 4.1), which contributes to 35% of the Mekong's discharge during the dry/early rising-water period, with snowmelt from mountains and the Tibetan Plateau being an important source of runoff. Its contribution to discharge is only 16% across the entire year [*Mekong River Commission*, 2005; *Kummu and Varis*, 2007, *Costa-Cabral et al*., 2008], as tributaries from the Lower Basin

dominate the Mekong's discharge during the rainy period [*Mekong River Commission*, 2005; *Costa-Cabral et al.,* 2008]. Source rocks collected from other rivers draining the Himalayas have been shown to contain petrogenic C, with the soil component exported by rivers emanating from the Tibetan Plateau being significantly aged [*Galy et al*. 2008; *Galy et al.* 2011]. Therefore, the Upper Basin appears to be the source of the aged C (of thousands of years old) exported by the Mekong during the low/early rising-water period. The Lower Basin lies entirely within tropical latitudes, where high precipitation and solar radiation leads to high primary production rates [*Clark et al*., 2001]. Thus, the young age of rainy-season FPOM suggests that the Lower Basin is a source of young soils, which are mobilized during the monsoon rains. This conclusion is corroborated by previous work suggesting that the dry-season lignin composition of Mekong FPOM is similar to Upper Basin vegetation, whereas rainy season FPOM resembles Lower Basin vegetation [*Ellis et al.*, 2012b].

To assess how C is partitioned amongst its possible sources, we constructed a mixing model and applied it to samples for the periods for which the $\Delta^{14}C$ of lignin was determined (Supplementary Discussion). For the high-water period, the $\Delta^{14}C$ of FPOC was assumed to be derived from plants ($\Delta^{14}C = 91.5‰$) and other soil-derived OM ($\Delta^{14}C$ is variable). The fraction of the plant-derived OM was estimated from lignin normalized to organic C contents of FPOM and vascular-plant end-members [*Ellis et al.*, 2012b]. During the rising-water period, we assumed that in situ production by phytoplankton ($\Delta^{14}C$ of -106‰) was responsible for organic C present in excess of high-water values, enabling the $\Delta^{14}C$ of the non-phytoplankton component to be determined. A second mixing model (as described for the high-water period) was then performed. Our results indicated that as the influence of phytoplankton decreased into the flood period, the contribution of vascular plants increased: Plants represented 15-33% of the FPOM during June 2009, and 35-76% during the rainy season (Table 4.2). Further, the $\Delta^{14}C$ of the soil

pool exported during June was more depleted (older) than during September. This is consistent with the Upper Basin exerting a strong influence during the rising-water season.

These results demonstrate that it is possible to obtain an average RT for vascular plants with fine resolution due to advances in our ability to date very small amounts of C [*Santos et al.* 2010]. Accordingly, we can detect change within a watershed at finer-scales than that which has been previously possible. Just as time series measurements in the ocean have provided insights into the marine C cycle, a similar approach conducted at the mouths of rivers can provide valuable insights as to how C cycling in terrestrial ecosystems is affected by climate change. For instance, if the RT of lignin increases, this implies that the catchment may be storing more C. Tropical biomes are most likely to experience unprecedented heat first [*Diffenbaugh and Scherer*, 2011**]**, and many tropical river catchments are becoming increasingly stressed by land-use change and impoundments. In the Mekong alone, eight mainstem dams are currently being installed in the Upper Basin, and up to eleven mainstem reservoirs may be constructed in the Lower Basin over the next several decades [*Mekong River Commission*, 2009]. Accordingly, it is imperative that biogeochemists develop an approach for assessing the effect of these changes on C storage in the tropics.

FURTHER METHODOLOGY

Sample collection and supporting analyses

Samples were collected on the Mekong River north of the confluence with the Tonle Sap River in Cambodia (11.595617°N, 104.94299°E), above any influence of salinity of the South China Sea. Samples were collected at mid-depth as described in *Ellis et al.* [2012b]. Coarse suspended sediment was first removed using a 63 μm sieve. Water was than filtered through precombusted QM/A quartz filters for radiocarbon analysis of FPOC. Filters were dried at 60°C

for 24 hours and stored for up to two years in precombusted foil. All supporting organic measurements (i.e. $\delta^{13}C$, wt % OC, C:N ratios, FSS and FPOC concentrations) were conducted as described in *Ellis et al.* [2012b]. We also collected large volumes of sieved water (up to 1,000 L) for radiocarbon analysis of the lignin phenols in FPOM. Fine sediments were concentrated within 48 hours using a Sharples T1 continuous flow centrifuge operated as in *Hedges et al.* [1986]. Sediments were then frozen immediately and stored up to two years. Sieved water was also filtered through GF/F filters to yield DOC, and the filtrate was collected into multiple 500-mL polycarbonate containers (for $\Delta^{14}C$ and $\delta^{13}C$) that had previously been soap and acid-washed, and then rinsed copiously with milliQ. Samples were stored in precombusted glass vials for measurements of DOC concentration. Samples were frozen immediately (for 1-2 years) and thawed just prior to analysis. DOC concentrations were measured on a Shimadzu TOC-V CPH carbon and nitrogen analyzer, and were acidified as in *Ellis et al.* [2012a].

Bulk radiocarbon analyses

Quartz filters containing the FPOC were acidified following *Komada et al.* [2008] prior to being transferred to 9 mm OD quartz tubes, where they were sealed and combusted following a specific protocol [*Santos et al*., 2007]. Cryogenically purified CO_2 was converted to graphite, and bulk radiocarbon analysis was performed at the Keck Carbon Cycle Accelerator Mass Spectrometry (KCCAMS) facility at the University of California, Irvine. Procedural blanks were conducted for both FPOC and DOC to assess contamination coming from the methodology reported here. DOC samples (between 250 mL to 500 mL) were acidified to pH 2 and dried by heating at 60°C using ultrapure N_2 gas. The concentrated sample was transferred to a precombusted quartz tube, where the drying process was completed using ultraclean techniques.

The 6 mm tube was then inserted into a 9 mm tube, sealed under vacuum, and combusted. The $\delta^{13}C$ of DOC was measured by following this same approach.

Lignin Analyses

Sediment samples were subject to oxidative hydrolysis by CuO in a microwave to liberate phenols from their complex polymers [*Goni and Montgomery*, 2000]. Between 7-12 g of sediment were analyzed for each sampling event, with 4 to 5 rounds of microwaving per sample. An aliquot of each sample was quantified by gas chromatography flame ionization detection (GC-FID) after derivitization with trimethylsilyl ethers and esters. Lignin phenols were purified using high performance liquid chromatography (HPLC) analysis and radiocarbon dated following *Ingalls et al.* [2010]. An initial separation was conducted in reserve phase, which was then followed by normal phase chromatography to obtain pure aliquots of individual lignin monomers. The samples were sent to the KCCAMS/UCI facility for AMS analyses, where they were reduced to graphite as in *Santos et al.* [2004] and *Santos et al.* [2007]. Procedural blanks were run of the entire analysis and used to correct ^{14}C values by accounting for contamination derived from the analytical protocol [*Ingalls et al.* 2010]. The modern C contamination was 0.5 ± 0.25 μg C (i.e. $\Delta 14C = 0‰$), whereas the dead C contamination was 0.8 ± 0.4 μg C. The age of each phenol was corrected as in *Santos et al.* [2007]. Further, all $\Delta^{14}C$ values were corrected for isotopic fractionation as described in *Santos et al.* [2007].

Table 4.1. Variability in particulate and dissolved OC composition and concentration[a].

Stage	Δ^{14}C FPOC	δ^{13}C FPOC	% OC of FSS	[FPOC]	Δ^{14}C DOC	δ^{13}C DOC	[DOC]
Rising	-267 ± 59 (2)	-26.7 ± 0.6 (4)	2.0 ± 0.2	1.9 ± 0.4	-3 (1)	-27.2	3.7 ± 0.5 (4)
High	-51 ± 62 (4)	-26.5 ± 0.6 (10)	1.3 ± 0.2	2.6 ± 0.6	30 ± 18 (4)	-26.7 ± 0.2	3.8 ± 1.8 (9)
Falling	-103 ± 20 (3)	-26.8 ± 0.8 (5)	2.1 ± 0.6	1.6 ± 0.9	-7 ± 44 (3)	-26.3 ± 0.8	5.1 ± 2.9 (4)
Low	-254 ± 68 (3)	-27.2 ± 1.4 (6)	4.8 ± 2.6	0.5 ± 0.1	52 (1)	-	2.5 ± 1.0 (6)

[a]Data are reported in mean ± s.d. (number of samples). The number of samples for % OC and [FPOC] is the same as for δ^{13}C of FPOC, whereas the number of samples for δ^{13}C of DOC equals that of Δ^{14}C of DOC. Δ^{14}C and δ^{13}C are in per mil (‰), whereas units of concentration are in mg/L.

Table 4.2. Apportioning of FPOC amongst end-members[a] during the rising and high-water seasons.

Date	Stage	%Phyto-plankton	% Vascular Plant	% Soil	Δ^{14}C Soil[b] (‰)
June 2009	Rising	26-49	15-33	30-58	-517 to -970
July 2009	Rising	10-38	26-56	26-64	-275 to -792
Sept 2008	High	0	35-76	24-65	-10 to -179

[a]% Phytoplankton, % Vascular Plant, and % Soil denote the percentage of FPOC that originates from these three pools, respectively, as calculated as described in Appendix 1.
[b]Δ^{14}C Soil denotes the range of values expected for the soil pool.

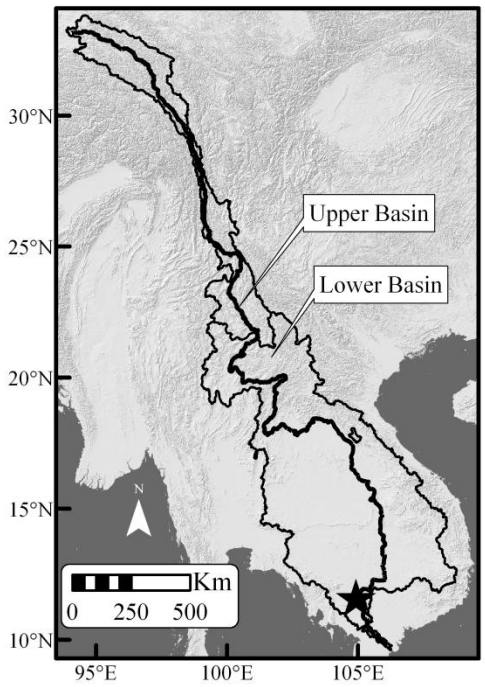

Figure 4.1. The Mekong basin of southeast Asia and the study site. From its headwaters on the eastern boundary of Tibetan Plateau, the Mekong River flows 4,800 km southward through China, Myanmar, Thailand, Lao People's Democratic Republic (Lao PDR), Cambodia, and Viet Nam until reaching the South China Sea [*Hori*, 2000]. The climate of the Mekong Basin varies considerably, with a cool, dry, temperate climate dominating at its headwaters in the Tibetan Plateau, where precipitation falls largely as snow, changing to a tropical climate in the Lower Basin (below China) [*Costa-Cabral et al*., 2008]. Further, its climate is dominated by a rainy season brought by the Southwest monsoon, and a dry season affiliated with the arrival of the northeast monsoon [*Mekong River Commission*, 2005]. The Upper and Lower Basins denote the catchment above and below China, respectively. The star denotes the sampling location.

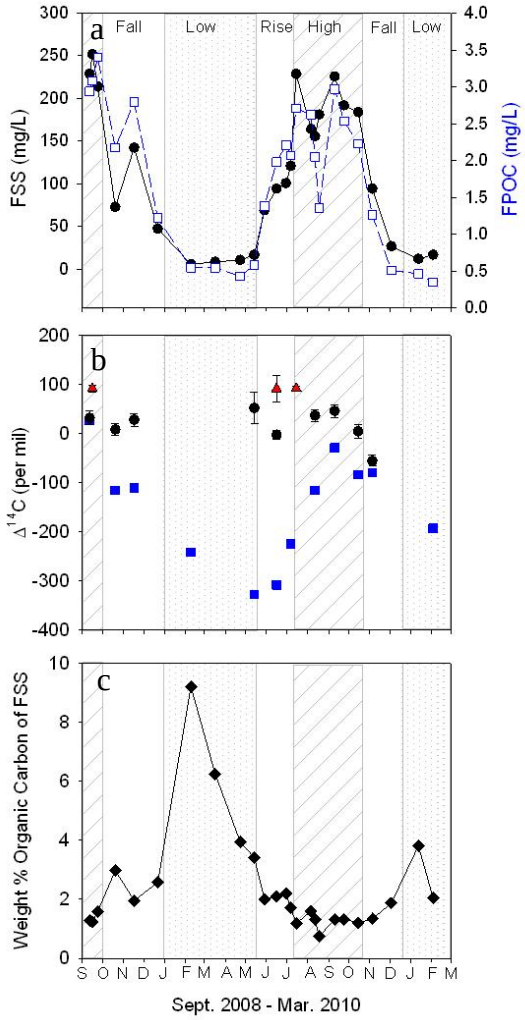

Figure 4.2. Seasonal variability in the concentration and composition of the material transported by the Mekong River. Dashed shading represents the high-water period, whereas light gray shading represents the dry season. (A) Variability in fine suspended sediment (FSS) (circles) and FPOC (squares) concentrations. (B) Seasonal changes in the $\Delta^{14}C$ of FPOC (squares), DOC (circles), and lignin (triangles) associated with FPOC. For each time period, the $\Delta^{14}C$ of lignin is the concentration-weighted average value. (C) Results for variability in the wt % OC content of FSS. Error bars represent one σ_x and are not shown if the symbol is larger than the error bars.

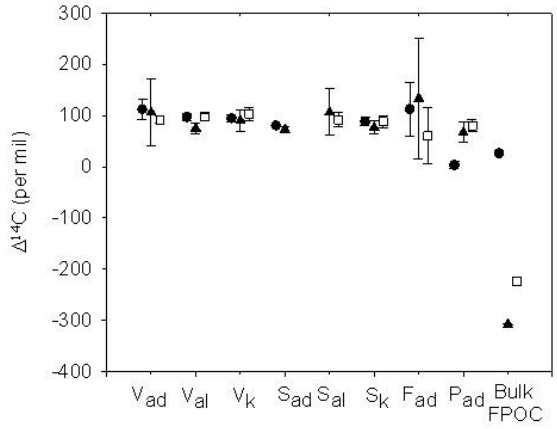

Figure 4.3. The $\Delta^{14}C$ of individual lignin monomers and bulk FPOC. Circles, triangles, and squares denote the sampling events of 10-17 September 2008, 15-19 June 2009, and 2-6 July 2009, respectively. The abbreviations for the individual monomers are as follows: V_{ad} (vanillic acid), V_{al} (vanillin), V_k (acetovanillone), S_{ad} (syringic acid), S_{al} (syringaldehyde), S_k (acetosyringone), F_{ad} (ferulic acid), P_{ad} (p-coumaric acid). Error bars are as described in figure 4.2.

Chapter 5: Sources and Temporal Variability of Branched and Isoprenoid Tetraether Lipids Exported by a Large Tropical River

INTRODUCTION

The organic carbon (OC) discharged by rivers is a key component of the global carbon cycle. Determining if this material will be permanently buried in marine sediments or returned to the atmosphere as carbon dioxide through processing in rivers is critical to accurately predicting the composition of the atmosphere and future climate change [*Hedges et al.,* 1992; *Hedges and Keil,* 1995; *Richey et al.,* 2002]. Rivers export between 0.38 - 0.53 Pg of OC each year [*Degens et al.* 1991; *Stallard et al.,* 1998; *Schlesinger and Melack,*1981]. Although much of this flux is mineralized within seawater and surficial sediments, terrigenous carbon burial is on the same order of magnitude as that of marine carbon burial in coastal sediments [*Schlunz and Schneider*, 2000]. Accordingly, terrestrially-derived organic matter preserved in marine sediments in coastal regions contains important archives for the reconstruction of changes in land-use, paleoclimate, and paleonvironmental change on continents over both short and long time-scales.

Accurate accounting of the proportion of terrestrial verses marine-derived organic matter preserved in coastal sediments is of considerable interest due to the paradox that less terrestrial carbon is preserved in ocean sediments than that predicted from riverine fluxes [*Hedges et al., 1997*]. A new proxy has been developed to trace the proportion of terrestrially verses marine-derived organic matter in coastal sediments, known as the branched/isoprenoid tetraether (BIT) index [*Hopmans et al.*, 2004]. The index is based on the relative abundance of two types of glycerol dialkyl glycerol tetraether (GDGT) membrane lipids occurring in these sediments: branched and isoprenoid lipids. Branched tetraethers (brGDGT I-III) (see Fig. 5.1 for structures) are derived from the membranes of anaerobic bacteria found ubiquitously in soils and peat bogs

[*Weijers et al,.* 2006], thus suggesting that brGDGT I-III are appropriate tracers for soils. Based on the stereoconfiguration of the glycerol backbone, brGDGTs are thought be derived from bacteria [*Weijers et al.,* 2006], and it has recently been suggested that *Acidobacteria* is a likely source [*Weijers et al.,* 2009; *Peterse et al.,* 2010; *Sinninghe-Damste et al*., 2011]. Crenarchaeol (GDGT IV) is the isoprenoid GDGT utilized in the BIT index (Fig. 5.1). This membrane lipid is produced by a group of archaea now provisionally assigned to Thaumarchaea (formerly crenarchaea) [*Sinninghe Damste et al.,* 2002; *Brochier-Armanet et al*., 2008; *Spang et al.,* 2010]. The BIT index is typically close to zero in open ocean sediments due to the lack of branched GDGTs and high concentrations of crenarchaeol. Originally, terrestrial end-members were suggested to have a theoretical BIT index value of 1 due to the presence of GDGTs I-III, but no GDGT IV. The terrestrial end-member has since been revised to be as low as values of 0.8 due to significant production of crenarchaeol in soils, peat bogs, and river sediments [*Walsh et al.,* 2008; *Weijers et al. 2006b*; *Kim et al.,* 2007; *Tierney and Russell,* 2009].

Although the BIT index has been widely applied since its original publication to assess terrestrial carbon burial in marine sediments, the variability of the BIT index and brGDGT I-III composition in suspended sediment carried by rivers remains largely uninvestigated. Because sediment exported by rivers just above the delta represents the most downstream point within a watershed that is uninfluenced by marine processes, the compositional signatures found at such locations should be viewed as the baseline terrestrial signature of material delivered to the ocean. Because the organic composition of material carried by rivers can vary significantly between seasons [*Paolini et al,* 1995; *Coynel et al.,* 2005; *Spencer et al, 2010*], the composition of the material delivered can only be known if the river is sampled at regular intervals throughout the year. Further to understand the source of riverine POM, a survey of sites throughout the watershed is also necessary.

Recently, the assumption that brGDGTs are produced only in soils has been questioned due to multiple lines of evidence suggesting in situ production of brGDGTs in lakes. Most recently, Tierney et al. [2012] provided support for this hypothesis based on measurements of intact and core brGDGT and isoprenoid GDGTs found in soil and lake sediment samples collected from a pond from Rhode Island. Intact polar head groups bound to tetraether lipids, such as sugars or phospholipids, are indications of viable cells [*Koga et al.*, 1993; *Schouten et al.,* 2008]. After death, polar head groups are enzymatically cleaved on time scales that range from days to weeks [*White et al.,* 1979, *Harvey et al.,* 1986; *Lipp et al.,* 2008], leaving behind core GDGTs. Therefore, based on the difference in the absolute concentration and the percentage of intact brGDGTs between soils and lake sediments, Tierney *et al.* [2012] concluded that in situ production was occurring in a Rhode Island pond. Thus, their results appear to offer an explanation as to why BIT index values between 0.02 to 1.0 were reported for particulate organic matter (POM) samples collected in a series of European lakes [*Blaga et al.,*. 2009]. However, it is unknown how widespread in situ production is across environmental types. Clearly if in situ production occurs in rivers, it has the potential to affect the BIT index and interpretations of terrestrial carbon preservation.

Here we determine the variability of the BIT index of suspended sediments carried by the Mekong River, in Cambodia, just upstream of the delta, over the course of one year. To aid in the interpretation of the variability, other measures of terrestrial carbon, such as lignin-derived phenols, N:C ratios, and $\delta^{13}C$ were concurrently measured for these same suspended sediments. A series of soils and sediment samples from pristine rainforest soils, rice paddies, river and lake beds, and river banks were analyzed to assess possible sources of tetraether lipids to the riverine suspended particles. Lastly, the proportion of intact lipids derived from viable cells was examined in various environments to further understand the conditions under which these lipids

are produced. In addition to impacting the BIT index, analysis of intact brGDGTs I-III is also relevant to studies of the MBT (methylation index of branched tetraethers) and CBT (cyclisation ratio of branched tetraethers) proxies, which are based on the relative degree of cyclization and number of methyl branches of brGDGTs. These proxies are used to reconstruct mean air temperature and soil pH [*Weijers et al.,* 2007; *Tierney and Russel*, 2009; *Sun et al*., 2011]. Therefore, if production is limited to niche environments or occurs in the river itself, there are implications for climate reconstructions based on this proxy. As very nearly "ophan" biomarkers, it is imperative to learn about their production.

The Mekong River, of Southeast Asia, was chosen for this study as it is a significant source of sediment to the ocean, ranking within the top ten rivers in the world [*Milliman and Svytski,* 1992; *Mekong River Commission*, 2005]). Furthermore, out of the 1.67 Mt of fine particulate organic carbon (FPOC) exported yearly, there is significant variability in the type of terrestrially-derived organic matter exported between the dry and rainy seasons [*Ellis et al.*, 2012b], suggesting that this river is an appropriate candidate to observe seasonal changes GDGT composition and in the BIT index. Given that anoxic conditions that may persist throughout the watershed during the rainy season, the Mekong catchment offer a diverse array of environmental types over which GDGT distribution on land can be assessed.

METHODS

Study area

The source waters of the Mekong River are found in the mountains of the Tibetan Plateau at an elevation of 5,000 m. During its 4,800 km journey to the South China Sea, it flows through China, Myanmar, the Laos People's Democratic Republic, Thailand, Cambodia, and Viet Nam to the South China Sea (see Fig. 5.1 in *Ellis et al.*, [2012b]) [*Hori,* 2000]. The drainage basin

(795,000 km^2) has been divided into the Upper and Lower Basin, which refer the region of the catchment above and below China, respectively. While in the Upper Basin, the Mekong descends 4,000 m in an incised channel through narrow gorges [*Mekong River Commission*, 2005]. As it enters the Lower Basin, the terrain is still almost entirely mountainous, but then the river velocity slows, with the channel widening. An extensive floodplain develops once the river reaches Kratie, Cambodia. Just past the confluence with the Tonle Sap River, the first distributaries form at Phnom Penh [*Mekong River Commission*, 2005].

The Mekong River basin is located in the humid tropics and is therefore characterized by a distinct rainy and dry period, corresponding to the arrival of the southwest and northeast monsoons, respectively. The dry season generally occurs during December through May, when discharges are less than 2,500 m^3/s. However, discharge can reach 40,000 m^3/s during October, at the height of the rainy season [*Mekong River Commission*, 2005]. The Upper Basin exerts more influence on the hydrograph during the dry season, when snowmelt from mountains are a significant source of flow to the Lower Mekong. However, during the rainy period, the Lower Basin exerts considerably more influence, with the left bank tributaries entering from Laos exerting significant influence on the hydrograph [*Mekong River Commission*, 2005; *Kummu and Varris*, 2007; *Wang et al.*, 2011].

Times series measurements of Mekong River suspended sediment composition were collected on the Mekong River near the city of Phnom Penh (11.595617°N 104.94299°E). This location was chosen because it lies just above the delta, therefore making it integrative of the entire fresh-water portion of the Mekong Watershed. This site was also selected because it is unaffected by the Tonle Sap River, as it is located upstream of the confluence with this river. The Tonle Sap River, which is connected to the Tonle Sap Lake, is unique in that the flow of the river reverses between the dry and rainy periods. During the rainy season, the Mekong River

flows up the Tonle Sap River, delivering some its sediment to the Tonle Sap Lake. However, during the low-water period, the direction of flow reverses such that the lake drains into the Tonle Sap River, which then joins the Mekong River (downstream of our sampling site on the Mekong) [*Kummu et al.*, 2008].

A variety of soil and sediment samples were collected from around Cambodia to further constrain sources of GDGTs (see Table 5.1 for locations). Several samples were collected from contrasting environmental types within close proximity to the location of the time series measurements on the Mekong River, including a river bed, river floodplain, lake bed, and rice paddy samples. A Van Veen Grab Sampler was used to collect sediments from the bed of the Tonle Sap River and the bed of the Preak Thom Lake. The Tonle Sap River site was sampled just above the confluence with the Mekong River during the rainy season, indicating that the Tonle Sap River was flowing towards the Tonle Sap Lake. The lake bed sediments came from Preak Thom Lake, which is also located within the Cambodian province of Kendal, and is about 10 km from the city of Phnom Penh. Using a steal auger, a surface sample was also collected from a rice paddy near Preak Thom Lake (henceforth referred to as Preak Thom Rice Field). Finally, the last site sampled near Phnom Penh included the Mekong River floodplain, which was collected about 25 m perpendicular to the bank of the Mekong River in Phnom Penh (henceforth referred to as the Mekong River Floodplain).

Multiple sites were sampled within the Cambodian province of Siem Reap, which were located ≈ 200-250 km from Phnom Penh. An additional floodplain sample was collected 45 m above the bank of the Sangkar River, which flows into the north end of the Tonle Sap Lake in Siem Reap. This site was located approximately 2.5 km upstream of the Tonle Sap Lake. The Tonle Sap Lake is typically 1 m above sea level during the rainy season, but then rises to 6 to 10 m above sea level during the rainy period, with its area increasing from 2,500 km^2 to15,000 km^2

[*Kummu et al.*, 2008]. Although the site was not inundated at the time of sampling (during the beginning of the rainy season), the site is seasonally inundated. It is subsequently referred to as the Tonle Sap Floodplain sample. An additional rice paddy sediment sample was collected outside of the city of Siem Reap (referred to as Siem Reap Rice Field). Finally, one upland soil sample was collected from a pristine rainforest found within the Phnom Kulen National Park in Northwest Cambodia (henceforth referred to as the Kulen Mountain Rainforest). Upon collection of sediment, samples were placed in dark plastic bags and immediately frozen until analysis for GDGTs. Surface soils were first air-dried, homogenized, and then later dried overnight at 60°C prior to analysis. Soil and floodplain samples were sieved with a 1 mm sieve after collection.

River suspended sediment collection

Mekong River suspended sediment samples were collected at half of the total depth of the river using an in-line submersible pump between 1 to 2 times a month from 6 January 2006 to 1 November 2006. Coarse particulate organic carbon was first removed with a 63 μm sieve because it is quantitatively insignificant relative to fine suspended sediment (data not shown). Fine suspended sediment (FSS) concentration was determined by filtering a known quantity of sieved water through 0.45 μm cellulose acetate filters, which were then weighed before and after collection. Sieved water was also filtered through precombusted GF/F filters, which were later analyzed for N:C ratios, $\delta^{13}C$, and GDGT compositions as in *Ellis et al.* [2012b]. All filters were dried for 24 hours at 60°C. The results of these bulk sediment measurements were previously published by Ellis *et al.* [2012b]. However, we present them again here as they are necessary for interpretation of the GDGT results.

We used the definitions applied by the Mekong River Commission to determine the onset of the different stages of the hydrograph as in [*Ellis et al.*, 2012b]. Discharge (measured at Kratie, Cambodia) was obtained from records provided by the Mekong River Commission

Laboratory analyses

The % OC and $\delta^{13}C$ of the soil and sediment samples were analyzed at the University of Washington's IsoLab using a Thermo-Finigan MAT 253 IRMS coupled with a Costech ECS4010 elemental analyzer with a precision that ranged from 0.1 to 0.3‰. A known quantity of sample was placed in silver boats, then transported to a dessicator, where samples were subjected to vapor phase acidification with 12 N HCl for twenty-four hours. Following acidification, samples were dried at 65°C also for twenty-four hours.

GDGT lipids from GF/F filters and soils were extracted ultrasonically at the University of Washington. Samples were placed in Teflon centrifuge tubes, and then sonicated three times each with methanol (MeOH), a 1:1 (v/v) mixture of MeOH and dichoromethane (DCM), and DCM for five minutes, for a total of nine extractions. Following each extraction, the sample was centrifuged for five minutes at 1,000 x G to remove particulates. Extracts were combined, dried at 45°C under a gentle flow of nitrogen gas using a TurboVap (Caliper LifeSciences) to 1 to 2 mL in volume. Total lipid extracts (TLE) were subsequently dried over a small glass Pasteur pipette filled with anhydrous sodium sulfate.

Lipids from wet sediment samples were soxhlet extracted. Sediment was transferred to a precombusted glass microfiber thimble (30 mm x 100 mm, Whatman), wetted with methanol to remove water, drained, and then the thimble was placed in the soxlet and extracted with 300 mL of DCM:MeOH (9:1, v:v) at 45°C for 72 hours. The extract was evaporated to 1 to 2 mL as described above, and then further dried over a column of anhydrous sodium sulfate.

Extracts (from all samples) were eluted sequentially into polar and apolar fractions using hexane:DCM (9:1 v/v) and DCM:MeOH (1:1, v/v), respectively, over a silica gel column. In some cases, the polar fraction, which contained the GDGTs, was split in two. One half was hydrolyzed prior to GDGT analyses, while the other was directly analyzed for core GDGTs. Samples were hydrolyzed in 5% HCl in MeOH (v/v) after flushing with N_2 gas. Capped vials were then held at a 70°C for 4 hours. Afterwards, DCM and MilliQ water were added to the vial, shaken, and then the DCM fraction was collected. The aqueous phase was then extracted four times to ensure complete recovery. The DCM fraction was then rinsed six times with MilliQ water to remove acid.

After the DCM fraction was dried, a known quantity of the internal GDGT standard (C_{46}) was added to both the hydrolyzed and non-hydrolyzed samples [*Huguet et al*., 2006]. The sample was then dissolved in hexane:propanol (99:1 v/v), sonicated for five minutes, and then filtered through a 0.45 µm PTFE filter prior to injection on the HPLC-MS.

Core GDGTs were analyzed using an Agilent 1100 Series Liquid Chromatograph (LC) coupled to an Agilent ion trap (XCT) mass spectrometer (LC-MS) following the methods described in [*Hopmans et al*., 2000]. Briefly, GDGTs were eluted isocratically with hexane:isopropanol (99:1, v/v) for five minutes, and then the gradient program linearly ramped to 1.8% isopropanol over the next 45 minutes. The flow rate was 0.2 mL/min for the duration of the elution. The HPLC was equipped with a Prevail Cyano column (2.1 x 150 mm; 3µm pore size) and a Prevail Cyano guard column (7.5 x 4.6 mm; 5µm pore size), which were held at 30°C. Between injections, the column was backflushed with hexane:isopropanol (90:10 v/v) for 8 minutes to clean the column, and then re-equilibrated for 10 minutes under the initial conditions. GDGTs were detected using atmospheric pressure chemical ionization (APCI), scanning from 730-1350 *m/z*, with spray chamber conditions as follows: dry gas, 6 L/min at

200ºC; nebulizer pressure, 60 psi; vaporizer temperature, 400°C; capillary voltage -3kV; corona 5µA (~3.2kV). GDGT peak areas were compared with that of the internal GDGT standard to determine absolute abundances. The analytical error estimated from triplicate injections was estimated to be 6%.

The abundance of intact and core GDGTs was calculated from the hydrolyzed and unhydrolyzed GDGT samples when both measurements were taken. The hydrolyzed samples yields the total amount of a given GDGTs within a sample (i.e. the intact and core GDGTs), whereas the unhydrolyzed sample provides only the amount of core GDGTs. Therefore, the abundance of intact GDGTs was determined by subtracting the unhydrolyzed sample from the hydrolyzed sample.

Index calculations:

The BIT index is based on the ratio of brGDGTs I-III to GDGT IV, and it is calculated as in *Hopmans et al*., [2004]:

$$BIT = ([I]+[II]+[III])/([I]+[II]+[III]+[IV]) \quad (1)$$

The cyclization ratio of branched tetraethers (CBT) is a measure of the average number of cyclopentyl moieties in branched GDGTs, whereas the methylation index of branched tetraethers (MBT) is based on the number of methyl groups in branched GDGTs. They are defined as follows [*Weijers et al.*, 2007]:

$$CBT = \log [([Ib]-[IIb])/([I]-[II])] \quad (2)$$

$$MBT = ([I]+[Ib]+[Ic])/([I]+[Ib]+[Ic]+[II]+[IIb]+[IIc]+[III]+[IIIb]+[IIIc]) \quad (3)$$

These indices can be related to pH of the lake water and mean air temperature (MAT) using the following calibrations from the global lakes dataset [*Sun et al.*, 2011]:

$$pH = 8.98 - 1.72*CBT \quad (4)$$

$$MAT = 3.949 - 5.593*CBT + 38.213*MBT \quad (5)$$

For the calibration for pH, $R^2 = 0.42$ and the root mean square error (RMSE) is 0.82. The MAT calibration is only to be applied in aquatic environments with pH < 8.5. The Mekong pH is < 8.5 over the course of the hydrograph, indicating that this is a suitable calibration for MAT. For this calibration, $R^2 = 0.73$, and RMSE is 4.27°C.

For the time series measurements, the air temperature predicted by the regression was compared to the mean air temperature for the day of sampling, which was determined as in [*Mitchell et al.*, 2004]. For the soil and sediment samples, the temperature derived from the MBT/CBT index was compared to the average yearly temperature obtained from records that span from 1950 to 2006 (also calculated as *in Mitchell et al.*, [2004]). River pH was calculated from the partial pressure of carbon dioxide in river water and from dissolved inorganic carbon concentrations (D. Lockwood, unpublished data), given that samples for both variables were collected concurrently with riverine suspended sediment samples. Unfortunately, pH measurements are not available for sites other than the Mekong River.

Statistical analyses

Statistical analyses were conducted using SPSS (version 15.0). Nonparametric statistics were used due to the limited amount of samples collected. To determine the significance of correlations between two variables, Spearman's rank order correlation procedure was used. The Mann-Whitney U test was used to determine significant differences in variables across two groups. For such comparisons, only differences between the low and high-water periods were assessed, as only two samples were collected during the rising-water period.

RESULTS

Seasonal variability in the concentration of core GDGTs attached to river particles

The concentration (ng/L) of brGDGT I-III (the sum of brGDGT I, II, and III), isoGDGT (henceforth refers to all isoprenoid GDGTs, excluding GDGT IV), and crenarchaeol (GDGT IV) ranged by two orders of magnitude over one year (Fig. 5.2a, Table. 5.2). brGDGT I-III ranged from 1.4 ng/L to 133.2 ng/L, whereas isoGDGT ranged from 0.4 to 69.8, and GDGT IV ranged from 0.1 to 25.7 ng/L (Table 5.2). Typically, the concentration of core GDGT (ng/L) exceeded isoGDGT IV concentrations, which exceeded GDGT IV concentrations in river water. Out of the branched GDGTs, I had the highest concentration, followed by II, and then III, with the latter occasionally not detected in river water particles. IIIb and IIIc were not detected in river particles (m/z ratio of 1048 and 1046, respectively), whereas IIc (m/z ratio of 1032) was often not detected; all other cyclopentyl moieties were present.

The concentration (ng/L) of each tetraether lipid category was positively correlated with discharge (brGDGT I-III: $r = 0.735$, $p = 0.001$); isoGDGTs: $r = 0.794$, $p < 0.0005$; GDGT IV: $r = 0.711$, $p = 0<0.0005$). The high-water period consistently had significantly greater concentrations than the low-water period for all GDGT categories (Table 5.2, Fig. 5.2a). For example, the average concentration of brGDGTs I-III was 68.8 ± 47.5 ng/L during the high-water period, and then decreased to 2.7 ± 1.1 ng/L during the low-water period ($U = 0.000$, $Z = -3.240$, $p < 0.0005$). The average concentration of GDGT IV during the high-water period was ≈25 times greater than values observed during the low-water period (Table 5.2).

FSS concentrations and FPOC concentrations were also positively correlated with brGDGT I-III, isoGDGTs, and GDGT IV concentrations (ng/L) (FSS: $r = 0.818$, 0.883, and 0.793, respectively; FPOC: $r = 0.788$, 0.838, and 0.750, respectively) (Table 5.3, Fig. 5.2b). GDGT IV peaked slightly before the maximum suspended sediment concentrations (Fig. 5.2a).

Maximum concentrations of brGDGT I-III were observed during the tropical storm Xangsane just past the peak of the rainy season. GDGT concentrations were not significantly correlated with N:C ratios or $\delta^{13}C$ of FPOC (see Table 5.3 for measures of bulk parameters). Instead, they were each negatively correlated with % OC (brGDGT I-III: $r = -0.786$, $p < 0.0005$; IsoGDGTs: $r = -0.842$, $p < 0.0005$; GDGT IV: $r = -0.798$, $p < 0.0005$) (Fig. 5.2c).

When core GDGT abundances were normalized to OC content (i.e. μg GDGT/g OC), all were correlated with discharge (brGDGT I-III: $r = 0.667$, $p = 0.003$; isoGDGTs: $r = 0.912$, $p < 0.0005$; GDGT IV: 0.532, $p = 0.028$) (Fig. 5.2d). All high-water values normalized to OC were statistically different from low-water values, with high-water values exceeding low-water values in all cases (Table 5.2). When normalized by OC, the mean abundance for brGDGT I-III, isoGDGTs, and GDGT IV was 10.5 ± 9.3, 5.3 ± 4.0, and 3.1 ± 3.0 μg GDGT/g OC, respectively.

When core GDGT abundances from river particles were normalized by mass (i.e. ng GDGT/g sediment), there was no significant correlation with discharge for GDGT I-III, GDGT IV, or Isoprenoid-GDGT IV (Fig. 5.2e). Further, there was no significant difference between seasons for any of these parameters when normalized by mass. Mean core brGDGT I-III, isoGDGTs, and GDGT IV abundances were 322.5 ± 174.6, 174.0 ± 107.6, and 107.6 ± 97.9 ng GDGT/g sediment, respectively).

Out of the brGDGTs, there was a statistically significant difference between the fractional abundance of GDGT IIb ($p = 0.047$), I ($p = 0.021$) and Ib ($p = 0.004$) between the low and the high-water seasons (m/z ratio of 1034 and 1020, respectively). brGDGTs IIb and Ib had a higher fractional abundance during the low-water period, whereas the abundance of brGDGT I decreased during that period (Fig. 5.3).

Variability in total (core + intact) tetraether lipids normalized to OC across environmental samples

The concentration of total (core + intact) brGDGT I-III normalized to OC varied by one order of magnitude across sites (Fig. 5.4a-c), from 16.7 (Mekong low-water FPOM) to 307.7 μg/g OC (Preak Thom Lake bed sediment). The upland soil sample also had very low concentrations of total brGDGT I-III (27.7 μg/g OC), with only 4% (Fig. 5.4d) of the total brGDGT I-III being intact. brGDGT I-III concentrations were generally low in samples collected in or near the Mekong River, including river particles (25.4 to 68.1 μg/g OC), the river bank (15.3 μg/g OC), and surface sediment collected from the Tonle Sap River (53.6 μg/g OC). The latter site was sampled just upstream of the confluence with the Mekong River and likely represents sediment deposited by the Mekong. Despite the low concentrations, the percentage of intact brGDGTs (relative to total brGDGTs) found in river particles were the highest measured across all sites, ranging between 47 and 65% for the high and low-water periods, respectively (Fig. 5.4e). Additional sites with high brGDGT I-III concentrations include the Tonle Sap floodplain and the Siem Reap rice field, with 217.8 and 229.4 μg/g OC, respectively. However, the percentage of intact brGDGTs was highly variable, ranging between not detectable (Tonle Sap floodplain) to 24% of the total (Preak Thom Lake).

Concentrations of GDGT IV normalized to OC were always less than values of branched GDGTs for both intact and core lipids (Fig. 5.4g-i). Concentrations of total (core and intact) GDGT IV ranged from 0.6 to 13.4 μg/g OC, with soils from the Kulen Mountains having the lowest concentration, and Tonle Sap bed sediments having the highest concentration. In contrast to brGDGTs, the samples collected in or near the Mekong River had comparable (or higher) concentrations relative to the other locations. Values found within riverine suspended sediments range from 3.2 to 13.6 between the low and the high-water season, respectively, which lies

within the range found within almost all environmental types. Intact GDGT IV was found in all environmental samples (Fig. 5.4j-l), with the percentage of intact GDGT IV usually exceeding the percentage of intact brGDGTs (with the exception being the Mekong river particles where between 47 to 59% of GDGT IV was intact). The highest percentage of intact GDGT IV was found in the Preak Thom rice paddy sediment sample (68%), whereas the lowest value was found in the Tonle Sap Lake floodplain sample (11%).

Variability in the composition of total branched lipids across environmental types

The relative abundance of branched GDGTs (intact + core) on river particles was compared to that found in other environmental types to further understand potential terrestrial and aquatic origins. The percentage that each type of branched GDGT (including cyclopentyl moieities) contributed to the total was calculated (Fig. 5.5). The composition of the soil sample differed most from the other samples, as it was composed of ≈99% GDGT I-Ic in both the core (Fig. 5.5a) and living fractions (Fig. 5.5b). All of the samples influenced by lacustrine or riverine processes (including bank and floodplain samples) contained GDGT II-IIc, and GDGT III-IIIc, although the fractional abundance of GDGT III-IIIc consistently represented 5% or less of the total brGDGT I-III for both the core and intact fractions. GDGT I-Ic represented the highest proportion of the GDGTs in the non-soil samples, representing between 57-93% the total in the core and intact pools. The composition between the living and intact fractions of many sites (e.g. the Kulen rainforest, Siem Reap rice field, the Tonle Sap floodplain) was quite similar to each other. If the composition differed, it was generally due to differences in the relative contribution of GDGT I-Ic and II-IIc to the total. For example, the core and living fractions differed significantly for the Preak Thom rice field and the Mekong bank sample, with GDGT II-c comprising a larger component of the total in the intact fraction in both cases. However, there was no general trend across all samples, as the intact pool of the high-water FSS and the Tonle

Sap bed sediment contained less GDGT II-c. Out of all sample types, the core brGDGT composition of the Mekong suspended sediment was most similar to the Mekong bank samples, whereas the intact brGDGT composition during the high-water period was most similar to sediments from the Preak Thom Lake bed.

Variability in indices across environmental types: BIT, MBT, and CBT

The BIT index measured on core lipids was generally high, ranging between 0.75 to 0.99. The soil, rice field, floodplain (Tonle Sap), and lake bottom (Preak Thom) samples all had high core BIT values, with values measuring greater than 0.97. The lowest core BIT value was measured on the Mekong bank sample (Fig. 5.6a-c). Intact BIT indices were generally similar to core values, although three sites had significantly lower BIT indices relative to core measurements: Mekong bank sediment (intact: 0.25, core: 0.75), Tonle Sap River bed sediment (intact: 0.82, core: 0.37), and the Preak Thom rice field sediment (intact: 0.58, intact 0.97). The low BIT values were due to higher proportions of crenarchaeol found in the intact samples. For the riverine FSS samples where both core and intact values were available, there was little variation between the BIT index for the core and intact samples (high-water core: 0.80, high-water intact: 0.88; low-water core: 0.84, low-water intact: 0.74).

There was a high variation in CBT core and intact values across environmental samples, ranging between 0.35 to 2.07 and 0.37 to 1.86 in core and intact lipids, respectively (Fig. 5.6 d-f). The CBT index was unable to be calculated in the Kulen Mountain soil sample, as not all GDGTs were detected. All samples collected in or near the Mekong River generally had lower CBT indices relative to samples from other locations. The highest values were observed in the samples collected near Siem Reap, including the Siem Reap rice field and the Tonle Sap floodplain. Comparisons between intact and core CBT indices indicated that many sites had similar values. For those sites with different values, there was no consistent trend between core

and intact values. The largest difference between core and intact CBT values was observed in the bed sample taken from the Preak Thom lake (core: 0.75, intact: 1.39).

The intact and core MBT values from the soil sample was higher (ranging between 0.99 and 1.00) than that observed in all other samples due to the predominance of GDGT I-Ic in that sample. Variability in the MBT Index ranged from 0.62 to 0.90 and 0.46 to 0.92 across core and intact GDGTs for all other sample types (Fig. 5.6 g-i). Similar to the CBT, many intact and core MBT values were not different from each other. The largest differences were observed in the Mekong River bank sample, the Tonle Sap bed sample, and Preak Thom rice paddy sample, although there was no consistent trend in the offset between sample types.

Seasonal variability in indices measured on FSS transported by the Mekong River

The BIT index of riverine FSS was highly variable, ranging from 0.56 to 0.93 from Jan. – Nov. 2006. There was no significant difference between low and high-water BIT indices, nor was there a significant correlation between the BIT index and discharge (Fig. 5.7a). However, the CBT, which ranged between 0.51 to 1.03 was significantly correlated with discharge ($r=0.891$, $p<0.0005$) (Fig. 5.7b), with high water values being significantly greater than low-water values (high-water CBT: 0.63 ± 0.10; low-water CBT: 0.84 ± 0.10) ($U=3.000$, $Z = -2.893$, $p = .002$). The MBT index was also positively correlated with discharge (Fig. 5.7c), although the correlation was not as strong as with the CBT index ($r = 0.527$, $p = 0.030$). Values ranged from 0.59 to 0.75.

The BIT index was not correlated with any measurements made on the bulk suspended sediment ($\delta^{13}C$, N:C ratios, % OC, FPOC concentration (Table 5.2), nor measurements of lignin-derived phenols normalized to OC, such as λ_8, and Σ_8 . In contrast, GDGT concentrations were correlated with lignin concentrations (core brGDGT I-III: $r=0.818$, $p<0.0005$; GDGT IV:

r=0.750, p=0.001), and λ_8 (GDGT I-III: r=0.820, p=0.<0.0005, n=17; GDGT IV: r=0.791, p<0.0005) (Fig. 5.8).

DISCUSSION

While application of the BIT index is widespread, few studies have examined this index in suspended particles within a river and even fewer have investigated it in time series studies of river particles. Existing temporal measurements have focused on determining changes recorded in surface sediment collected kilometers downstream from a river mouth [*Kim et al.* 2006]. Marine sediment BIT values are averaged over a relatively long time interval and may be biased by depositional and post-depositional processes. Thus, it is imperative to examine the composition of riverine suspended sediments prior to being exported to the ocean to accurately decipher terrestrial carbon preservation. Here we investigate seasonal variability in the BIT index and the constituent tetraether lipids in riverine suspended particles. Because an understanding the origin of the biomarkers that constitute the BIT index is imperative to understanding variation in this index, we began our discussion with lessons gained from measuring both intact and core brGDGT and GDGT IV found in suspended river particles and other environmental samples in order to constrain possible regions of GDGT production within the lower portion of the Mekong River catchment.

Insights into the source of riverine branched GDGTs

Since branched GDGTs are very nearly "orphan" biomarkers, with nearly no known biological source [*Sinninghe Damsté et al.*, 2011], any clues that can be gathered from environmental distributions of branched GDGTs can extend our understanding of the habitat and lifestyle of organisms making these compounds. So far, nearly all studies of branched GDGTs in the environment have focused on the core lipids, which have demonstrated that these GDGTs are found in rivers and lake sediments in addition to watershed soils [*Blaga et al.*, 2009; *Tierney and*

Russel, 2009; *Sun et al.,* 2011]. Support for in situ production has recently arisen as both core and intact branched and isoprenoid GDGTs have been found in sediment samples taken from a Rhode Island pond [*Tierney et al.,* 2012]. Our analyses of core and intact lipid abundance in the Mekong River basin corroborate these findings and suggest that branched GDGT-producing organisms are produced within rivers, lakes, and other environments that are seasonally inundated (Fig. 5.4). Although the carbon-normalized concentration of GDGTs found in Mekong River sediment was relatively low, strong support for in situ production is derived from the observation that between 47 to 65% of the branched GDGTs in Mekong River suspended sediment are intact during the rainy and dry seasons, respectively. In fact, river particles represent the highest proportion of intact brGDGTs observed across all environmental types examined in this study (Fig. 5.4). In addition to the river particles, surface sediments collected from the bottom of Preak Thom lake also contain high percentages of intact lipids (24%).

The presence of intact branched GDGTs in aquatic environments is significant because they are traditionally implied to be specific to organisms living in soils and peat bogs [*Hopmans et al.,* 2004; *Weijers et al*., 2006a; *Kim et al*., 2006; *Liu et al.* 2010]. Although we cannot eliminate the possibility that intact riverine GDGTs are produced within watershed soils and subsequently mobilized into the river or lake, there are several lines of evidence that suggest these biomarkers are likely produced in situ. First, we utilized measurements of the CBT index derived from core lipids to reconstruct measurements of river pH using the correlation between in situ measurements of pH and the CBT index derived from sediment samples taken from the global lakes dataset [*Sun et al.,* 2011]. The basis for this is that it has been suggested that the bacteria producing branched GDGTs I-III vary the amount of cyclopentyl moieties in their membrane lipids according to the pH of their environment [Weijers et al. 2007b]. The similarity between the 1) pH predicted from branched GDGTs and 2) pH calculated from measurements of

the partial pressure of carbon dioxide and dissolved inorganic carbon collected at the time of sampling [D. E. Lockwood, unpublished data] is striking: there is a strong correlation between these measurements ($r=0.836$, $p = 0.001$), with the predicted pH derived from branched lipids closely following the seasonal variability observed in the pH of the Mekong River (Fig. 5.7b). This is due to differences in the fractional abundance of GDGT Ib and IIb between seasons (m/z ratio of 1020 and 1034, respectively), as significantly higher proportions of these lipids are observed during the low-water period relative to the more acidic high-water period (Fig. 5.3). The pH of the river is strongly controlled by weathering, with maximum values occurring during the low-water season [D. E. Lockwood, unpublished data]. The close similarity between the two estimates of pH supports the notion that in situ production of brGDGTs is occurring within the river. It seems highly unlikely that intact brGDGTs mobilized from soils would also be experiencing the same pH conditions observed in the Mekong River at this lowland sampling location. This is especially true considering that 50% of the sediment exported by the Mekong River comes from the Upper Basin [*Kummu and Varis*, 2007; *Walling*, 2005]. Furthermore, when the CBT index is calculated using only intact brGDGTs, the predicted pH was even more similar to the measured pH during the high and low-water periods (Fig. 5.7b), which would be expected if intact brGDGTs are truly produced in situ.

The degree of methylation of branched-GDGTs varies with temperature [*Weijers et al.*, 2007] which is the basis of the MBT/CBT paleoclimate proxy used to reconstruct air temperature. Measurements of air temperature calculated from the MBT index of riverine core brGDGTs (again using the regression of MBT and air temperature derived from the global lakes dataset [*Sun et al.*, 2011]) were also correlated with the mean air temperature observed during the day of sampling ($r=0.506$, $p = 0.038$) (Fig. 5.7c). Although the predicted air temperature was generally cooler than observed (Fig. 5.7c), the difference between the measurements was within

the error of the regression (5.2°C) [*Sun et al.*, 2011]. However, considering that source organisms in soils would be more likely to respond to changes in air temperature, rather than organisms living in river-water, it is tenuous to conclude that this is evidence for in situ production of brGDGTs I-III in river water.

The low percentage of intact GDGTs (<5%) combined with the relatively low concentrations of brGDGTs I-III (27.9 µg/g OC) suggest that the upland soils from the Kulen Mountain rainforest are likely not sites of high productivity for the organisms producing brGDGTs. Previous work has demonstrated that some of the highest abundances of branched GDGTs in soils have been observed in peat bogs, with the highest concentrations occurring in the anoxic part of the profile [*Weijers et al.*, 2006]. Therefore, it appears that the lack of anoxic conditions, or water-logged pore spaces, limits the activity of brGDGT-producing organisms in upland soils. In addition, compositional differences between the relative abundance of brGDGT I-III between the soil and river particles differ significantly, considering that the soil sample is comprised almost entirely of GDGT I (Fig. 5.5). Differences in the relative composition of brGDGTs between lakes and soils have led to the speculation that in situ production of brGDGTs occurs in lakes [*Blaga et al.* 2009; *Tierney and Russel*, 2009; *Sun et al.* 2011]. Although the distribution of these GDGTs vary with temperature, soils generally contain a higher fractional abundance of GDGT I, and less GDGT III, whereas lake sediments contain proportionally more GDGT II and III, suggesting that these brGDGTs may be produced in the water column [*Sun et al.*, 2011]. This is consistent with our observations of the relative contribution of brGDGT I-III between riverine/lacustrine sediment samples and soils (Fig. 5.5), providing additional support that intact GDGTs in these environments are derived from in situ production.

Measurements of the percentage of intact brGDGTs and the concentration of brGDGTs in aquatic environments (including their floodplains) provide clues as to which locations are ideal

for active brGDGT production versus depositional environments for brGDGTs produced elsewhere. For example, Preak Thom Lake is an amenable site for production considering that its bed sediments contained the highest abundance of branched GDGTs (308 µg BrGDGT I-III/100 µg C) observed in this study, with a relatively high percentage of intact lipids (23%) (Fig. 5.4). While sampling, ebullition occurred as the bottom sediments were disturbed, suggesting anoxic conditions. Although the BIT index and MBT index was almost identical between core and intact lipids, the CBT index was notably higher on intact lipids (Fig. 5.6). In contrast to Preak Thom Lake, the Tonle Sap floodplain appears to be a depositional environment for brGDGTs I-III, which is supported by the high concentrations of BrGDGT I-III (218 µg/g OC), but undetectable intact brGDGT I-III concentrations. This site was sampled during the beginning of the rising-water period, and therefore the soils were not waterlogged. However, this site is inundated during the rainy period [*Kummu et al.*, 2008] . Therefore, we speculate that the high abundance of core brGDGT I-III is either due to the deposition of lake brGDGTs during the rainy period, or due to production within the sediment once it is inundated. The other site with notably high GDGT abundances was the Siem Reap rice field, where 14% of the brGDGTs were intact. The BIT, MBT, and CBT indices were virtually identical between the intact and core fractions, suggesting this rice field actively supports brGDGT production (Fig. 5.6). Therefore, work in the Mekong catchment corroborates previous work suggesting that anoxic environments are important regions of branched GDGT production [*Weijers et al.* 2006], and are likely an important source of brGDGTs to the Mekong River.

Mekong suspended particles are compositionally most similar to soil from the bank of the Mekong River based on the relative abudance of core brGDGT I, II, and III (Fig. 5.5b). Therefore, one interpretation of these observations could be that Mekong bank soils are significant contributors to riverine particles. However, the entire sediment load discharged to the

South China Sea by the Mekong can be accounted for by that measured at an upstream mainstem location relative to our site (in Pakse, Laos) [*Milliman and Syvitski*, 1992; *Walling et al*., 2008]. Further, once the Mekong reaches Kratie, Cambodia (250 km upstream from our site), the channel widens, the river slows, and an extensive floodplain develops [*Mekong River Commission*, 2005]. Therefore, it is more likely that the similarity between the composition of brGDGTs found in Mekong river particles and bank sediment samples reflect that the bank is composed of sediments deposited by the river.

Implications for the BIT Index

The BIT index varied dramatically over the course of one year: values ranged from 0.53 to 0.96 in suspended sediment of the Mekong River (Fig. 5.7). Terrestrial end-member values less than 1 are due to quantitatively significant amounts of GDGT IV being produced in soils and peat, which can reduce the BIT index to values as low as 0.8 in these end-members [*Weijers et al*. 2006]. We found relatively high concentrations of intact GDGT IV in Mekong river particles, and bed sediments suggesting that this compound is also produced in the catchment (Fig. 5.4). Thus, production of both branched GDGTs and GDGT IV within the Mekong catchment influence BIT values of particles reaching a river mouth and later being deposited in coastal regions. Therefore, down-core and spatial variability in the BIT index of river delta and coastal sediments is likely influenced by the in situ production of both branched and isoprenoid GDGTs in aquatic environments in addition to the delivery of tetraether lipids from sources outside the river.

In this study, the lack of correlation between the BIT index and other tracers of terrestrial carbon, such as lignin-phenols, is likely caused by the in situ production of GDGTs in the river and differences in the relative sources of these biomarkers. The suspended sediments analyzed here for BIT index values were concurrently examined for lignin-phenol composition [*Ellis et*

al., 2012b], and no correlation was observed between the BIT index and any measure of lignin phenols (i.e. lignin concentrations, lignin normalized to organic carbon, or lignin normalized to dry weight), or any measure of bulk organic carbon (such as N:C ratios and $\delta^{13}C$). However, in spite of this observation, our results indicate that the mobilization of sediment is controlling both GDGT and lignin concentrations. For example, the concentration of brGDGTs I-III and GDGT IV were positively correlated with 1) discharge measurements, 2) FSS concentrations, 3) FPOC concentrations, 4) lignin phenol concentrations, and 5) each other (Fig. 5.2, and Fig. 5.8). Further, there was no significant difference in the concentration between seasons when any of these biomarkers were normalized by dry weight, indicating that the sediment is equally enriched in all three of these biomarkers between seasons. Finally, when normalized to organic carbon content, the rainy season is significantly more enriched in all three biomarkers relative to the dry season (Fig. 5.2). The latter observation has been attributed to the phytoplankton bloom that occurs during the low-water season, which produces a carbon-rich source of organic matter that dilutes the contribution of the aforementioned biomarkers to total carbon [*Ellis et al*., 2012b]. Thus, these results indicate that the increased mobilization of sediment during the rainy season is an important factor that delivers particulate branched GDGTs, isoprenoid GDGTs, and lignin-derived phenols to the river.

How is it possible that seasonal variability in GDGT concentrations and lignin concentrations are highly correlated with each other and primarily governed by the flux of sediment into the Mekong River, but there is no correlation between the BIT index and lignin? Lignin is primarily a tracer of allochthonous carbon, whereas GDGTs are tracing both allochthonous and autochthonous carbon. For example, the Mekong is largely confined to its channel for the majority of its journey to the South China Sea [*Mekong River Commission*, 2005], and its vascular plant composition reflects that found on land [Ellis et al. 2012b]. In

contrast, we have observed that between 47 to 65% of the bacteria producing branched GDGTs, and between 47 to 58% of the archaea producing GDGT IV are living within the river during the dry and rainy season.

The BIT index is ultimately defined by the ratio of brGDGT I-III to GDGT IV, and this ratio is likely governed by a separate suite of factors, such as anoxic conditions and nutrient availability, that are unrelated to lignin mobilization. Because we only measured intact GDGTs once during the dry season and once during the flood season, we are currently unable to assess how the relative amounts of in situ production of these biomarkers influence the BIT index. However, considering that the BIT index was not correlated with any measure of terrestrially-derived carbon or bulk suspended sediment, or any parameter measured in this study, we hypothesize that the role of in situ production in controlling the variability of the BIT index in this study is substantial. Thus, when interpreting the BIT index, it is necessary to consider that hydrologic factors and sediment mobilization influence production of branched GDGTs in the river itself and that the signal observed in a offshore core may is likely a function of in-river processing.

Several studies have compared the BIT index to the proportion of carbon derived from vascular plants ($\lambda 8$) in fjords and have found a weak correlation between the two parameters [*Smith et al.*, 2010] or no correlation at all [*Walsh et al.,* 2008]. Considering that the BIT index has been proposed to be a tracer of soil-derived carbon, the lack of strong correlations between the BIT index and lignin in these studies has been attributed to the deposition of undeveloped soils (poor in branched GDGTs) and fresh woody debris (rich in lignin) in Vancouver Island fjords sediments [*Walsh et al*., 2008], or soil-rich and vascular-plant-poor organic matter in a New Zealand fjord [*Smith et al*., 2010]. We now suggest that in situ production of GDGTs I-III

and GDGT IV in aquatic environments may also contribute to the lack of correlation between these two tracers of terrestrial carbon in certain environments, such as the Mekong River.

CONCLUSIONS

Our finding that 47 to 65% of branched GDGTs associated with suspended and bed sediment of the Mekong River are intact, suggests that in situ production is occurring within the Mekong River. Further, the percentage of intact and branched GDGTs found in river bed and lake bed sediments, and suspended sediments generally exceed that found in soils. Finally, significant concentrations of intact isoprenoid GDGTs were also present in these same environments. These findings suggest the possibility for significant in alteration of BIT index values during transport within a river, imparting a modified BIT index value to particles delivered to the ocean compared to that found in terrestrial soils. Considering that the BIT index of riverine FSS was not correlated with any measure of terrestrially-derived carbon, such as lignin phenols, N:C ratios, or $\delta^{13}C$, we hypothesize that the relative ratios of branched GDGTs and GDGT IV produced within the river are responsible for this variation. Accordingly, more studies are needed to assess how the in situ production of branched GDGTs alters the BIT index and other indices, such as the MBT and CBT indices, in order to accurately interpret marine carbon preservation or proxies of past environmental change.

Table 5.1. Location and description of study sites from within Cambodia.

Name	*Abbreviation*	*Type*	*Province*	*Lat. (°N)*	*Long. (°E)*	*Soil/sediment Depth*
Mekong River FSS	M FSS	FSS	Phnom Penh	11.60385	104.9397	Surface
Mekong Bank	M Bank	Sediment	Phnom Penh	11.600854	104.957522	0-19 cm
Tonle Sap River Bed	TS Bed	Sediment	Phnom Penh	11.60725	104.92255	Surface
Tonle Sap Floodplain	TS Floodplain	Sediment	Siem Reap	13.240317	103.66035	0-13 cm
Preak Thom Lake Bed	PT Lake Bed	Sediment	Kandal	11.512344	105.016267	Surface
Preak Thom Rice Field	PT Rice	Sediment	Kandal	11.506017	105.01085	Surface
Siem Reap Rice Field	SR Rice	Sediment	Siem Reap			Surface
Kulen Mountain Rainforest	K Rainforest	Soil	Siem Reap	13.573483	104.092556	0-13 cm

Table 5.2. Seasonal variability in branched and isoprenoid GDGT concentrations associated with Mekong River suspended sediment. All values refer to measurements taken on the core fraction.

Date	brGDGT I-III (ng/L)	IsoGDGT (ng/L)	GDGT IV (ng/L)	brGDGT I-III (ng/gdw)	IsoGDGT (ng/gdw)	GDGT IV (ng/gdw)	brGDGT I-III (µg/g OC)	IsoGDGT (µg/g OC)	GDGT IV (µg/g OC)
					Low-water Stage				
06 Jan. 2006	3.2	0.6	0.4	120.8	24.0	16.5	3.4	0.7	0.5
20 Jan. 2006	2.3	1.7	0.5	213.2	158.6	44.2	2.7	2.0	0.6
03 Feb. 2006	1.7	0.9	0.7	276.3	151.5	123.8	3.4	1.8	1.5
17 Feb. 2006	2.4	0.6	0.3	351.4	87.3	47.3	3.3	0.8	0.4
02 Mar. 2006	2.1	0.4	0.1	300.1	56.3	19.9	2.9	0.5	0.2
17 Mar. 2006	4.2	1.0	0.7	530.3	127.4	91.6	6.1	1.5	1.1
31 Mar. 2006	1.4	1.6	1.0	226.7	260.8	169.3	2.4	2.7	1.8
21 Apr. 2006	4.2	1.8	1.0	336.8	142.2	83.4	6.8	2.9	1.7
Average	*2.7*	*1.1*	*0.6*	*294.4*	*126.0*	*74.5*	*3.9*	*1.6*	*1.0*
Standard deviation	*1.1*	*0.6*	*0.3*	*120.9*	*72.6*	*53.2*	*1.7*	*0.9*	*0.6*
					Rising-water Stage				
09 Jun. 2006	15.8	14.4	12.5	538.5	492.2	425.4	13.5	12.3	10.7
23 Jun. 2006	17.8	6.8	6.7	484.9	185.8	181.6	17.2	6.6	6.4
Average	*16.8*	*10.6*	*9.6*	*511.7*	*339.0*	*303.5*	*15.4*	*9.5*	*8.6*
Standard deviation	*1.4*	*5.4*	*4.1*	*37.9*	*216.7*	*172.4*	*2.6*	*4.0*	*3.0*
					High-water Stage				
07 Jul. 2006	116.4	36.2	22.3	591.8	183.9	113.5	29.2	9.1	5.6
21 Jul. 2006	75.4	31.5	25.7	553.2	231.4	188.3	23.0	9.6	7.8
04 Aug. 2006	91.0	69.8	21.3	350.1	268.7	81.8	14.4	11.0	3.4
18 Aug. 2006	25.0	14.0	5.3	144.2	80.5	30.5	6.6	3.7	1.4
06 Oct. 2006	133.2	37.0	18.4	606.7	168.7	84.0	30.2	8.4	4.2
20 Oct. 2006	19.3	23.7	8.4	187.6	229.6	81.8	7.1	8.7	3.1
01 Nov. 2006	21.4	22.5	9.4	103.9	109.2	45.7	7.0	7.4	3.1
Average	*68.8*	*33.5*	*15.8*	*362.5*	*181.7*	*89.4*	*16.8*	*8.3*	*4.1*
Standard deviation	*47.5*	*18.0*	*8.0*	*221.3*	*68.3*	*51.5*	*10.6*	*2.3*	*2.1*

Table 5.3. Characterization of riverine particulate organic matter at the bulk level.

Date	FSS *Mg/L*	FPOC *Mg/L*	% OC	N:C	$\delta^{13}C$
		Low-water Stage			
06 Jan. 2006	26.2	0.94	3.6	0.06	-30.3
20 Jan. 2006	10.8	0.86	8.0	0.07	-29.9
03 Feb. 2006	6.1	0.50	8.2	0.10	-31.3
17 Feb. 2006	6.7	0.72	10.7	0.09	-29.2
02 Mar. 2006	7.0	0.73	10.5	0.09	-28.8
17 Mar. 2006	7.9	0.68	8.6	0.10	-30.4
31 Mar. 2006	6.1	0.58	9.5	0.09	-29.4
21 Apr. 2006	12.4	0.61	5.0	0.10	-29.3
Average	*10.4*	*0.70*	*8.0*	*0.09*	*-29.8*
Standard deviation	*6.8*	*0.15*	*2.5*	*0.01*	*0.8*
		Rising-water Stage			
09 Jun. 2006	29.3	1.17	4.0	0.07	-30.4
23 Jun. 2006	36.7	1.04	2.8	0.07	-30.5
Average	*33.0*	*1.10*	*3.4*	*0.07*	*-30.5*
Standard deviation	*5.2*	*0.09*	*0.8*	*0.00*	*0.1*
		High-water Stage			
07 Jul. 2006	196.7	3.99	2.0	0.09	-29.5
21 Jul. 2006	136.3	3.28	2.4	0.09	-29.3
04 Aug. 2006	259.8	6.34	2.4	0.08	-30.1
18 Aug. 2006	173.6	3.78	2.2	0.09	-29.0
06 Oct. 2006	219.6	4.41	2.0	0.08	-29.7
20 Oct. 2006	103.1	2.71	2.6	0.06	-31.1
01 Nov. 2006	206.1	3.04	1.5	0.09	-29.8
Average	*185.0*	*3.94*	*2.2*	*0.08*	*-29.8*
Standard deviation	*52.6*	*1.21*	*0.4*	*0.01*	*0.7*

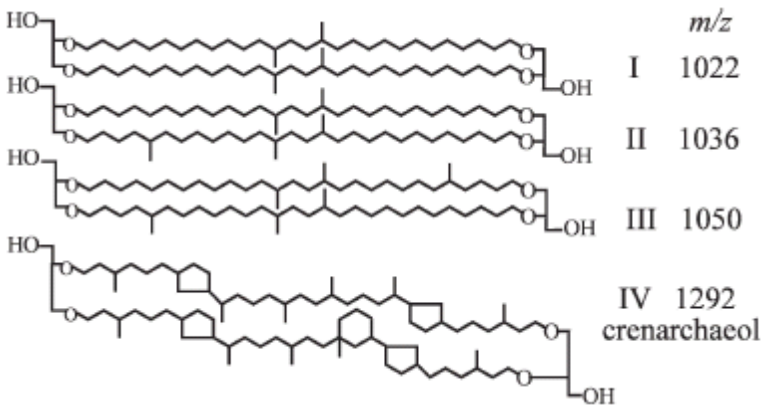

Figure 5.1[3]. The structures of the core glycerol dialkyl glycerol tetraether (GDGT) membrane lipids used in the BIT index. I-III are the branched membrane lipids produced by bacteria. IV is crenarcaeol, which is produced by a group of archaea now provisionally assigned to Thaumarchaea (formerly crenarchaea) [*Sinninghe Damste et al.*, 2002; *Brochier-Armanet et al.*, 2008; *Spang et al.*, 2010].

[3] Copyright, 2008 by the Association for the Sciences of Limnology and Oceanography, Inc. Walsh, E. M., A. E. Ingalls, and R. G. Keil. Sources and transport of terrestrial organic matter in Vancouver Island fjords and the Washington-Vancouver Margin: A multiproxy approach using $\delta^{13}C_{org}$, lignin phenols, and the ether lipid BIT index. Limnol. Oceanograph. 53(3) , 2008, p. 1055.

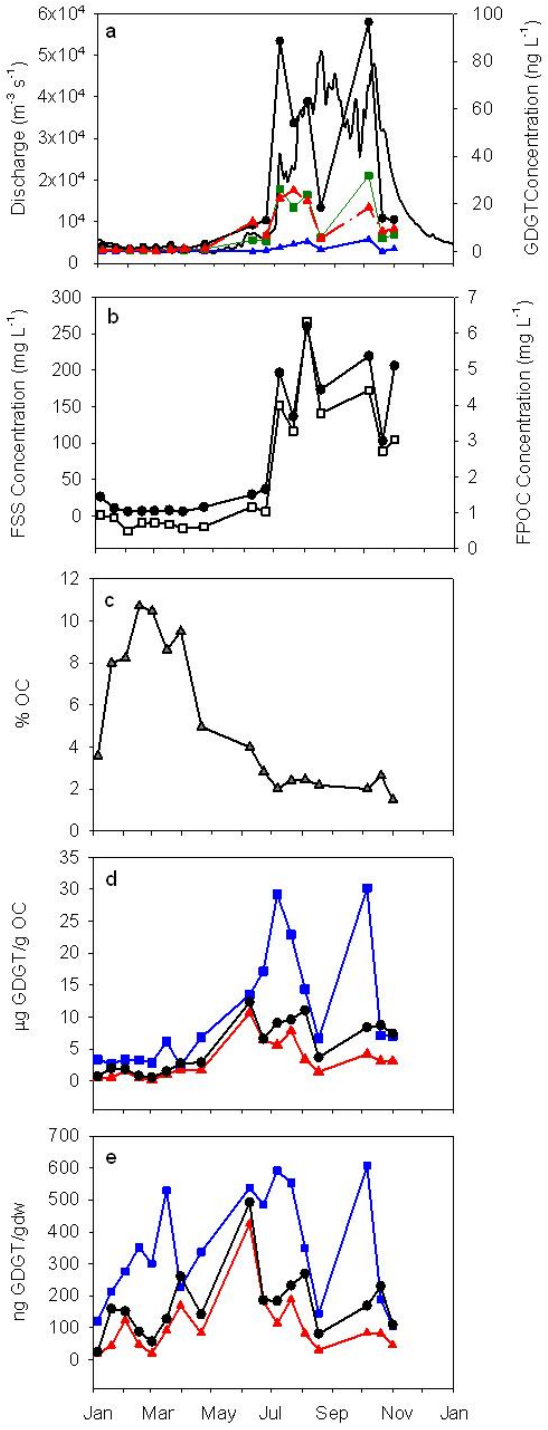

Figure 5.2. Variability in FPOM composition. (A) The concentration (ng/L) of core GDGTs. brGDGT I, II, and III are denoted by black circles, green squares, and blue triangles, respectively. GDGT IV is represented by red triangles. The black line is discharge. (B) The concentration of FSS (circles) and FPOC (squares). (C) The percentage of FSS that is organic carbon. (D) GDGT abundances normalized by organic carbon. Concentrations of BrGDGT I-III, isoGDGTs, and GDGT IV are represented by squares, circles, and triangles, respectively. (E) GDGT abundances normalized by weight.

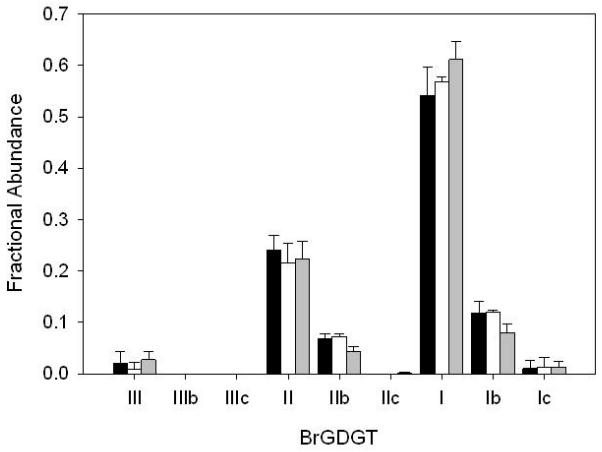

Figure 5.3. The fractional abundance of BrGDGT I-III and their cyclopentyl moieties from core riverine GDGTs during the low-, rising-, and high-water periods. Black, white, and gray represent low, rising, and high-water periods, respectively.

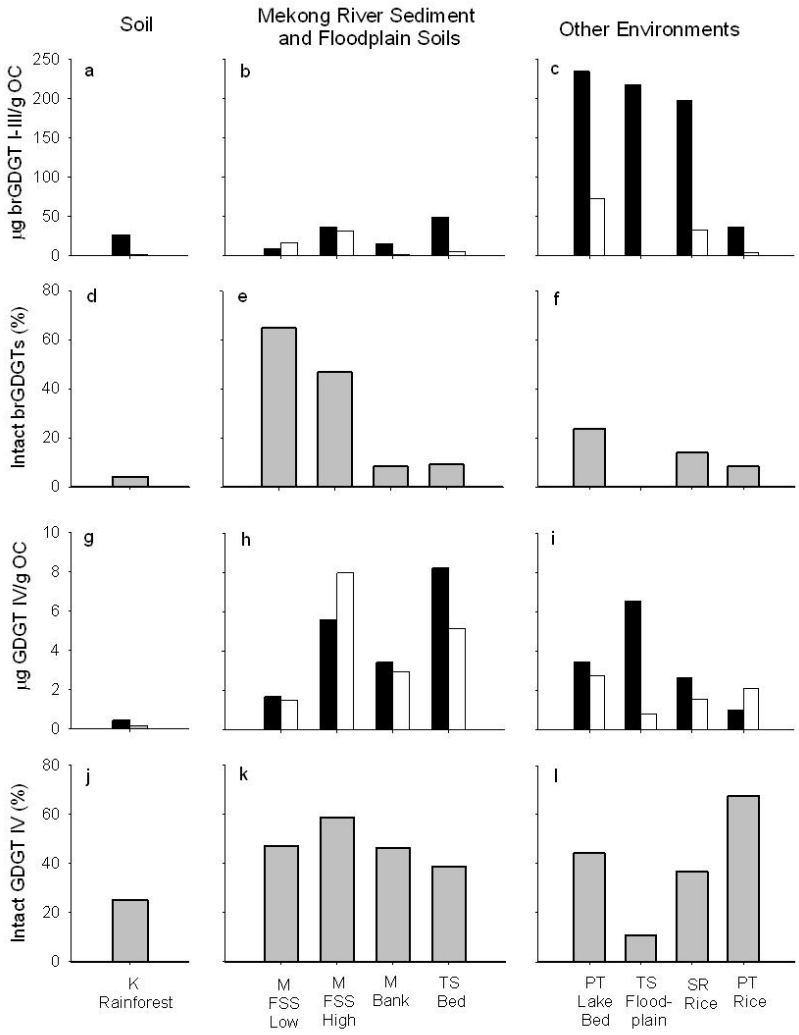

Figure 5.4. The relative abundance of total (intact + core) branched and isoprenoid GDGTs between sampling sites (µg GDGT/g OC). Site abbreviations are described in Table 1. Black and white shading represents core and intact lipids, respectively. (A-C) The concentration of brGDGT (I-III including cyclopentyl moieties); (D-F) The percentage of intact brGDGT I-III; (G-I) The concentration of GDGT IV; (J-K) The percentage of intact GDGT IV.

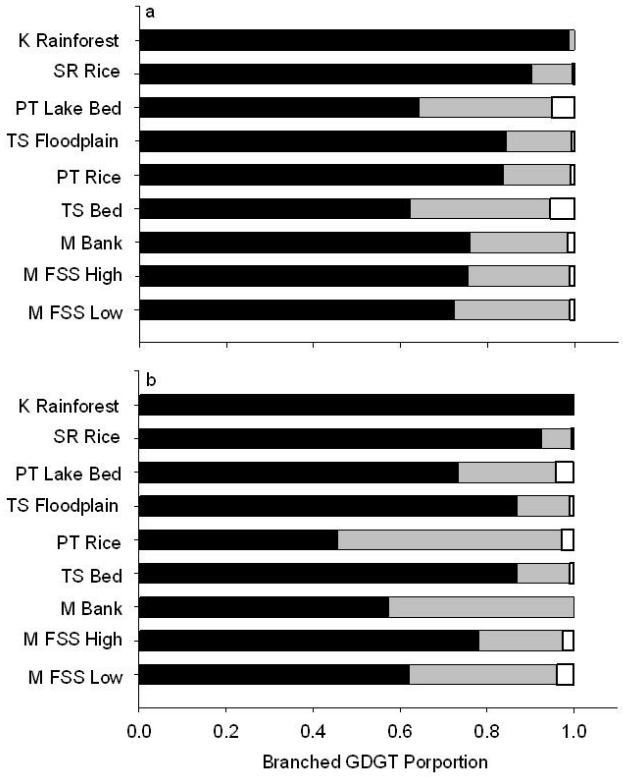

Figure 5.5. The fractional abundance of brGDGT I-III in (A) core lipids and (B) intact lipids. Black, gray, and white shading represents the fraction of brGDGT I-Ic, brGDGT II-IIc, and brGDGT III-IIIc, respectively.

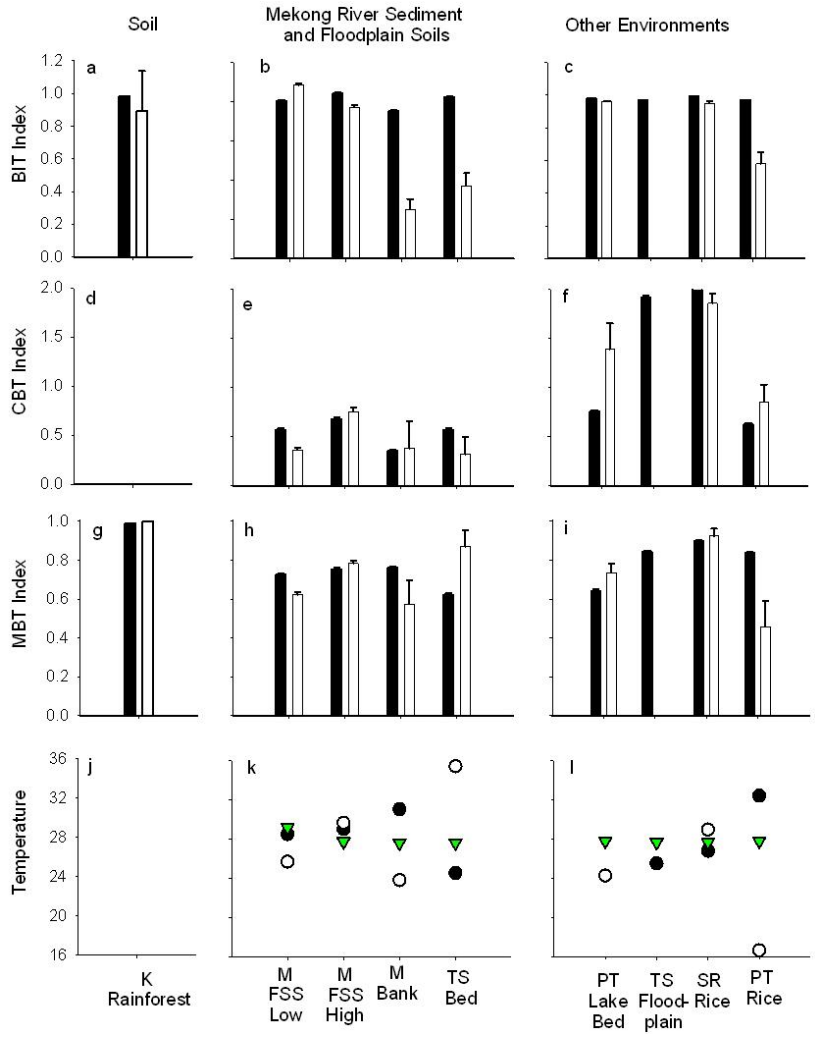

Figure 5.6. Variability in indices and predicted temperatures across sites. Black and white shading represents core and intact lipids, respectively. (A-C) the BIT index; (D-F) the CBT index; (G-I) the MBT index; (J-L) Temperature. Green triangles represent the average air temperature from 1950-2006 for a particular site. White and black circles represent the predicted air temperature calculated from intact lipids and core lipids, respectively.

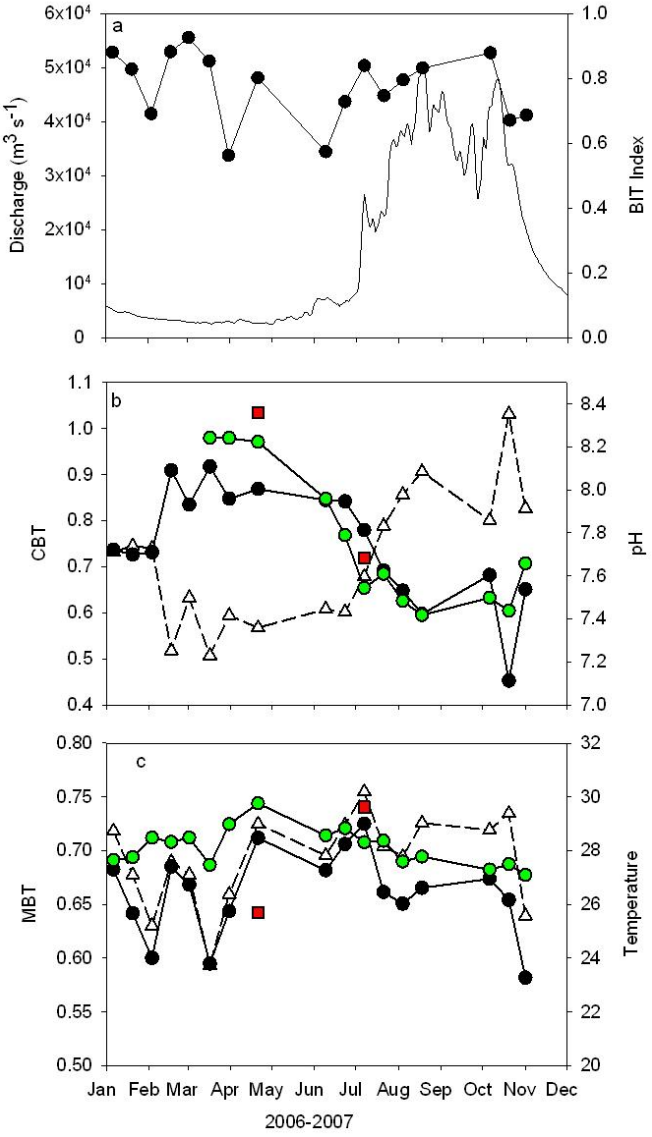

Figure 5.7. Seasonal variability in BIT, CBT, and MBT indices measured on Mekong River FSS. (A) Variability in the BIT index of Mekong River FSS; (B) Variability in the CBT index and pH. White triangles represent the CBT index, whereas black circles represent calculations of pH based on the regression for global lake sediment by *Sun et al.* [2011]. Green circles represent measured values of pH [D. E. Lockwood, unpublished data]. Red squares are the pH calculated from intact lipids; (C) Variability in the MBT index and temperature. White triangles are the MBT index, whereas black circles are MAAT calculated from *Sun et al.* [2011]. Green circles represent the average air temperature of the day the sample was collected. Red squares are calculates of air temperature using only intact lipids.

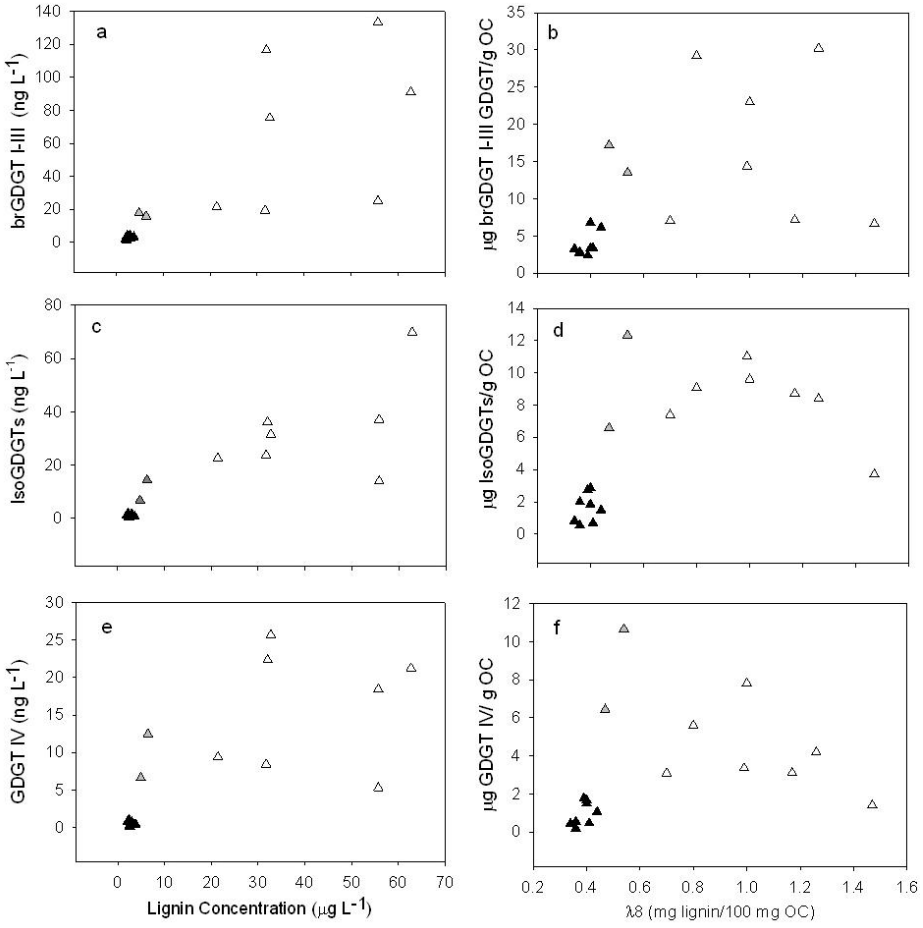

Figure 5.8. Correlations between GDGT lipids and lignin-phenols. Black, gray, and white triangles represent the low, rising, and high-water periods, respectively. Fig. A, C, E compare concentrations of brGDGT I-III and lignin-phenols normalized to volume concentrations normalized to volume (ng/L or µg/L), whereas Fig. B, D, and F compare concentrations normalized to organic carbon.

REFERENCES

Alin, S. R., M. F. L. Rasera, C. I. Salimon, J. E. Richey, G. W. Holtgrieve, A. V. Krusche, and A. Snidvongs (2011), Physical controls on carbon dioxide transfer velocity and flux in low-gradient river systems and implications for regional carbon budgets, *J. Geophy. Res., 116*, doi:10.1029/2010JG001398.

Amon, R., and R. Benner (1996), Bacterial utilization of different size classes of dissolved organic matter, *Limnol. Oceanogr., 41*(1), 41-51.

Amon, R., and R. Benner (1996), Photochemical and microbial consumption of dissolved organic carbon and dissolved oxygen in the Amazon River system, *Geochim. Cosmochim. Acta, 60*(10), 1783-1792, doi:10.1016/0016-7037(96)00055-5.

Araujo-Lima, C. A., B. R. Forsberg, R. Victoria, and L. Martinelli (1986), Energy sources for detritivorous fishes in the Amazon, *Science, 234*(4781), 1256-1258, doi:10.1126/science.234.4781.1256.

Aufdenkampe, A. K., J. I. Hedges, J. E. Richey, A. V. Krusche, and C. A. Llerena (2001), Sorptive fractionation of dissolved organic nitrogen and amino acids onto fine sediments within the Amazon Basin, *Limnol. Oceanogr., 46*(8), 1921-1935.

Aufdenkampe, A. K., E. Mayorga, P. Raymond, J. Melack, S. Doney, S. Alin, R. Aalto, and K. Yoo (2011), Riverine coupling of biogeochemical cycles between land, oceans, and atmosphere *Front. Ecol. Environ., 9*, 53-60, doi:10.1890/100014.

Aumont, O., J. Orr, P. Monfray, W. Ludwig, P. Amiotte-Suchet, and J. Probst (2001), Riverine-driven interhemispheric transport of carbon, *Global Biogeochem. Cycles, 15*(2), 393-405, doi:10.1029/1999GB001238.

Battin, T. J., L. A. Kaplan, S. Findlay, C. S. Hopkinson, E. Marti, A. I. Packman, J. D. Newbold, and F. Sabater (2008), Biophysical controls on organic carbon fluxes in fluvial networks, *Nat. Geosci., 1*(2), 95-100, doi:10.1038/ngeo101.

Battin, T. J., S. Luyssaert, L. A. Kaplan, A. K. Aufdenkampe, A. Richter, and L. J. Tranvik (2009), The boundless carbon cycle, *Nat. Geosci., 2*(9), 598-600, doi:10.1038/ngeo618.

Benner, R., M. L. Fogel, and E. K. Sprague (1991), Diagenesis of below-ground biomass of *Spartina Alterniflora* in salt marsh sediments, *Limnol. Oceanogr., 36*(7), 1358-1374.

Benner, R., S. Opsahl, G. ChinLeo, J. Richey, and B. Forsberg (1995), Bacterial carbon metabolism in the Amazon River system, *Limnol. Oceanogr., 40*(7), 1262-1270.

Benson, B. B., D. Krause (1984), The concentration and isotopic fractionation of oxygen dissolved in fresh-water and seawater in equilibrium with the atmosphere, *Limnol. Oceanogr., 29*(3), 620-632.

Bernardes, M., L. Martinelli, A. Krusche, J. Gudeman, M. Moreira, R. Victoria, J. Ometto, M. Ballester, A. Aufdenkampe, J. Richey, and J. Hedges (2004), Riverine organic matter composition as a function of land use changes, Southwest Amazon, *Ecol. Appl., 14*(4), S263-S279.

Berner, R. A. (1989), Biogeochemical cycles of carbon and sulfer and their effects on atmospheric oxygen over Phanerozoic time, *Paleogeography, Paleoclimatology, and Paleoecology 72*, 97-122.

Bianchi, T. S. (2011), The role of terrestrially derived organic carbon in the coastal ocean: a changing paradigm and the priming effect, *P. Natl. Acad. Sci. USA, 108*(49), 19473-19481, doi:10.1073/pnas.1017982108.

Bianchi, T. S., L. A. Wysocki, M. Stewart, T. R. Filley, and B. A. McKee (2007), Temporal variability in terrestrially-derived sources of particulate organic carbon in the lower Mississippi River and its upper tributaries, *Geochim. Cosmochim. Acta, 71*(18), 4425-4437, doi:10.1016/j.gca.2007.07.011.

Blaga, C. I., G. Reichart, O. Heiri, and J. S. Sinninghe Damsté (2009), Tetraether membrane lipid distributions in water-column particulate matter and sediments: a study of 47 European lakes along a north–south transect, *J. Paleolimnol., 41*(3), 523-540, doi:10.1007/s10933-008-9242-2.

Blair, N., E. Leithold, and R. Aller (2004), From bedrock to burial: the evolution of particulate organic carbon across coupled watershed-continental margin systems, *Mar. Chem., 92*(1-4), 141-156, doi:10.1016/j.marchem.2004.06.023.

Bott, T. L., D. S. Montgomery, J. D. Newbold, D. B. Arscott, C. L. Dow, A. K. Aufdenkampe, J. K. Jackson, and L. A. Kaplan (2006), Ecosystem metabolism in streams of the Catskill Mountains (Delaware and Hudson River watersheds) and Lower Hudson Valley, *J. N. Am. Benthol. Soc., 25*(4), 1018-1044.

Brochier-Armanet, C., B. Boussau, S. Gribaldo, and P. Forterre (2008), Mesophilic Crenarchaeota: proposal for a third archaeal phylum, the Thaumarchaeota, *Nat. Rev. Microbiol., 6*(3), 245-252, doi:10.1038/nrmicro1852.

Burdige, D., and K. Gardner (1998), Molecular weight distribution of dissolved organic carbon in marine sediment pore waters, *Mar. Chem., 62*(1-2), 45-64, doi:10.1016/S0304-4203(98)00035-8.

Canadell, J. G., C. Le Quere, M. R. Raupach, C. B. Field, E. T. Buitenhuis, P. Ciais, T. J. Conway, N. P. Gillett, R. A. Houghton, and G. Marland (2007), Contributions to accelerating atmospheric CO_2 growth from economic activity, carbon intensity, and efficiency of natural sinks, *Proc. Natl. Acad. Sci. U. S. A., 104*(47), 18866-18870, doi:10.1073/pnas.0702737104.

Chaplot, V., C. Rumpel, and C. Valentin (2005), Water erosion impact on soil and carbon redistributions within uplands of Mekong River, *Global Biogeochem. Cycles, 19*(4), GB4004, doi:10.1029/2005GB002493.

Clark, I., P. Fritz (1997), *Environmental isotopes in hydrogeology*, Lewis Publishers, Boca Raton.

Clark, D., S. Piper, C. Keeling, and D. Clark (2003), Tropical rain forest tree growth and atmospheric carbon dynamics linked to interannual temperature variation during 1984-2000, *Proc. Natl. Acad. Sci. U. S. A., 100*(10), 5852-5857, doi:10.1073/pnas.0935903100.

Cole, J. J., N. F. Caraco, G. W. Kling, and T. K. Kratz (1994), Carbon dioxide supersaturation in the surface waters of lakes, *Science, 265*(5178), 1568-1570, doi:10.1126/science.265.5178.1568.

Cole, J. J., Y. T. Prairie, N. F. Caraco, W. H. McDowell, L. J. Tranvik, R. G. Striegl, C. M. Duarte, P. Kortelainen, J. A. Downing, J. J. Middelburg, and J. Melack (2007), Plumbing the global carbon cycle: Integrating inland waters into the terrestrial carbon budget, *Ecosystems, 10*(1), 171-184, doi:10.1007/s10021-006-9013-8.

Costa-Cabral, M. C., J. E. Richey, G. Goteti, D. P. Lettenmaier, C. Feldkotter, and A. Snidvongs (2008), Landscape structure and use, climate, and water movement in the Mekong River basin, *Hydrol. Process., 22*(12), 1731-1746, doi:10.1002/hyp.6740.

Coynel, A., P. Seyler, H. Etcheber, M. Meybeck, and D. Orange (2005), Spatial and seasonal dynamics of total suspended sediment and organic carbon species in the Congo River, *Global Biogeochem. Cycles, 19*(4), doi:10.1029/2004GB002335.

da Cunha, L., L. Serve, F. Gadel, and J. Blazi (2001), Lignin-derived phenolic compounds in the particulate organic matter of a French Mediterranean river: seasonal and spatial variations, *Org. Geochem., 32*(2), 305-320.

Dagley, S. (1975), A biochemical approach to some problems of environmental pollution, *Essays in Biochemistry, 11*(1), 81-138.

Damste, J. S., S. Schouten, E. C. Hopmans, A. C. van Duin, and J. A. Geenevasen (2002), Crenarchaeol: the characteristic core glycerol dibiphytanyl glycerol tetraether membrane lipid of cosmopolitan pelagic crenarchaeota, *J. Lipid Res., 43*(10), 1641-1651.

Davidson, E., I. Janssens (2006), Temperature sensitivity of soil carbon decomposition and feedbacks to climate change, *Nature, 440*(7081), 165-173, doi:10.1038/nature04514.

Davis, W. M., J. S. Nickels, J. D. King, and R. J. Bobbie (1979), Determination of the sedimentary microbial biomass by extractable lipid phosphate, *Oecologia, 40*(1), 51-62.

De Haan, H., G. Werlemark, and T. Deboer (1983), Effect of pH on molecular-weight and size of fulvic acids in drainage water from Peaty Grassland in NW Netherlands, *Plant Soil, 75*(1), 63-73.

de Rouw, A., S. Huon, B. Soulileuth, P. Jouquet, A. Pierret, O. Ribolzi, C. Valentin, E. Bourdon, and B. Chantharath (2010), Possibilities of carbon and nitrogen sequestration under conventional tillage and no-till cover crop farming (Mekong valley, Laos), *Agriculture Ecosystems & Environment, 136*(1-2), 148-161, doi:10.1016/j.agee.2009.12.013.

Degens, E. T., S. Kempe, and J. E. Richey (1991), Biogeochemistry of major world rivers, John Wiley and Sons, Inc, New York.

del Giorgio, P. A., and M. L. Pace (2008), Relative independence of dissolved organic carbon transport and processing in a large temperate river: The Hudson River as both pipe and reactor, *Limnol. Oceanogr., 53*(1), 185-197, doi:10.4319/lo.2008.53.1.0185.

Devol, A. H., B. R. Forsberg, J. E. Richey, and T. P. Pimentel (1995), Seasonal variation in chemical distributions in the Amazon (Solimoes) River - a multiyear time series, *Global Biogeochem. Cycles, 9*(3), 307-328, doi:10.1029/95GB01145.

Devol, A. H., and J. I. Hedges (2001), Organic matter and nutrients in the mainstem Amazon River, in *The biogeochemistry of the Amazon Basin, ,* edited by R. L. McClain et al, pp. 275-306, Oxford University Press.

Devol, A. H., P. D. Quay, J. E. Richey, and L. A. Martinelli (1987), The Role of Gas-Exchange in the Inorganic Carbon, Oxygen, and Rn-222 Budgets of the Amazon River, *Limnol. Oceanogr., 32*(1), 235-248.

Dickens, A., Y. Gelinas, C. Masiello, S. Wakeham, and J. Hedges (2004), Reburial of fossil organic carbon in marine sediments, *Nature, 427*(6972), 336-339, doi:10.1038/nature02299.

Diffenbaugh, N. S., and M. Scherer (2011), Observational and model evidence of global emergence of permanent, unprecedented heat in the 20th and 21st centuries *Clim. Change, 107*(3-4), 615-624, doi:10.1007/s10584-011-0112-y.

Downing, J. A., J. J. Cole, J. J. Middelburg, R. G. Striegl, C. M. Duarte, P. Kortelainen, Y. T. Prairie, and K. A. Laube (2008), Sediment organic carbon burial in agriculturally eutrophic impoundments over the last century, *Global Biogeochem. Cycles, 22*(1), GB1018, doi:10.1029/2006GB002854.

Drenzek, N. J., D. B. Montlucon, M. B. Yunker, R. W. Macdonald, and T. I. Eglinton (2007), Constraints on the origin of sedimentary organic carbon in the Beaufort Sea from coupled molecular C-13 and C-14 measurements, *Mar. Chem., 103*(1-2), 146-162, doi:10.1016/j.marchem.2006.06.017.

Duarte, C., Y. Prairie (2005), Prevalence of heterotrophy and atmospheric CO_2 emissions from aquatic ecosystems, *Ecosystems, 8*(7), 862-870, doi:10.1007/s10021-005-0177-4.

Dunne, T., L. Mertes, R. Meade, J. Richey, and B. Forsberg (1998), Exchanges of sediment between the flood plain and channel of the Amazon River in Brazil, *Geological Society of America Bulletin, 110*(4), 450-467, doi:10.1130/0016-7606(1998)110<0450:EOSBTF>2.3.CO;2.

Eckard, R. S., P. J. Hernes, B. A. Bergamaschi, R. Stepanauskas, and C. Kendall (2007), Landscape scale controls on the vascular plant component of dissolved organic carbon across a freshwater delta, *Geochim. Cosmochim. Acta, 71*(24), 5968-5984, doi:10.1016/j.gca.2007.09.027.

Ellis, E. E., J. E. Richey, A. K. Aufdenkampe, A. V. Krusche, P. D. Quay, C. Salimon, and H. B. da Cunha (2012a), Factors controlling water-column respiration in rivers of the central and southwestern Amazon Basin, *Limnol. Oceanogr., 57*(2), 527-540, doi:10.4319/lo.2012.57.2.0527.

Ellis, E. E., R. G. Keil, A. E. Ingalls, J. E. Richey, and S. R. Alin (2012b), Seasonal variability in the sources of particulate organic matter of the Mekong River as discerned by elemental and lignin analyses *Journal of Geophysical Research, 117*, doi:10.1029/2011JG001816.

Engle, D. L., J. M. Melack, R. D. Doyle, and T. R. Fisher (2008), High rates of net primary production and turnover of floating grasses on the Amazon floodplain: implications for aquatic respiration and regional CO_2 flux, *Global Change Biol., 14*(2), 369-381, doi:10.1111/j.1365-2486.2007.01481.x.

Ertel, J., and J. I. Hedges (1984), The lignin component of humic substances - distribution among soil and sedimentary humic, fulvic, and base-insoluble fractions, *Geochim. Cosmochim. Acta, 48*(10), 2065-2074, doi:10.1016/0016-7037(84)90387-9.

Feeley, K. J., S. J. Wright, M. N. N. Supardi, A. R. Kassim, and S. J. Davies (2007), Decelerating growth in tropical forest trees, *Ecol. Lett., 10*(6), 461-469, doi:10.1111/j.1461-0248.2007.01033.x.

Field, C., M. Behrenfeld, J. Randerson, and P. Falkowski (1998), Primary production of the biosphere: Integrating terrestrial and oceanic components, *Science, 281*(5374), 237-240, doi:10.1126/science.281.5374.237.

Galy, V., O. Beyssac, C. France-Lanord, and T. Eglinton (2008), Recycling of graphite during Himalayan erosion: A geological stabilization of carbon in the crust, *Science, 322*(5903), 943-945, doi:10.1126/science.1161408.

Galy, V., T. Eglinton (2011), Protracted storage of biospheric carbon in the Ganges-Brahmaputra basin, *Nat. Geosci., 4*(12), 843-847, doi:10.1038/NGEO1293.

Galy, V., T. Eglinton, C. France-Lanord, and S. Sylya (2011), The provenance of vegetation and environmental signatures encoded in vascular plant biomarkers carried by the Ganges-Brahmaputra rivers, *Earth Planet. Sci. Lett., 304*(1-2), 1-12, doi:10.1016/j.epsl.2011.02.003.

Galy, V., C. France-Lanord, and B. Lartiges (2008), Loading and fate of particulate organic carbon from the Himalaya to the Ganga-Brahmaputra delta, *Geochim. Cosmochim. Acta, 72*(7), 1767-1787, doi:10.1016/j.gca.2008.01.027.

Goericke, R., B. Fry (1994), Variations of marine plankton $\delta^{13}C$ with latitude, temperature, and dissolved CO_2 in the world ocean, *Global Biogeochem. Cycles, 8*(1), 85-90, doi:10.1029/93GB03272.

Goni, M. A., and J. I. Hedges (1995), Sources and reactivities of marine-derived organic matter in coastal sediments as determined by alkaline Cuo oxidation, *Geochim. Cosmochim. Acta, 59*(14), 2965-2981, doi:10.1016/0016-7037(95)00188-3.

Goni, M. A., and S. Montgomery (2000), Alkaline CuO oxidation with a microwave digestion system: Lignin analyses of geochemical samples, *Anal. Chem., 72*(14), 3116-3121, doi:10.1021/ac991316w.

Grossart, H. P., and H. Ploug (2000), Bacterial production and growth efficiencies: direct measurements on riverine aggregates, *Limnol. Oceanogr., 45*(2), 436-445.

Grumbine, R. E., J. Xu (2011), Mekong Hydropower Development, *Science, 332*(6026), 178-179, doi:10.1126/science.1200990.

Gupta, A., L. Hock, X. Huang, and P. Chen (2002), Evaluation of part of the Mekong River using satellite imagery, *Geomorphology, 44*(3-4), 221-239, doi:10.1016/S0169-555X(01)00176-3.

Harvey, H. R., R. D. Fallon, and J. S. Patton (1986), The effect of organic matter and oxygen on the degradation of bacterial membrane lipids in marine sediments, *Geochim. Cosmochim. Acta, 50*(5), 795-804, doi:10.1016/0016-7037(86)90355-8.

Hedges, J. I., and P. L. Parker (1976), Land-derived organic matter in surface sediments from the Gulf of Mexico, *Geochim. Cosmochim. Acta, 40*(9), 1019-1029.

Hedges, J. I., R. A. Blanchette, K. Weliky, and A. H. Devol (1988), Effects of Fungal Degradation on the CuO Oxidation-Products of Lignin - a Controlled Laboratory Study, *Geochim. Cosmochim. Acta, 52*(11), 2717-2726, doi:10.1016/0016-7037(88)90040-3.

Hedges, J. I., W. A. Clark, P. D. Quay, J. E. Richey, A. H. Devol, and U. D. Santos (1986), Compositions and fluxes of particulate organic material in the Amazon River, *Limnol. Oceanogr., 31*(4), 717-738.

Hedges, J. I., G. L. Cowie, J. E. Richey, P. D. Quay, R. Benner, M. Strom, and B. R. Forsberg (1994), Origins and processing of organic matter in the Amazon River as indicated by carbohydrates and amino acids, *Limnol. Oceanogr., 39*(4), 743-761.

Hedges, J. I., J. R. Ertel, and E. S. Leopold (1982), Lignin geochemistry of a late Quaternary sediment core from Lake Washington, *Geochim. Cosmochim. Acta, 46*(10), 1869-1877, doi:10.1016/0016-7037(82)90125-9.

Hedges, J. I., R. G. Keil, and R. Benner (1997), What happens to terrestrial organic matter in the ocean? *Org. Geochem., 27*(5-6), 195-212, doi:10.1016/S0146-6380(97)00066-1.

Hedges, J. I., and D. C. Mann (1979), Characterization of plant tissues by their lignin oxidation products, *Geochim. Cosmochim. Acta, 43*(11), 1803-1807, doi:10.1016/0016-7037(79)90028-0.

Hedges, J., E. Mayorga, E. Tsamakis, M. McClain, A. Aufdenkampe, P. Quay, J. Richey, R. Benner, S. Opsahl, B. Black, T. Pimentel, J. Quintanilla, and L. Maurice (2000), Organic matter in Bolivian tributaries of the Amazon River: A comparison to the lower mainstream, *Limnol. Oceanogr., 45*(7), 1449-1466.

Hedges, J., and J. Oades (1997), Comparative organic geochemistries of soils and marine sediments, *Org. Geochem., 27*(7-8), 319-361, doi:10.1016/S0146-6380(97)00056-9.

Hedges, J. I. (1992), Global biogeochemical cycles: progress and problems , *Mar. Chem., 39*(1-3), 67-93, doi:10.1016/0304-4203(92)90096-S.

Hedges, J. I., R. G. Keil (1995), Sedimentary organic matter preservation: an assessment and speculative synthesis *Mar. Chem., 49*(2-3), 81-115, doi:10.1016/0304-4203(95)00008-F.

Hernes, P. J., A. C. Robinson, and A. K. Aufdenkampe (2007), Fractionation of lignin during leaching and sorption and implications for organic matter "freshness", *Geophys. Res. Lett., 34*(17), L17401, doi:10.1029/2007GL031017.

Holtgrieve, G. W., D. E. Schindler, T. A. Branch, and Z. T. A'mar (2010), Simultaneous quantification of aquatic ecosystem metabolism and reaeration using a Bayesian statistical model of oxygen dynamics, *Limnol. Oceanogr., 55*(3), 1047-1063, doi:10.4319/lo.2010.55.3.1047.

Hopmans, E. C., J. W. H. Weijers, E. Schefuß, L. Herfort, J. S. Sinninghe Damsté, and S. Schouten (2004), A novel proxy for terrestrial organic matter in sediments based on branched and isoprenoid tetraether lipids *Earth Planet. Sci. Lett., 224*(1-2), 107-116, doi:10.1016/j.epsl.2004.05.012.

Hori, H. (2000), *The Mekong: Environment and development*, United Nations University Press, Tokyo, Japan.

Houghton, R. A. (2007), Balancing the global carbon budget, *Annu. Rev. Earth Planet. Sci., 35*, 313-347, doi:10.1146/annurev.earth.35.031306.140057.

Hua, Q., M. Barbetti (2004), Review of tropospheric bomb C-14 data for carbon cycle modeling and age calibration purposes, *Radiocarbon, 46*(3), 1273-1298.

Huang, Y., K. Freeman, T. Eglinton, and F. Street-Perrott (1999), $\delta^{13}C$ analyses of individual lignin phenols in Quaternary lake sediments: A novel proxy for deciphering past terrestrial vegetation changes, *Geology, 27*(5), 471-474, doi:10.1130/0091-7613(1999)027<0471:CAOILP>2.3.CO;2.

Huguet, C., E. C. Hopmans, W. Febo-Ayala, D. H. Thompson, J. S. Sinninghe Damsté, and S. Schouten (2006), An improved method to determine the absolute abundance of glycerol dibiphytanyl glycerol tetraether lipids *Org. Geochem., 37*(9), 1036-1041, doi:10.1016/j.orggeochem.2006.05.008.

Hutyra, L. R., J. W. Munger, S. R. Saleska, E. Gottlieb, B. C. Daube, A. L. Dunn, D. F. Amaral, P. B. de Camargo, and S. C. Wofsy (2007), Seasonal controls on the exchange of carbon and water in an Amazonian rain forest, *J. Geophys. Res., 112*(G3), G03008, doi:10.1029/2006JG000365.

Ingalls, A. E., E. E. Ellis, G. M. Santos, K. E. McDuffee, L. Truxal, R. G. Keil, and E. R. M. Druffel (2010), HPLC purification of higher plant-dervied lignin phenols for compound specific radiocarbon analysis, *Anal. Chem., 82*(21), 8931-8938, doi:10.1021/ac1016584.

Ittekot, V., R. W. P. M. Laane (1991), Fate of riverine particulate organic matter, in *Biogeochemistry of major world rivers,* , edited by E. T. Degens et al, pp. 233-243, New York, John Wiley and Sons, Inc.

Johnson, M. S., J. Lehmann, S. J. Riha, A. V. Krusche, J. E. Richey, J. P. H. B. Ometto, and E. G. Couto (2008), CO_2 efflux from Amazonian headwater streams represents a significant fate for deep soil respiration, *Geophys. Res. Lett., 35*(17), L17401, doi:10.1029/2008GL034619.

Keil, R. G., and J. A. Neibauer (2009), Analysis of cooking spices in natural waters, *Limn. Oceanogr. Methods, 7*, 848-855.

Kiem, R., I. Kogel-Knabner (2003), Contribution of lignin and polysaccharides to the refractory carbon pool in C-depleted arable soils, *Soil Biol. Biochem., 35*(1), 101-118, doi:10.1016/S0038-0717(02)00242-0.

Kim, J., W. Ludwig, S. Schouten, P. Kerhervé, L. Herfort, J. Bonnin, and J. S. Sinninghe Damsté (2007), Impact of flood events on the transport of terrestrial organic matter to the ocean: A study of the Têt River (SW France) using the BIT index *Org. Geochem., 38*(10), 1593-1606, doi:10.1016/j.orggeochem.2007.06.010.

Koga, Y., M. Akagawa-Matsushita, M. Ohga, and M. Nishihara (1993), Taxonomic Significance of the Distribution of Component Parts of Polar Ether Lipids in Methanogens *Syst. Appl. Microbiol., 16*(3), 342-351, doi:10.1016/S0723-2020(11)80264-X.

Komada, T., M. R. Anderson, and C. L. Dorfmeier (2008), Carbonate removal from coastal sediments for the determination of organic carbon and its isotopic signatures, δ^{13}C andC: comparison of fumigation and direct acidification by hydrochloric acid, *Limnol. Oceanogr.-Methods, 6*, 254-262.

Kritzberg, E., J. Cole, M. Pace, W. Graneli, and D. Bade (2004), Autochthonous versus allochthonous carbon sources of bacteria: Results from whole-lake C-13 addition experiments, *Limnol. Oceanogr., 49*(2), 588-596.

Kummu, M., D. Penny, J. Sarkkula, and J. Koponen (2008), Sediment: Curse or Blessing for Tonle Sap Lake? *Ambio, 37*(3), 158-163, doi:10.1579/0044-7447(2008)37[158:SCOBFT]2.0.CO;2.

Kummu, M., J. Sarkkula (2008), Impact of the Mekong River flow alteration on the Tonle Sap flood pulse, *Ambio, 37*(3), 185-192, doi:10.1579/0044-7447(2008)37[185:IOTMRF]2.0.CO;2.

Kummu, M., O. Varis (2007), Sediment-related impacts due to upstream reservoir trapping, the Lower Mekong River *Geomorphology, 85*(3-4), 275-293, doi:10.1016/j.geomorph.2006.03.024.

Levin, I., B. Kromer (2004), The tropospheric CO_2 ^{14}C-level in mid-latitudes of the Northern Hemisphere (1959-2003), *Radiocarbon, 46*(3), 1261-1272.

Lipp, J. S., Y. Morono, F. Inagaki, and K. U. Hinrichs (2008), Significant contribution of Archaea to extant biomass in marine subsurface sediments *Nature, 454*(7207), 991-994, doi:10.1038/nature07174.

Lipp, J. S., and K. Hinrichs (2009), Structural diversity and fate of intact polar lipids in marine sediments, *Geochim. Cosmochim. Acta, 73*(22), 6816-6833, doi:10.1016/j.gca.2009.08.003.

Malhi, Y., D. Wood, T. Baker, J. Wright, O. Phillips, T. Cochrane, P. Meir, J. Chave, S. Almeida, L. Arroyo, N. Higuchi, T. Killeen, S. Laurance, W. Laurance, S. Lewis, A. Monteagudo, D. Neill, P. Vargas, N. Pitman, C. Quesada, R. Salomao, J. Silva, A. Lezama, J. Terborgh, R. Martinez, and B. Vinceti (2006), The regional variation of aboveground live biomass in old-growth Amazonian forests, *Global Change Biol., 12*(7), 1107-1138, doi:10.1111/j.1365-2486.2006.01120.x.

Marschner, B., S. Brodowski, A. Dreves, G. Gleixner, A. Gude, P. M. Grootes, U. Hamer, A. Heim, G. Jandl, R. Ji, K. Kaiser, K. Kalbitz, C. Kramer, P. Leinweber, J. Rethemeyer, A. Schäffer, M. W. I. Schmidt, L. Schwark, and G. L. B. Wiesenberg (2008), How relevant is recalcitrance for the stabilization of organic matter in soils? *J. Plant Nutr. Soil Sc., 171*(1), 91-110, doi:10.1002/jpln.200700049.

Mayorga, E., A. Aufdenkampe, C. Masiello, A. Krusche, J. Hedges, P. Quay, J. Richey, and T. Brown (2005), Young organic matter as a source of carbon dioxide outgassing from Amazonian rivers, *Nature, 436*(7050), 538-541, doi:10.1038/nature03880.

Mayorga, E., M. Logsdon, M. Ballester, and J. Richey (2005), Estimating cell-to-cell land surface drainage paths from digital channel networks, with an application to the Amazon basin, *J. of Hydrol., 315*(1-4), 167-182, doi:10.1016/j.jhydrol.2005.03.023.

Mayorga, E. (2004), Isotopic constraints on sources and cycling of riverine dissolved inorganic carbon in the Amazon Basin, Ph.D. thesis, Univ. of Washington.

Mayorga, E., S. P. Seitzinger, J. A. Harrison, E. Dumont, A. H. W. Beusen, A. F. Bouwman, B. M. Fekete, C. Kroeze, and G. Van Drecht (2010), Global Nutrient Export from WaterSheds 2 (NEWS 2): Model development and implementation, *Environ. Modell. Softw., 25*(7), 837-853, doi:10.1016/j.envsoft.2010.01.007.

Mekong River Commission (2005), Overview of the hydrology of the Mekong Basin, Mekong River Commission, Vientiane, Lao PDR.

Mekong River Commission (2007), Annual Mekong Flood Report 2006, Mekong River Commission, Vientiane, Lao PDR.

Mekong River Commission (2009), Economic, Environmental and Social Impact Assessment of Basin-Wide Water Resources Development Scenarios, Mekong River Commission, Vientiane, Lao PDR.

Meybeck, M. (1982), Carbon, Nitrogen, and Phosphorus Transport by World Rivers, *Am. J. Sci., 282*(4), 401-450.

Milliman, J. D., J. P. M. Syvitski (1992), Geomorphic/tectonic control of sediment discharge to the ocean: The importance of small mountainous rivers *J. Geol., 100*(5), 525-544, doi:10.1086/629606.

Mitchell, T.D., T. R. Carter, P. D. Jones, M. Hulme and M. New (2004), A comprehensive set of high-resolution grids of monthly climate for Europe and the globe: the observed record (1901-2000) and 16 scenarios (2001-2100). Working Paper 55. Tyne Centre for Climate Change Research, University of East Anglia, Norwich, UK (for CRU TS 2.02).

Moody, J. A., and R. H. Meade (1994), Evaluation of the method of collecting suspended sediment from large rivers by discharge-weighted pumping and separation by continuous-flow centrifugation, *Hydrol. Process., 8*(6), 513-530, doi:10.1002/hyp.3360080603.

Opsahl, S., and R. Benner (1995), Early diagenesis of vascular plant tissues - Lignin and cutin decomposition and biogeochemical implications, *Geochim. Cosmochim. Acta, 59*(23), 4889-4904, doi:10.1016/0016-7037(95)00348-7.

Paolini, J. (1995), Particulate organic carbon and nitrogen in the Orinoco river (Venezuela) *Biogeochemistry, 29*(1), 59-70, doi:10.1007/BF00002594.

Peterse, F., G. W. Nicol, S. Schouten, and J. S. Sinninghe Damsté (2010), Influence of soil pH on the abundance and distribution of core and intact polar lipid-derived branched GDGTs in soil, *Org. Geochem., 41*(10), 1171-1175, doi:10.1016/j.orggeochem.2010.07.004.

Quay, P. D., D. O. Wilbur, J. E. Richey, A. H. Devol, R. Benner, and B. R. Forsberg (1995), The O-18/O-16 of dissolved oxygen in rivers and lakes in the Amazon Basin - Determining the ratio of respiration to photosynthesis rates in fresh-waters, *Limnol. Oceanogr., 40*(4), 718-729.

Quay, P. D., D. O. Wilbur, J. E. Richey, J. I. Hedges, A. H. Devol, and R. L. Victoria (1992), Carbon cycling in the Amazon River - Implications from the ^{13}C compositions of particles and solutes, *Limnol. Oceanogr., 37*(4), 857-871.

Randerson, J., I. Enting, E. Schuur, K. Caldeira, and I. Fung (2002), Seasonal and latitudinal variability of troposphere $\Delta^{14}CO_2$: Post bomb contributions from fossil fuels, oceans, the stratosphere, and the terrestrial biosphere, *Global Biogeochem. Cycles, 16*(4), 1112, doi:10.1029/2002GB001876.

Rasse, D. P., M. Dignac, H. Bahri, C. Rumpel, A. Mariotti, and C. Chenu (2006), Lignin turnover in an agricultural field: from plant residues to soil-protected fractions, *Eur. J. Soil Sci., 57*(4), 530-538, doi:10.1111/j.1365-2389.2006.00806.x.

Raymond, and P., J. Bauer (2001), Use of ^{14}C and ^{13}C natural abundances for evaluating riverine, estuarine, and coastal DOC and POC sources and cycling: a review and synthesis, *Org. Geochem., 32*(4), 469-485, doi:10.1016/S0146-6380(00)00190-X.

Raymond, P., J. Bauer, N. Caraco, J. Cole, B. Longworth, and S. Petsch (2004), Controls on the variability of organic matter and dissolved inorganic carbon ages in northeast US rivers, *Mar. Chem., 92*(1-4), 353-366, doi:10.1016/j.marchem.2004.06.036.

Reimer, P., T. Brown, and R. Reimer (2004), Discussion: Reporting and calibration of post-bomb ^{14}C data, *Radiocarbon, 46*(3), 1299-1304.

Remington, S., A. Krusche, and J. Richey (2011), Effects of DOM photochemistry on bacterial metabolism and CO_2 evasion during falling water in a humic and a whitewater river in the Brazilian Amazon, *Biogeochemistry, 105*(1-3), 185-200, doi:10.1007/s10533-010-9565-8.

Rezende, C. E., W. C. Pfeiffer, L. A. Martinelli, E. Tsamakis, J. I. Hedges, and R. G. Keil (2010), Lignin phenols used to infer organic matter sources to Sepetiba Bay - RJ, Brasil, *Estuarine Coastal and Shelf Science, 87*(3), 479-486, doi:10.1016/j.ecss.2010.02.008.

Richey, J. E., A. H. Devol, S. C. Wofsy, R. L. Victoria, and M. N. G. Riberio (1988), Biogenic gases and the xxidation and reduction of carbon in Amazon River and floodplain waters, *Limnol. Oceanogr., 33*(4), 551-561.

Richey, J. E., J. I. Hedges, A. H. Devol, P. D. Quay, R. L. Victoria, L. A. Martinelli, and B. R. Forsberg (1990), Biogeochemistry of carbon in the Amazon River, *Limnol. Oceanogr., 35*(2), 352-371.

Richey, J. E., A. V. Krusche, M. S. Johnson, H. B. da Cunha, and V. M. Ballester (2009), The role of rivers in the regional carbon balance, in *LBA Synthesis Volume - Amazonia and the Global Change*, edited by M. Keller et al, pp. 489-504, Washington, D.C., AGU.

Richey, J. E., J. M. Melack, A. K. Aufdenkampe, V. M. Ballester, and L. L. Hess (2002), Outgassing from Amazonian rivers and wetlands as a large tropical source of atmospheric CO_2 *Nature, 416*(6881), 617-620, doi:10.1038/416617a.

Rundel, P. W. (2007), Vegetation in the Mekong Basin, in *The Mekong: Biophysical environment of an international river basin*, edited by I. C. Campbell, pp. 143-160, New York, Academic Press.

Saleska, S., S. Miller, D. Matross, M. Goulden, S. Wofsy, H. da Rocha, P. de Camargo, P. Crill, B. Daube, H. de Freitas, L. Hutyra, M. Keller, V. Kirchhoff, M. Menton, J. Munger, E. Pyle, A. Rice, and H. Silva (2003), Carbon in Amazon forests: Unexpected seasonal fluxes and disturbance-induced losses, *Science, 302*(5650), 1554-1557, doi:10.1126/science.1091165.

Santos, G. M., J. R. Southon, K. C. Druffel-Rodriquez, S. Griffin, and M. Mazon (2004), Magnesium perchlorate as an alternative water trap in AMS graphite sample preparation: a report on sample preparation at KCCAMS at the University of California, Irvine, *Radiocarbon, 46*(1), 165-173.

Santos, G. M., R. B. Moore, J. R. Southon, S. Griffin, E. Hinger, and D. Zhang (2007), AMS C-14 sample preparation at the KCCAMS/UCI facility: Status report and performance of small samples, *Radiocarbon, 49*(2), 255-269.

Santos, G. M., J. R. Southon, N. J. Drenzek, L. A. Ziolkowski, E. Druffel, X. Xu, D. Zhang, S. Trumbore, T. I. Eglinton, and K. A. Hughen (2010), Blank assessment for ultra-small radiocarbon samples: chemical extraction and separation versus AMS, *Radiocarbon, 52*(3), 1322-1335.

Schlesinger, W. H., and J. M. Melack (1981), Transport of organic carbon in the world's rivers, *Tellus, 33*(2), 172-187, doi:10.1111/j.2153-3490.1981.tb01742.x.

Schlünz, B., and R. R. Schneider (2000), Transport of terrestrial organic carbon to the oceans by rivers: re-estimating flux- and burial rates, *Int. J. Earth Sci., 88*(4), 599-606, doi:10.1007/s005310050290.

Schmidt, J., J. Deming, P. Jumars, and R. Keil (1998), Constancy of bacterial abundance in surficial marine sediments, *Limnol. Oceanogr., 43*(5), 976-982.

Schmidt, M. W. I., M. S. Torn, S. Abiven, T. Dittmar, G. Guggenberger, I. A. Janssens, M. Kleber, I. Koegel-Knabner, J. Lehmann, D. A. C. Manning, P. Nannipieri, D. P. Rasse, S. Weiner, and S. E. Trumbore (2011), Persistence of soil organic matter as an ecosystem property, *Nature*, *478*(7367), 49-56, doi:10.1038/nature10386.

Schnitzer, M. (1978), Some observations on chemistry of humic substances, *Agrochimica*, *22*(3-4), 216-225.

Schouten, S., E. C. Hopmans, M. Baas, H. Boumann, S. Standfest, M. Konneke, D. A. Stahl, and J. S. Sinninghe Damste (2008), Intact membrane lipids of "Candidatus Nitrosopumilus maritimus," a cultivated representative of the cosmopolitan mesophilic group I Crenarchaeota, *Appl. Environ. Microbiol.*, *74*(8), 2433-2440, doi:10.1128/AEM.01709-07.

Sinninghe Damste, J. S., W. I. Rijpstra, E. C. Hopmans, J. W. Weijers, B. U. Foesel, J. Overmann, and S. N. Dedysh (2011), 13,16-Dimethyl octacosanedioic acid (iso-diabolic acid): A common membrane-spanning lipid of Acidobacteria subdivisions 1 and 3, *Appl. Environ. Microbiol.*, doi:10.1128/AEM.00466-11.

Sioli, H. (1984), *The Amazon: Limnology and landscape ecology of a mighty tropical river and its basin*, Kluwer Academic Publishers.

Smith, R. W., T. S. Bianchi, and C. Savage (2010), Comparison of lignin phenols and branched/isoprenoid tetraethers (BIT index) as indices of terrestrial organic matter in Doubtful Sound, Fjordland, New Zealand, *Org. Geochem.*, *41*(3), 281-290, doi:10.1016/j.orggeochem.2009.10.009.

Spang, A., R. Hatzenpichler, C. Brochier-Armanet, T. Rattei, P. Tischler, E. Spieck, W. Streit, D. A. Stahl, M. Wagner, and C. Schleper (2010), Distinct gene set in two different lineages of ammonia-oxidizing archaea supports the phylum Thaumarchaeota, *Trends Microbiol.*, *18*(8), 331-340, doi:10.1016/j.tim.2010.06.003.

Spencer, R. G. M., P. J. Hernes, R. Ruf, A. Baker, R. Y. Dyda, A. Stubbins, and J. Six (2010), Temporal controls on dissolved organic matter and lignin biogeochemistry in a pristine tropical river, Democratic Republic of Congo, *J. Geophys. Res.*, *115*(G3), doi:10.1029/2009JG001180.

Stallard, R. F. (1998), Terrestrial sedimentation and the carbon cycle: Coupling weathering and erosion to carbon burial, *Global Biogeochem. Cycles*, *12*(2), 231-257, doi:10.1029/98GB00741.

Sun, L., E. Perdue, J. Meyer, and J. Weis (1997), Use of elemental composition to predict bioavailability of dissolved organic matter in a Georgia river, *Limnol. Oceanogr.*, *42*(4), 714-721.

Sun, Q., G. Chu, M. Liu, M. Xie, S. Li, Y. Ling, X. Wang, L. Shi, G. Jia, and H. Lü (2011), Distributions and temperature dependence of branched glycerol dialkyl glycerol tetraethers in recent lacustrine sediments from China and Nepal, *J. Geophys. Res.*, *116*(G1), doi:10.1029/2010JG001365.

Tabachnick, B. G., and L. S. Fidell (2001), *Using multivariate statistics*, 4th ed., Harper and Rowe, New York.

Tan, F. C., and P. M. Strain (1983), Sources, sinks and distribution of organic carbon in the St. Lawrence Estuary, Canada, *Geochim. Cosmochim. Acta, 47*(1), 125-132, doi:10.1016/0016-7037(83)90096-0.

Tareq, S., N. Tanaka, and K. Ohta (2004), Biomarker signature in tropical wetland: lignin phenol vegetation index (LPVI) and its implications for reconstructing the paleoenvironment, *Sci. Total Environ., 324*(1-3), 91-103, doi:10.1016/j.scitotenv.2003.10.020.

Tierney, J. E., J. M. Russell (2009), Distributions of branched GDGTs in a tropical lake system: Implications for lacustrine application of the MBT/CBT paleoproxy, *Org. Geochem., 40*(9), 1032-1036, doi:10.1016/j.orggeochem.2009.04.014.

Tierney, J. E., S. Schouten, A. Pitcher, E. C. Hopmans, and J. S. Sinninghe Damsté (2012), Core and intact polar glycerol dialkyl glycerol tetraethers (GDGTs) in Sand Pond, Warwick, Rhode Island (USA): Insights into the origin of lacustrine GDGTs, *Geochim. Cosmochim. Acta, 77*(0), 561-581, doi:10.1016/j.gca.2011.10.018.

Townsend-Small, A., J. L. Noguera, M. E. McClain, and J. A. Brandes (2007), Radiocarbon and stable isotope geochemistry of organic matter in the Amazon headwaters, Peruvian Andes, *Global Biogeochem. Cycles, 21*(2), GB2029, doi:10.1029/2006GB002835.

Tranvik, L. J., J. A. Downing, J. B. Cotner, S. A. Loiselle, R. G. Striegl, T. J. Ballatore, P. Dillon, K. Finlay, K. Fortino, L. B. Knoll, P. L. Kortelainen, T. Kutser, S. Larsen, I. Laurion, D. M. Leech, S. L. McCallister, D. M. McKnight, J. M. Melack, E. Overholt, J. A. Porter, Y. Prairie, W. H. Renwick, F. Roland, B. S. Sherman, D. W. Schindler, S. Sobek, A. Tremblay, M. J. Vanni, A. M. Verschoor, E. von Wachenfeldt, and G. A. Weyhenmeyer (2009), Lakes and reservoirs as regulators of carbon cycling and climate, *Limnol. Oceanogr., 54*(6), 2298-2314, doi:10.4319/lo.2009.54.6_part_2.2298.

Trumbore, S. E. (1993), Comparison of carbon dynamics in tropical and temperate soils using radiocarbon measurements, *Global Biogeochem. Cycles, 7*(2), 275-290, doi:10.1029/93GB00468.

Walling, D. E. (2005), Evaluation and analysis of sediment data from the Lower Mekong River, report, 61 pp., Mekong River Commission, Vientianne, Laos PDR.

Walling, D. E. (2008), The Changing Sediment Load of the Mekong River, *Ambio, 37*(3), 150-157, doi:10.1579/0044-7447(2008)37[150:TCSLOT]2.0.CO;2.

Walsh, E. M., A. E. Ingalls, and R. G. Keil (2008), Sources and transport of terrestrial organic matter in Vancouver Island fjords and the Vancouver-Washington Margin: A multiproxy approach using $\delta^{13}C_{org}$, lignin phenols, and the ether lipid BIT index, *Limnol. Oceanogr., 53*(3), 1054-1063, doi:10.4319/lo.2008.53.3.1054.

Wang, J. J., X. X. Lu, and M. Kummu (2011), Sediment load estimates and variations in the Lower Mekong River, *River Research and Applications, 27*(1), 33-46, doi:10.1002/rra.1337.

Weijers, J. W. H., E. Panoto, J. van Bleijswijk, S. Schouten, W. I. C. Rijpstra, M. Balk, A. J. M. Stams, and J. S. S. Damsté (2009), Constraints on the biological source(s) of the orphan branched tetraether membrane lipids, *Geomicrobiol. J., 26*(6), 402-414, doi:10.1080/01490450902937293.

Weijers, J. W. H., S. Schouten, E. C. Hopmans, J. A. J. Geenevasen, O. R. P. David, J. M. Coleman, R. D. Pancost, and J. S. Sinninghe Damsté (2006), Membrane lipids of mesophilic anaerobic bacteria thriving in peats have typical archaeal traits, *Environ. Microbiol., 8*(4), 648-657, doi:10.1111/j.1462-2920.2005.00941.x.

Weijers, J. W. H., S. Schouten, O. C. Spaargaren, and J. S. Sinninghe Damsté (2006), Occurrence and distribution of tetraether membrane lipids in soils: Implications for the use of the TEX86 proxy and the BIT index, *Org. Geochem., 37*(12), 1680-1693, doi:10.1016/j.orggeochem.2006.07.018.

Weijers, J. W. H., S. Schouten, J. C. van den Donker, E. C. Hopmans, and J. S. Sinninghe Damsté (2007), Environmental controls on bacterial tetraether membrane lipid distribution in soils, *Geochim. Cosmochim. Acta, 71*(3), 703-713, doi:10.1016/j.gca.2006.10.003.

Weiss, R. F. (1970), Solubility of nitrogen, oxygen and argon in water and seawater, *Deep-Sea Res., 17*(4), 721-&, doi:10.1016/0011-7471(70)90037-9.

Weiss, R. F. (1974), Carbon dioxide in water and seawater: the solubility of a non-ideal gas, *Mar. Chem., 2*(3), 203-215, doi:10.1016/0304-4203(74)90015-2.

Wetzel, R. G., and G. E. Likens (1991), *Limnological Analyses, 2nd ed.*, Springer-Verlag.

Wilde, F. D., and D. B. Radtke (2003), National field manual for the collection of water-quality data, *U.S. Geol. Surv. Tech. Water Resour. Invest., Book 9.*

Wissmar, R. C., J. E. Richey, R. F. Stallard, and J. M. Edmond (1981), Plankton metabolism and carbon processes in the Amazon River, its tributaries, and floodplain waters, Peru-Brazil, May-June 1977, *Ecology, 62*(6), 1622-1633, doi:10.2307/1941517.

Xue, Z., J. P. Liu, and Q. Ge (2011), Changes in hydrology and sediment delivery of the Mekong River in the last 50 years: connection to damming, monsoon, and ENSO, *Earth Surf. Process. Landforms, 36*(3), 296-308, doi:10.1002/esp.2036.

Zeng, N., J. Yoon, J. A. Marengo, A. Subramaniam, C. A. Nobre, A. Mariotti, and J. D. Neelin (2008), Causes and impacts of the 2005 Amazon drought, *Environ. Res. Lett., 3*(1), 014002, doi:10.1088/1748-9326/3/1/014002.

Zhang, J., P. Quay, and D. O. Wilbur (1995), Carbon isotope fractionation during gas-water exchange and dissolution of CO_2, *Geochim. Cosmochim. Acta, 59*(1), 107-114, doi:10.1016/0016-7037(95)91550-D.

Appendix 1: Supplementary Information from Chapter 4

We constructed a simple model to assess how the partitioning of carbon amongst its end-members changes between seasons. The model was applied for those time periods in which the $\Delta^{14}C$ of lignin phenols and FPOC was determined, with two different approaches used for the rising and high-water periods. For the high-water period, FPOC was assumed to be derived from either vascular plants found in soils (F_{plant}) or other soil-derived OM (F_{soil}). The following binary mixing model was constructed:

$$\Delta^{14}C_{FPOC} = F_{plant}\,\Delta^{14}C_{plant} + F_{soil}\,\Delta^{14}C_{soil} \qquad (1)$$

$$1 = F_{plant} + F_{soil} \qquad (2)$$

where $\Delta^{14}C_{FPOC}$ is the $\Delta^{14}C$ of the bulk FPOC sample, $\Delta^{14}C_{plant}$ is the $\Delta^{14}C$ of lignin (91.5‰) (determined by averaging the three concentration-weighted values reported in Fig. 4.2b), and $\Delta^{14}C_{soil}$ is the leftover soil component, which likely contains a mixture of petrogenic C and refractory soil C.

We used carbon-normalized yields of lignin, λ_8 (mg lignin/100 mg OC), in sediments and vascular plants to deduce the vascular plant contribution to Mekong FPOM (i.e. determine F_{plant}). This approach has been applied in marine settings to estimate the contribution of terrestrial OM to bulk POM [*Hedges and Parker*, 1976; *Hedges et al.*, 1997]. Angiosperm leaves were chosen as the plant end-member given that the lignin phenol composition of Mekong FPOM appears to trend toward this end-member during the high-water season [*Ellis et al.* 2012]. Given the high variability in λ_8 of Mekong Basin angiosperm leaves, we calculated λ_8 from only the most common regional plant types [*Rundel et al*., 2007] reported in [*Ellis et al*., 2012], yielding a λ_8 of 4.9 ± 1.8 ($n = 7$). In addition to using the average λ_8 value, we also employed a range from 3.1 to 6.7 to determine the maximum and minimum possible vascular plant contribution to FPOM,

respectively. Although λ_8 has not been reported for gymnosperms in the Mekong Basin, the range of λ_8 values utilized here encompasses the average values reported for gymnosperm woods and needles in other river basins [*da Cunha et al.*, 2001]. Therefore, this model is also applicable to the early stages of the rising-water period, as it has been suggested that gymnosperms influence the lignin phenol composition of Mekong FPOM at that time [*Ellis et al.,* 2012]. The model employed λ_8 values for Mekong FPOM of 2.34, 1.03, and 1.74 for September 2008, June 2009, and July 2009, respectively, as determined from the concentration of lignin in the sediment during these three periods (data not shown). Once F_{plant} had been determined, $\Delta^{14}C_{soil}$ could be obtained using equation (1).

During the rising-water period, phytoplankton also contributes to FPOM composition [*Ellis et al.*, 2012]. We assumed that in situ production by phytoplankton was responsible for organic carbon present elevated beyond average high-water values, thus enabling the fraction of phytoplankton (F_{phyto}) to be determined:

$$F_{phyto} = (\%OC_{FPOM} - \%OC_{HW})/\%OC_{FPOM} \qquad (3)$$

where $\%OC_{FPOM}$ is the wt % OC content of FPOM, and $\%OC_{HW}$ is the average wt % OC content of sediments collected during the high-water period. Model input values ranged from 1.06 to 1.54% given that the average $\%OC_{HW}$ value was 1.30 ± 0.24% (n=10). Next, a binary mixing model was utilized to determine the $\Delta^{14}C$ of the terrestrial component as follows:

$$\Delta^{14}C_{FPOC} = F_{phyto}\,\Delta^{14}C_{phyto} + F_{terr}\,\Delta^{14}C_{terr} \qquad (4)$$

$$1 = F_{phyto} + F_{terr} \qquad (5)$$

Where $\Delta^{14}C_{phyto}$ is the $\Delta^{14}C$ of phytoplankton (which was assumed to equal the $\Delta^{14}C$ of dissolved inorganic carbon during the rising water stage (-106‰) (S. Alin, unpublished data)), F_{terr} is the fraction of carbon derived from terrestrial sources (plants and non-plant organic matter in soils),

and $\Delta^{14}C_{terr}$ is the Δ^{14}C of this organic carbon. After determining the radiocarbon content of the terrestrial component, an additional mixing model was employed:

$$\Delta^{14}C_{terr} = F_{plant}\,\Delta^{14}C_{plant} + F_{soil}\,\Delta^{14}C_{soil} \qquad (6)$$

$$1 = F_{plant} + F_{soil} \qquad (7)$$

Where all abbreviations are the same as in equations (1) and (3). This equation was then solved as outlined for equations (1) and (2), with the only difference being that the λ_8 of FPOM was corrected so as to remove the influence of phytoplankton on these values.

Model results were considered to be physically impossible and therefore rejected if Δ^{14}C values were < -1,000‰.

Table S4.1. Variability in suspended sediment concentration and the organic composition of riverine FPOC[a].

Date	[FSS] (mg/L)	[FPOC] (mg/L)	$\Delta^{14}C$ (‰)	$\delta^{13}C$ (‰)	wt. % OC	C:N
			High-Water Stage			
12 Sep 2008	228.8	2.9	25.9 ± 2.2	-26.4	1.3	9.3
16 Sep 2008	251.8	3.1	-	-26.6	1.2	10.0
24 Sep 2008	214.0	3.4	-	-26.7	1.6	10.0
15 Jul 2009	228.7	2.7	-	-26.2	1.2	7.4
6 Aug 2009	163.9	2.6	-	-26.3	1.6	9.1
12 Aug 2009	155.7	2.0	-115.7 ± 1.7	-27.0	1.3	9.6
18 Aug 2009	181.0	1.4	-	-27.7	0.7	5.1
10 Sep 2009	225.7	3.0	-29.5 ± 2.0	-25.3	1.3	8.1
24 Sep 2009	192.0	2.5	-	-26.3	1.3	8.2
15 Oct 2009	184.1	2.2	-83.5 ± 1.7	-26.9	1.2	8.8
Average	202.6	2.6	-50.7	-26.5	1.3	8.6
s. d.	31.7	0.6	62.2	0.6	0.2	1.5
			Falling-Water Stage			
20 Oct 2008	73.0	2.2	-116.2 ± 2.3	-26.1	3.0	7.8
17 Nov 2008	142.5	2.8	-111.2 ± 1.8	-26.0	2.0	9.2
22 Dec 2008	47.3	1.2	-	-27.3	2.6	10.9
5 Nov 2009	94.5	1.3	-80.1 ± 2.0	-26.4	1.3	11.8
3 Dec 2009	26.9	0.5	-	-27.9	1.9	8.7
Average	76.8	1.6	-102.5	-26.8	2.1	9.7
s. d.	44.7	0.9	19.5	0.8	0.6	1.6
			Low-Water Stage			
9 Feb 2009	5.9	0.5	-241.9 ± 3.0	-25.5	9.2	12.9
17 Mar 2009	8.7	0.5	-	-26.6	6.2	9.4
23 Apr 2009	10.8	0.4	-	-26.8	4.0	7.0
14 May 2009	17.0	0.6	-327.7 ± 1.6	-26.7	3.4	9.8

Table S4.1continued.

Date	[FSS] (mg/L)	[FPOC] (mg/L)	$\Delta^{14}C$ (‰)	$\delta^{13}C$ (‰)	wt. % OC	C:N
			Low-Water Stage			
12 Jan 2010	12.1	0.5	-	-29.2	3.8	9.2
3 Feb 2010	17.0	0.3	-193.2 ± 3.6	-28.4	2.0	7.5
Average	11.9	0.5	-254.3	-27.2	4.8	9.3
			Rising-Water Stage			
29 May 2009	69.2	1.4		-26.8	2.0	8.2
16 Jun 2009	94.6	2.0	-308.4 ± 1.8	-26.0	2.1	10.0
30 Jun 2009	100.7	2.2		-27.4	2.2	12.8
7 Jul 2009	121.1	2.1	-224.6 ± 3.1	-26.4	1.7	8.9
Average	96.4	1.9	-266.5	-26.7	2.0	10.0
s.d.	21.4	0.4	59.3	0.6	0.2	2.0

[a]FSS: fine suspended sediment, FPOC: fine particulate organic carbon, $\Delta^{14}C$: the $\Delta^{14}C$ of FPOC, $\delta^{13}C$: the $\delta^{13}C$ of FPOC, wt% OC: the weight % organic carbon of FSS, C:N: the carbon to nitrogen ratio of FPOM. The ± symbol denotes one standard error.

Table S4.2. The concentration, ^{14}C values, and $\delta^{13}C$ of DOC.

Date	[DOC] (mg/L)	$\Delta^{14}C$[a] (‰)	$\delta^{13}C$ (‰)
		High-Water Stage	
12 Sep 2008	1.4	31.7 ± 14.6	-26.6
16 Sep 2008	1.5	-	-
24 Sep 2008	-	-	-
15 Jul 2009	4.6	-	-
6 Aug 2009	4.4	-	-
12 Aug 2009	4.3	36.4 ± 11.3	-26.8
18 Aug 2009	3.2	-	-
10 Sep 2009	3.7	45.5 ± 12.4	-26.4
24 Sep 2009	3.7	-	-
15 Oct 2009	7.6	4.2 ± 14.4	-26.9
Average	3.8	29.5	-26.7
s. d.	1.8	17.8	0.2
		Falling-Water Stage	
20 Oct 2008	9.2	7.8 ± 11.7	-26.3
17 Nov 2008	4.8	28.0 ± 12.9	-25.5
22 Dec 2008	2.4	-	-
5 Nov 2009	-	-55.7 ± -11.2	-27.0
3 Dec 2009	4.1	-	-
Average	5.1	-6.6	-26.3
s. d.	2.9	43.6	0.8
		Low-Water Stage	
9 Feb 2009	2.8	-	-
17 Mar 2009	3.0	-	-
23 Apr 2009	2.5	-	-
14 May 2009	3.9	51.6 ± 32.5	-
12 Jan 2010	1.7	-	-
3 Feb 2010	1.1	-	-
Average	2.5	51.6	
s. d.	1.0		

[a]The ± symbol denotes one standard error.

Table S4.2 continued

Date	[DOC] (mg/L)	$\Delta^{14}C$[a] (‰)	$\delta^{13}C$ (‰)
	Rising-Water Stage		
29 May 2009	4.4	-	-
16 Jun 2009	3.4	-3.0 ± -9.4	-27.2
30 Jun 2009	3.5	-	-
7 Jul 2009	3.3	-	-
Average	3.7	-3.0	-27.2
s.d.	0.5		

[a]The ± symbol denotes one standard error.

Table S4.3. Radiocarbon analyses of individual lignin phenols[a] isolated from suspended sediment during September 2008, June 2009, and July 2009.

UCIAMS #	Lignn Phenol	Date	Size (mg C)	Fraction Modern	±	$\Delta^{14}C$	±	^{14}C age (BP)	±
93862	V_{ad}	Sep. 2008	0.07	1.1051	0.0063	96.9	6.3	-800	50
93864	V_{ad}	Jun. 2009	0.043	1.083	0.0105	75	10.5	-630	80
93863	V_{ad}	Jul. 2009	0.055	1.105	0.0083	96.9	8.3	-790	70
93867	V_{al}	Sep. 2008	0.026	1.12	0.0189	111.7	18.9	-900	140
93868	V_{al}	Jun. 2009	0.008	1.114	0.0651	105.9	65.1	-860	470
93869	V_{al}	Jul. 2009	0.061	1.0998	0.0072	91.8	7.2	-750	60
93826	V_{k}	Sep. 2008	0.061	1.1027	0.0072	94.6	7.2	-780	60
93827	V_{k}	Jun. 2009	0.023	1.0978	0.0203	89.7	20.3	-740	150
93828	V_{k}	Jul. 2009	0.034	1.1109	0.0135	102.7	13.5	-830	100
93845	S_{ad}	Jun. 2009	0.011	1.1146	0.0455	106.4	45.5	-860	330
93846	S_{ad}	Jul. 2009	0.033	1.0999	0.0136	91.8	13.6	-750	100
93841	S_{al}	Sep. 2008	0.163	1.0885	0.0026	80.5	2.6	-675	20
93842	S_{al}	Jun. 2009	0.076	1.0806	0.0057	72.6	5.7	-615	45
93822	S_{k}	Sep. 2008	0.059	1.0963	0.0074	88.2	7.4	-730	60
93823	S_{k}	Jun. 2009	0.034	1.0845	0.0133	76.5	13.3	-640	100
93824	S_{k}	Jul. 2009	0.041	1.0956	0.011	87.6	11	-720	90
93831	F_{ad}	Sep. 2008	0.01	1.1203	0.0528	112.1	52.8	-900	380
93832	F_{ad}	Jun. 2009	0.005	1.1419	0.1178	133.5	117.8	-1060	830
93833	F_{ad}	Jul. 2009	0.009	1.068	0.0546	60.1	54.6	-520	420
93836	P_{ad}	Sep. 2008	0.063	1.0104	0.0065	2.9	6.5	-70	60
93837	P_{ad}	Jun. 2009	0.024	1.0748	0.0195	66.9	19.5	-570	150
93838	P_{ad}	Jul. 2009	0.036	1.0879	0.0123	79.9	12.3	-670	100

[a]Abbreviations for individual monomers are as follows: V_{ad} (vanillic acid), V_{al} (vanillin), V_{k} (acetovanillone), S_{ad} (syringic acid), S_{al} (syringaldehyde), S_{k} (acetosyringone), F_{ad} (ferulic acid), and P_{ad} (p-coumaric acid). The error (±) denotes one σ_{x}.

Curriculum Vitae

Erin E. Ellis

Education

2012 Ph.D. Chemical Oceanography.
University of Washington, School of Oceanography, Seattle, WA.
2007 M.S. Chemical Oceanography.
University of Washington, School of Oceanography, Seattle, WA.
2002 B.A. Biology.
Carleton College, Department of Biology, Northfield, MN.

Professional Experience

2011-2012 Visiting Faculty, The Evergreen State College, Olympia, WA. Program: Introduction to Natural Science.

2009 -2012 Doctoral Candidate, School of Oceanography, University of Washington, Seattle, WA. Dissertation: *Elucidating the sources and cycling of organic matter exported by tropical rivers.* Advisors: Dr. Jeffrey E. Richey and Dr. Anitra E. Ingalls.

2004 - 2009 Graduate Research Assistant**,** University of Washington, School of Oceanography.

2003 - 2004 Research Staff Assistant, University of Washington, School of Oceanography. Supervisors: Dr. Paul Quay and Mr. Johnny Stutsman.

2002 - 2003 Environmental Education Program Coordinator, Northwest Environmental Education Council, Seattle, WA. AmeriCorps position. Supervisor: Mr. Erick McWayne.

2002 Research Assistant, University of Washington, Biology Department. Supervisor: Dr. Roger del Moral.

2001 Research Assistant, Carleton College, Biology Department. Supervisor: Dr. Philip Camill.

Awards and Honors

2009 Huckabay Teaching Fellowship, University of Washington.
2006-2009 National Science Foundation Graduate Research Fellowship.
2003 AmeriCorps Education Award.
2001 Hughes Foundation Summer Research Fellowship, Carleton College.

Courses Designed and Taught

2011-2012 Introduction to Natural Science. The Evergreen State College. Taught general chemistry lectures, labs, and workshops. Supervised student-led independent research projects.

2010 Biogeochemical Cycles and Ecosystem Functioning. School of Oceanography, University of Washington. Taught undergraduates

Teaching Assistantship

2012 Ocean 201: Introduction to Oceanography Laboratory. School of Oceanography, University of Washington.
2006 Ocean 400: Chemical Oceanography. School of Oceanography, University of Washington.

Refereed Journal Articles

Ellis, EE, Richey JE, Aufdenkampe AK, Krusche AV, Quay PD, Salimon C, and Brandao da Chunha H. 2012. Factors controlling water-column respiration in rivers of the central and southwestern Amazon Basin. Limnolology and Oceanography. 57: 527-540.

Ellis, EE., Keil RG, Ingalls AE, and Richey JE. 2012. Seasonal variability in the sources of particulate organic matter of the Mekong River as discerned by elemental and lignin analyses. Journal of Geophysical Research-Biogeosciences. 117, GO1038, doi:101029/2011JG001816.

Ingalls AE, Ellis EE, Santos GM, McDuffee KE, Truxal L, Keil RG, Druffell ERM. 2010. HPLC Purification of Higher Plant-Derived Lignin Phenols for Compound Specific Radiocarbon Analysis. Analytical Chemistry. 82: 8931- 8938.

Del Moral R., Ellis EE. 2004. Gradients in compositional variation on lahars, Mount St. Helens, Washington, USA. Plant Ecology. 175: 273-286.

Camill P, McKone MJ, Sturges S, Severud W, Ellis E, Limmer J, Martin C, Navratil RT, Purdie A, Sandel BS, Talukder S, Trout A. 2004. Community and ecosystem-level changes in a species-rich tallgrass prairie restoration. Ecological Applications. 15: 1680-1694.

In Preparation

Ellis EE, Ingalls AE, Keil RG, Truxal L, Richey JE. Variation in glycerol dialkyl glycerol tetraether (GDGTs) distribution in the Mekong River and surrounding soils.

Ellis EE, Ingalls AE, Keil RG, Truxal L, Richey JE, Santos GM, Druffel ERM. Young plant-derived organic matter is consistently exported from sediments of the Mekong River Basin despite high variability in the age of the bulk sediments.

Small GE, Mayorga E, Ardon M, Aufdenkampe AK, Ellis EE, Genereux D, Hernes PJ, Holmes RM, Johnson M, Kaplan LA, McDowell W, Pringle C, Ramierez A, Richey JE, Six J, Spencer R, Taylor B, Townsend-Small A, Whiles M, and Wohl E. Human impacts on carbon transport and processing in tropical rivers: current understanding and knowledge gaps.

Conference Presentations

AGU Fall Meeting, December 2011, San Francisco, CA. Poster. Seasonal variability in glycerol dialkyl glycerol tetraethers (GDGTs) associated with suspended sediment transported by the Mekong River, Cambodia. Ellis EE, Richey JE, Truxal L, Keil RG, Ingalls AE.

International Exploratory Workshop: Pushing the size limits of radiocarbon analysis, September 2011, Zurich, Switzerland. Oral Presentation. The age of plant-derived organic carbon transported by the Mekong River, Cambodia: A comparison between lignin-derived phenols and bulk organic matter. Ellis EE, Ingalls AE, Richey JE, Keil RG, Truxal LT, Santos GM, Druffel ERM.

ASLO Aquatic Sciences Meeting, February 2011, San Juan, Puerto Rico. Oral presentation. Seasonal variability in the sources of Particulate Organic Carbon on the Mekong River, Cambodia. Ellis EE, Richey JE, Ingalls AI, Keil RG.

ASLO Aquatic Sciences Meeting, February 2011, San Juan, Puerto Rico. Oral presentation. A synthesis of carbon transport and processing in tropical streams and rivers: Effects of global change. Small GE, Ardon M, Ellis EE, Genereux DP, Hernes PJ, Johnson MS, Mayorga E, McDowell WH, Pringle CM, Six JW.

ASLO Aquatic Sciences Meeting, February 2011, San Juan, Puerto Rico. Oral presentation. How carbon dynamics in large tropical rivers might respond to global change. Richey JE, Krusche AV, Ellis EE.

AGU/ASLO Ocean Sciences Meeting, February, 2010, Portland, OR. Oral Presentation. HPLC purification of higher plant-derived lignin phenols for radiocarbon dating. Ellis EE, Ingalls AE, McDuffee K, Keil RG, Santos GM, Druffel ERM.

AGU/ASLO Ocean Sciences Meeting, March 2008, Orlando, FL. Poster. The Importance of pH, Particulate Carbon, and Photosynthesis in Controlling Water-Column Respiration Rates in the Amazon Basin. Ellis EE, Richey JE, Aufdenakmpe AK, Quay PD, Krusche AV.

LBA-ECO Annual Meeting, September 2007, Salvador, Brazil. Oral Presentation. The Importance of pH, Particulate Carbon, and Photosynthesis in Controlling Water-Column Respiration Rates in the Central and Southwestern Amazon Basin. Presentation: Ellis EE, Richey JE, Aufdenkampe AK, and Krusche AV.

AGU Fall Meeting, December 2006, San Francisco, CA. Poster. Factors Controlling Respiration Rates and Respired CO_2 Signatures in Riverine Ecosystems of the Amazon Basin. Ellis EE, Aufdenkampe AK, Quay PD, Krusche AV, Alin SR, Richey JE.

ESA Annual Meeting, August 2002, Tuscon, AZ. Poster: Community and system-level constraints on NPP and C and N pool dynamics in restored tallgrass prairies. Annual meeting of the Ecological Society of America. Camill P, Limmer J, Ellis E, Sturges S, McKone M.

Synergistic Activities

2012	co-Chair of special session "Riverine Organic Matter as an Integrated Signal of Basin-Scale Processes, Climate and Land-Use Change" at the American Geophysical Union's fall meeting in San Francisco, CA.
2011	Reviewer for *Limnology and Oceanography*.
2011	Invited to International Workshop on Small Scale Radiocarbon Analysis, Eidgenössische Technische Hochschule Zürich, Sept. 13-16.
2010	Invited to the NOSAMS Compound Specific Radiocarbon Analyses Workshop, Woods Hole Oceanographic Institution, June 29- 30.

2010	Invited to the workshop "Carbon Transport and Processing in Tropical Streams and Rivers", at La Selva Biological Station in Costa Rica, April 15-17.
2010	Facilitator, Annual TA Conference on Teaching and Learning, University of Washington's Center for Instructional Development and Research.
2010	Reviewer for *Biogeochemistry*.
2010	Presenter, Bennett Elementary Family Science Night, Shoreline, WA.
2009	Developer and instructor, 3-day course on "Carbon Cycling and Remote Sensing for Large Tropical Rivers", at Resource Development International-Cambodia (RDIC), Kandol, Cambodia.
2009	Presenter, Lake Forest Park Elementary Family Science Night, Lake Forest Park, WA.
2008	Presenter, "Microworlds" course, University of Washington, visiting class of 5th Graders.
2006-2009	Facilitator, College of Ocean and Fishery Science TA Training Workshop, University of Washington.

Professional Societies:

American Society of Limnology and Oceanography
American Geophysical Union

Collaborators:

Druffel, ERM (UC Irvine), Santos, GM (UC Irivine), Krusche, AV (CENA-University of Sao Paulo), Victoria, R (CENA-University of Sao Paulo), Aufdenakmpe, AK (Stroud Water Research Center), Solomon, CI (Federal University of Acre, Brazil), Alin, SR (NOAA-PMEL), Shantz, A (Resource Development International-Cambodia). UW Collaborators: Quay, PD, Keil, R G, Richey, JE and Ingalls, AE.

Fieldwork:

2009	Kandol and Siem Reap, Cambodia. Organized field campaign to collect water, sediment, soil, and vegetation samples for inorganic and organic carbon analyses. Employed centrifuge ultrafiltration to isolate suspended sediment from river water. June – July.
2009	Willapa Bay, Washington, USA. Collected marine and riverine sediment cores. August.
2008	Kandol and Siem Reap, Cambodia. Trained local collaborators in field collection methods. Organized field campaign to collected water, sediment, soil, and vegetation samples for inorganic and organic carbon analyses. July – September.
2006	Acre and Amazonas, Brazil. Organized field campaign to collect water samples for community respiration measurements. July – September.

2005 Acre and Amazonas, Brazil. Organized field campaign to measure *in situ* respiration rates in Amazonian Rivers. Collected samples for the analysis of particulate and dissolved organic matter and dissolved inorganic carbon.

2004 Acre and Amazonas, Brazil. Collected samples to be analyzed for organic matter composition. June – August.

2002 Mount St. Helens, Washington, USA. Assessed diversity of native plant communities on lahars. July - September.

2001 Northfield, Minnesota, USA. Collected soil cores and analyzed soil composition in tallgrass prairie ecosystems. June - September.